AN INDIVIDUAL-BASED MODEL TO EVALUATE JUVENILE CHINOOK SALMON MIGRATION IN THE COLUMBIA RIVER ESTUARY

By

Katherine J. Morrice

A DISSERTATION

Presented to the Division of Environmental and Biomolecular Systems
and the Oregon Health & Science University
School of Medicine
in partial fulfillment of
the requirements for the degree of

Doctor of Philosophy
June 2020

School of Medicine

Oregon Health & Science University

CERTIFICATE OF APPROVAL

This is to certify that the PhD dissertation of
Katherine J. Morrice
has been approved

_____
Dr. António Baptista

_____
Dr. Tawnya Peterson

_____
Dr. Richard Johnson

_____
Dr. Brian Burke

_____
Dr. Laurie Weitkamp

Table of Contents

List of Tables

List of Figures

List of Acronyms

SELFE	Semi-implicit Eulerian-Lagrangian Finite Element model
NCOM	Naval Research Laboratory Navy Coastal Ocean Model
IBM	Individual-Based Model
CH0	Subyearling Chinook Salmon
CH1	Yearling Chinook Salmon
BCRW	Biased Correlated Random Walk
RW	Random Walk
RAS	Restricted-Area Search
PA	Predator Avoidance
USGS	United States Geological Survey
NOAA	National Oceanic and Atmospheric Administration
JSATS	Juvenile Salmon Acoustic Telemetry System
PIT	Passive Integrated Transponder
PTAGIS	PIT Tag Information System
CC	Clifton Channel
CB	Cathlamet Bay

Acknowledgements

I would like to thank the faculty, staff, and students from Oregon Health & Science University's former Institute of Environmental Health. I would especially like to thank members of the Baptista lab, both past and present, including Jesse Lopez, Mojgan Rostaminia, Tuomas Kärnä, Paul Turner, and Charles Seaton. I am also grateful to the NOAA scientists that provided guidance throughout the development of this model, including David Huff and Curtis Roegner. I would also like to thank Matt Morris for his guidance regarding the pair-trawl data, as well as those who were involved in the collection of JSATS data, including George McMichael, Ryan Harnish, and Gary Johnson. I would also like to acknowledge the Columbia Basin PIT Tag Information System (PTAGIS), the Fish Passage Center's Smolt Monitoring Program, Columbia Basin Research out of the School of Aquatic and Fishery Sciences at the University of Washington, and the Lower Columbia River Estuary Program for providing data that was used to inform the model simulations.

I am very grateful for the members of this dissertation committee for their time and service, including Richard Johnson, Tawnya Peterson, Brian Burke, and Laurie Weitkamp. Michiko Nakano has also been wonderful in helping me progress through this program amidst many transitions, and I will forever be grateful for her support. Lastly, I would like to extend special thanks to my advisor Antonio Baptista for his guidance and support and for providing me with this opportunity to conduct research that has been of great interest.

This research was partially funded through the project "Sustaining NANOOS, the Pacific Northwest component of the U.S. Integrated Ocean Observing Systems", Award NA16NOS0120019 of the National Oceanic and Atmospheric Administration.

Abstract

An individual-based model (IBM) was developed to explore juvenile Chinook salmon (*Oncorhynchus tshawytscha*) migration patterns in the Columbia River estuary. The model used outputs from the hydrodynamic model SELFE as a virtual environment. There were several sub-models, including a movement model that simulated Lagrangian transport and active swimming and a bioenergetics model that computed growth. A predation model was also developed to explore potential impacts of avian predators on survival. Migration was simulated for yearling and subyearling Chinook salmon, and swimming behaviors were developed based on assumptions regarding habitat usage. Yearling Chinook salmon behaviors optimized efficient migration, while subyearling Chinook salmon behaviors prioritized growth. Passive drift and random walk behaviors for both life-history types served as null models to compare the more sophisticated behaviors against.

Migration periods for juvenile Chinook salmon were simulated in 2010 to evaluate how flow conditions and swimming behaviors influenced migration. Observational data from the pair-trawl survey near Jones Beach as well as Juvenile Salmon Acoustic Telemetry System (JSATS) data from the lower estuary were used to assess simulated travel times. With the exception of one behavior that optimized growth, simulated travel times for juvenile Chinook salmon between Bonneville Dam and Jones Beach and between JSATS arrays were within several hours of observed values. Overall, this evaluation helped establish the legitimacy of the IBM as a tool for modeling migration.

River flows largely drove estuarine residence times, and the timing of marine entry occurred primarily during the ebb phase of the tide. With the exception of one subyearling Chinook salmon behavior, residence times and migration rates across behaviors showed little

variability suggesting that flows were primarily responsible for variability in migration over time. Looking at trends across the estuary's hydrogeomorphic reaches, simulated migration rates tended to be reduced in the lower estuary (rkm 0 – 50), which was likely due to the increased interaction of river discharge and tidal activity. Simulations that considered predation indicated that survival was associated with residence times. Individuals that spent less time in the estuary were more likely to survive to marine entry.

River temperatures and large-scale indices influenced juvenile Chinook salmon growth rates. Warm temperatures during low flow years were associated with increased yearling Chinook salmon growth. However, subyearling Chinook salmon that migrated during summer months in low flow years experienced much warmer temperatures that limited growth. This was especially true when large-scale climate indices contributed to warmer than average conditions. Across the estuary, simulated growth rates were reduced in the lower estuary, where there was a greater extent of open water compared to other reaches.

This IBM was effective for investigating how juvenile Chinook salmon utilize estuarine habitat and how environmental conditions and behavioral decision-making influence migration and growth. While this work did not consider the influence of management decisions, the IBM could benefit managers seeking to understand how estuarine migration and growth could be impacted under different flow management scenarios. Similarly, the model could prove useful for better understanding potential impacts associated with warming temperatures and shifting hydrographs.

1 Introduction

1.1 The Columbia River estuary

The Columbia River has the second highest discharge of major river basins in the United States and accounts for 77% of the freshwater input into the Pacific Ocean from San Francisco to the Strait of Juan de Fuca (Barnes et al. 1972). The river basin extends from the headwaters in Canada to the United States, with the majority of the basin across Washington, Idaho, and Oregon, draining an area of approximately 660,480 km^2. The river and its tributaries are heavily managed due to hydropower operations and flood management, with a total of 29 federally managed major dams and hundreds of smaller impoundments. Daily river discharge measured at Bonneville Dam ranges from 3,200 to 10,500 m^3s^{-1} with spring freshets typically exceeding 10,000 m^3s^{-1} (Chawla et al. 2008). While the spring freshet has a strong seasonal signal due to snowmelt, flow management dampens this signal, leading to reduced spring freshets and higher than historic summer and winter flows.

The Columbia River estuary extends from Bonneville River Dam to the estuary mouth, covering a distance of approximately 234 river kilometers (rkm). Tidal amplitudes in the lower estuary range from 2 to 3.6 m based on the spring-neap cycle (Chawla et al. 2008), and tidal influence extends to Bonneville Dam. The estuary as described in Simenstad et al. (2011) is made up of eight major hydrogeomorphic reaches that differ based on the influence of various hydrologic and geomorphic processes (Figure 1.1). More specifically, these processes include river flows, tidal activity, salinity, flooding and turbidity. While the river-dominated mesotidal estuary is strongly influenced by river discharge and semi-diurnal tides, upstream reaches are more dominated by riverine processes, whereas the reaches near the mouth are more impacted by

the tides and coastal processes. These differences have relevant impacts on the availability of optimal habitat for outmigrating salmonids.

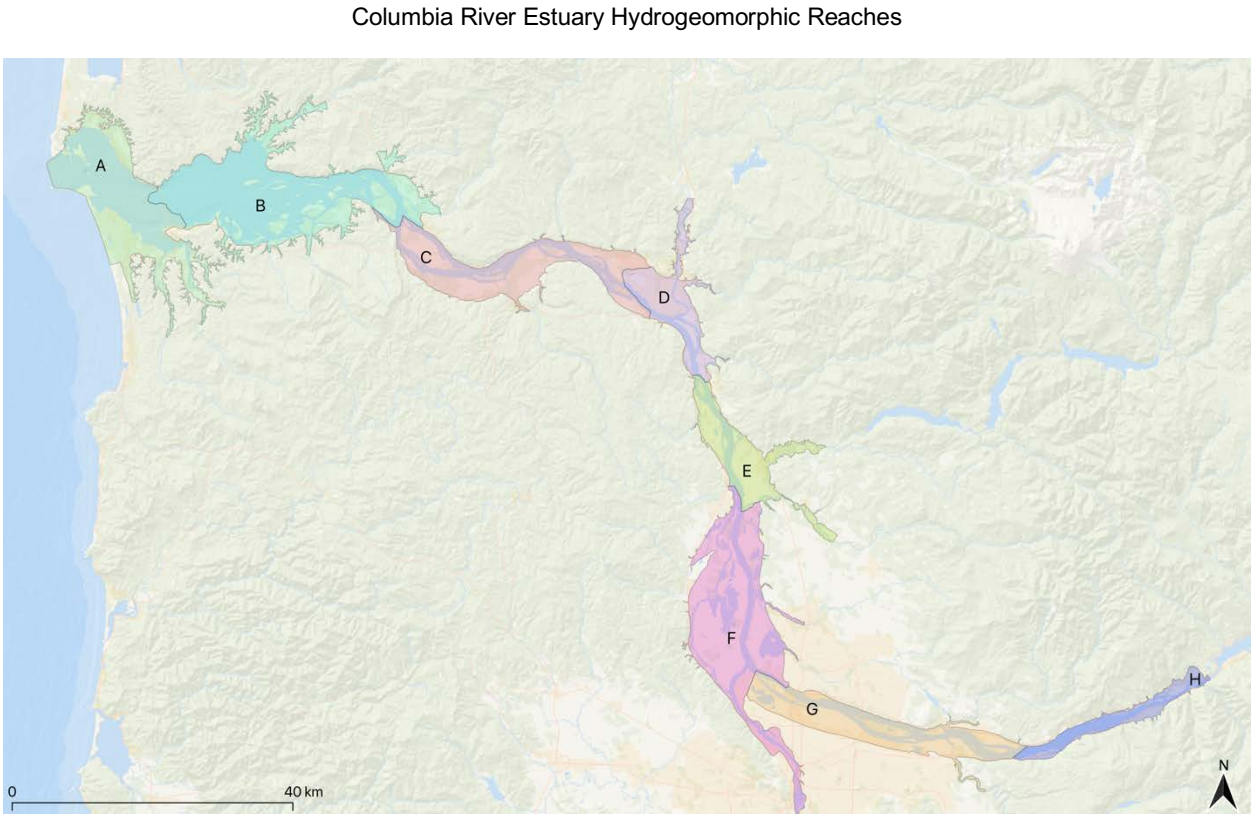

Figure 1.1. Map of hydrogeomorphic reaches A – H for the Columbia River estuary as defined in Simenstad et al. (2011).

1.2 Salmonids in the Columbia River Estuary

The Columbia River has historically supported large populations of Pacific salmon (*Oncorhynchus* spp.); however, starting in the late-1800s, many of these populations declined, with an estimated 90% loss from historical levels (Bottom et al. 2011). Several activities contributed to this decline, including the construction of hydroelectric dams along the Columbia River, loss of wetland habitat, and overharvesting. In addition, the increasing reliance on hatcheries as a strategy to maintain populations has limited genetic diversity (Bottom et al. 2005). Currently, there are twenty evolutionarily significant units (ESUs) that inhabit the basin,

thirteen of which are listed as threatened or endangered under the Endangered Species Act (https://www.fisheries.noaa.gov/species-directory/threatened-endangered). Facing ongoing declines of salmonids in the Columbia River basin, in addition to the listing of numerous stocks under the Endangered Species Act has necessitated improving our understanding of how the Columbia River estuary supports salmonids.

Bottom et al. (2005) effectively conveyed the importance of the estuary to juvenile salmonids and its potential role in supporting the recovery of Columbia River salmon. Understanding how the estuary supports juvenile salmonids has been an ongoing area of research. Groups have sought to investigate marsh habitat and the macroinvertebrate food webs that support salmonids (Bottom et al. 2008) and how avian predation has impacted juvenile salmonid survival (Collis et al. 2002; Evans et al. 2012). Studies employing acoustic telemetry have been especially helpful in better understanding travel times and survival throughout the system (Ledgerwood et al. 2004; McMichael et al. 2010).

Modeling studies have attempted to describe how the estuary supports juvenile salmonids by quantifying the amount of optimal habitat available and how that varies under different hydrological and marine conditions. For example, previous modeling work used temperature, velocity, depth, and salinity criteria from hydrodynamic models to calculate habitat area or volume in the estuary (Bottom et al. 2005; Burla 2009; Rostaminia 2017). These Eulerian-based approaches have been informative and have effectively conveyed how various reaches of the system function as habitat over time, but there are recognized limitations with these approaches as they quantify potential habitat but do not consider behavioral decision-making by an active agent.

IBMs have become increasingly popular tools to examine population-level patterns through modeling individual behaviors and responses to a changing environment. IBMs simulate multiple individuals that differ in their environmental histories, growth, and mortality. This approach effectively describes the heterogenous environmental conditions that fish experience in ways that Eulerian-based methods cannot. Similarly, IBMs offer greater perspective on the habitats that are most beneficial to fish in terms of growth opportunities or reduced mortality risks. Fish IBMs can take advantage of hydrodynamic model outputs that provide a virtual environment. Incorporating swimming behaviors and bioenergetics models to simulate growth then allows for a greater understanding of how individual behavior in a simulated environment can have population-level effects.

While previous modeling approaches to quantify salmon habitat have proven useful, there is a need to advance from that framework to simulate active agents, and this calls for the development of an IBM to understand how juvenile salmonids utilize estuarine habitat and how changing environmental conditions and habitats influence their growth and migration. This dissertation describes the development of an IBM using a three-dimensional circulation model of the Columbia River estuary.

Specific objectives of this work include:

1. Develop a spatially-explicit and time-varying IBM of juvenile Chinook salmon in the Columbia River estuary that simulates individual trajectories based on realistic environmental flows and behavioral decision making.
2. Implement a bioenergetics model that relates to wetland-based food webs.

3. Implement a predation model to assess avian predation impacts on juvenile Chinook salmon.
4. Assess how interannual variability in river conditions, temperatures, and larger scale indices influences migration patterns and growth for yearling and subyearling Chinook salmon.
5. Describe how migration and growth patterns differ across the estuary's hydrogeomorphic reaches.

This dissertation is organized into five separate chapters. Chapter 1 describes the Columbia River estuary and provides a brief history on salmon in the Columbia River estuary. This chapter also lays the ground for the benefits of an IBM to better understand juvenile salmonid migration dynamics in the estuary.

Chapter 2 describes the development of the IBM, including details about the virtual environment and the rationale for multiple swimming behaviors simulated for both yearling and subyearling Chinook salmon. In this chapter, passive particles are likewise simulated to assess the relative skill of the Lagrangian particle tracking model upon which more complex swimming behaviors are built. Model-data comparisons are also conducted for this chapter to assess the performance of the IBM against observed travel times from the annual Jones Beach pair-trawl study and the 2010 JSATS study in the lower estuary as described in Harnish et al. (2012).

Chapter 3 models juvenile Chinook salmon in the lower Columbia River estuary from 2000 – 2015 and explores the association between migration patterns and growth with interannual variability in river conditions and larger-scale ocean indices. Spatial patterns in

migration and growth rates are also described for the eight hydrogeomorphic reaches of the estuary.

Chapter 4 describes the development of a predation sub-model to simulate the potential impacts of avian predation on the survival of outmigrating yearling Chinook salmon in the lower Columbia River estuary. The model is based on the foraging ranges of two common avian predators, double-crested cormorants (*Phalacrocorax auritus*) and Caspian terns (*Hydroprogne caspia*), and considers the role of marine forage fish as alternate prey. Years 2010 – 2015 were simulated to capture a range of flow conditions. Survival and its relation to residence times and growth are described across different flow regimes and swimming behaviors to account for how environmental drivers and behavioral decision-making influence growth and survival outcomes.

Chapter 5 provides an overall summary of the dissertation and discusses future work.

2 Environmental and behavioral controls on juvenile Chinook salmon migration pathways in the Columbia River estuary[1]

Abstract

Juvenile Chinook salmon population dynamics in the Columbia River estuary are influenced by physical processes, hatchery practices, and behavioral decision-making. To better understand how environmental forcing and swimming behavior influence estuarine migration and travel times, we developed an individual-based model (IBM) that uses 3-D outputs from a hydrodynamic model to simulate Lagrangian transport as well as swimming and bioenergetics sub-models to simulate active swimming and growth. Simulations were run in 2010 during the migration seasons for yearling and subyearling Chinook salmon. For both life-history types, alternative behaviors were simulated, from random walks to behaviors that optimized efficient system migration for yearling Chinook salmon and growth for subyearling Chinook salmon. Simulation results compared well against observed data on travel times and common migration pathways; the simulated travel times for both yearling and subyearling Chinook salmon were within several hours of the observed travel times. In general, residence times and pathways were largely driven by river discharge and the phase of the tide. During periods of greater river discharge, simulated estuarine residence times were reduced and variability across individuals was minimal. The timing of estuarine exit was closely tied to the phase of the tide, with most simulated individuals exiting the system during the ebb phase. While travel times were largely driven by flow velocities, swimming behavior was likewise important. Simulated yearling

[1] Morrice, K.J., Baptista, A.M., and B.J. Burke. 2020. Environmental and behavioral controls on juvenile Chinook salmon migration pathways in the Columbia River estuary. *Ecological Modelling,* 427, 109003.

Chinook salmon behaviors that optimized movement with surrounding flows resulted in reduced estuarine residence times when compared to passive and random walk behaviors. Similarly, simulated subyearling Chinook salmon behaviors that optimized growth directed individuals to shallow peripheral habitats, resulting in longer residence times and higher growth rates. Even if potentially important factors such as predator avoidance were not included, this IBM provides an informative tool to model migration pathways, growth, and residence times of juvenile salmon in an estuarine environment and could be used to inform management decisions by evaluating various scenarios.

2.1 Introduction

The Columbia River basin serves as important habitat for anadromous fish in the Pacific Northwest. The river and its surrounding tributaries have historically supported large runs of several species of salmonids; however, habitat loss, hydropower development, navigation improvements, and overfishing in the past century, have all contributed to their decline (Bottom et al. 2005). Furthermore, an increasing shift of hatcheries towards production-oriented practices has reduced salmonid diversity and residency in the Columbia River estuary (Bottom et al. 2005). Due to these ongoing stressors, thirteen stocks are now listed under the Endangered Species Act (ESA) as threatened or endangered (Myers et al. 1998). As a result of these listings, there is a pressing need for an improved understanding of salmonid survival and migratory behaviors to inform recovery efforts and habitat restoration.

The importance of estuarine habitat has been of particular interest, especially with regards to how the Federal Columbia River Hydropower System (FCRPS) has altered juvenile rearing habitats and overall production. Estuaries are important rearing habitats for salmonids that provide multiple services, including food resources, shelter from predators, and a transitional

habitat to physiologically adapt to increasing salinities (Bottom et al. 2005; Simenstad et al. 1982; Thorpe 1994). However, estuaries can also be challenging environments due to tides, strong and dynamic salinity gradients, and increasing interactions with predators. Juvenile Pacific salmon use estuaries to varying degrees (Bottom et al. 2005; Healey 1982; Simenstad et al. 1982), and populations have adapted to using freshwater and estuarine habitats in different capacities.

Diverse migration patterns across life-history types result in a wide range of estuarine residence times (Weitkamp et al. 2014). For yearling salmonids, estuarine residence times are on the order of days to weeks, while estuarine residence times for subyearling salmonids often last weeks to months (Healey 1982; Simenstad et al. 1982). Yearling salmonids migrate to the ocean after rearing in freshwater for a year or more (i.e., coho, sockeye, steelhead, and stream-type Chinook) and typically travel quickly through the estuary, using it as a migration corridor. They are often assumed to minimally interact with estuarine habitat outside of the main channels; however, recent work by McNatt and Hinton (2017) observed yearling Chinook salmon in wetland habitats, thereby challenging this assumption. Subyearling salmonids (i.e., ocean-type Chinook and chum) spend less time rearing in freshwater and instead migrate earlier and spend longer periods in estuaries (Healey 1982; Quinn 2005; Weitkamp et al. 2014). Whereas yearling salmonids do not spend much time in shallow habitats, smaller subyearling salmonids frequently occupy shallow nearshore wetland habitats (McCabe et al. 1986; Simenstad et al. 1982).

Smolts generally migrate between May and July, responding to environmental cues such as the spring freshet. Juvenile salmon that have shorter estuarine residence migrate earlier in the season, while those with longer estuarine residence migrate mid-summer (Healey 1982; Roegner et al. 2012; Weitkamp et al. 2012). As juveniles migrate from freshwater to marine

environments, they experience different habitats and environmental conditions, and this variation impacts the timing of their migration and size at ocean entry. Smolt migration rate and survival are affected by a number of factors, including predation, physiology, river flows, and ocean conditions. Although there have been concerted efforts to study smolt survival along the hydropower system upstream of Bonneville Dam, less is known about how survival changes downstream of Bonneville Dam as smolts continue their migration through the estuary.

Field-based campaigns and modeling efforts have advanced our understanding of juvenile salmonid habitat preference, survival, and migration in the estuary. However, these studies are often of limited temporal or spatial scope and may underrepresent distributions of juvenile salmon, particularly in shallow nearshore environments. Passive integrated transponder (PIT) tag (Ledgerwood et al. 2004; Prentice et al. 1990) and the Juvenile Salmon Acoustic Telemetry System (JSATS) tag (McMichael et al. 2010) data have been especially useful for tracking survival and migration rates; however such data are typically collected at a select few locations and thus lack comprehensive information about the entire migratory pathway.

Modeling approaches have also been used to quantify optimal habitat for juvenile Chinook salmon and how that changes based on river discharge (Kukulka and Jay 2003a; Kukulka and Jay 2003b), tides, and seasons. Salmon habitat opportunity (Bottom et al. 2005; Burla 2009), an area-based metric, and salmon habitat (Rostaminia 2017), a volume-based metric have both been used to compute the amount of optimal salmon habitat available in specific hydrogeomorphic reaches of the estuary. Although these methods are informative to understanding how different reaches of the estuary function as habitat over time, these Eulerian-based approaches do not account for how juvenile salmon interact with and respond to changing environmental conditions along a migration route. Furthermore, these methods have relied solely

on physical variables (e.g., temperature, salinity, flow velocities, and water depths) and do not account for biological habitat components.

A more in-depth investigation of how the estuary supports stocks of juvenile salmon is needed and requires a modeling technique that tracks estuarine residence and migration pathways of individual salmon. This can be addressed with an individual-based model (IBM) that simulates juvenile salmon migration in the estuary, providing a means to characterize how system variability and behavioral decisions affect estuarine migration pathways. IBMs are effective tools for tracking the spatial and temporal distributions of organisms and their response to biotic and abiotic environmental conditions. When coupled with bioenergetics models, IBMs can offer insight into the response of individual growth to environmental variability (Fiechter et al. 2015a; Hinckley et al. 1996).

IBMs vary in their level of sophistication. Some IBMs simulate extensive life-history processes and consider foraging, growth, mortality, and reproduction, while others are simpler and employ rule-based methods to approximate movement patterns and habitat use (Giske et al. 1998; Tyler and Rose 1994). IBMs are frequently used to describe distributions of marine fish populations (Miller 2007) and have been adapted to simulate salmon migration pathways in the ocean (Byron and Burke 2014). In addition, IBMs have been applied to the upstream reaches of the Columbia River to investigate juvenile salmon passage through the hydropower system (Goodwin et al. 2006), as well as to the Columbia River plume (Brosnan 2014) and coastal ocean off Oregon and Washington (Burke et al. 2014; Burke et al. 2016). Although IBMs have been used in upstream reaches of the Columbia River and off the mouth of the estuary, there have been few attempts to simulate juvenile Chinook salmon in the estuary.

The objectives of this work were to investigate potential estuarine migration pathways of yearling and subyearling Chinook salmon in the Columbia River estuary using different swimming behaviors and to explore how environmental conditions and behavioral decisions influence migration pathways, travel times, and growth rates. To address these objectives, an IBM coupled with a bioenergetics model was used to simulate movement due to advection and active swimming and growth based on the local environment. Results from model simulations were then validated against observations to assess model performance. Chinook salmon were the focus of this study as they are the most estuarine-dependent salmonid species in the Columbia River (Healey 1982). In addition, there are multiple species of Chinook salmon listed as endangered or threatened under the ESA, and multiple life-history strategies for each species, allowing for an intra-specific behavioral comparison.

2.2 Methods

2.2.1 Overview

An IBM was used to simulate juvenile Chinook salmon migration in the Columbia River estuary from Bonneville Dam to the estuary mouth (Figure 2.1). The virtual environment wherein fish movement and growth were modeled utilized outputs from a hydrodynamic model. Data collected at Bonneville Dam and various locations in the estuary informed model design (e.g., simulation timing, starting fish lengths, and length-weight relationships). In addition, acoustic telemetry data from multiple regions of the Columbia River estuary were used to assess the performance of the IBM. Wetland habitat quality, adapted from the Lower Columbia Estuary Partnership (LCEP) land cover dataset (Sanborn Map Company 2011) was used as a proxy for feeding success in the bioenergetics model. Fish were modeled using different swimming behaviors, and results from these simulations were then analyzed to describe travel times,

migration pathways, and growth. In addition, the effects of river and tidal forcing were considered.

The year of focus for this work was 2010. This year was selected because there was a large number of detections of juvenile Chinook salmon in the Columbia River estuary pair-trawl experiment in 2010 and because there were abundant JSATS data in the lower estuary. Flows in 2010 started below average but rose substantially by early June (Figure 2.2), with above-average flows for most of June. Major flows associated with the spring freshet were slightly delayed when compared to historical mean flows. Temperatures recorded at Bonneville Dam were relatively low at Bonneville during the spring season; however, by late summer, temperatures exceeded 20 °C.

The following sections describe the juvenile salmon data used to inform simulation design and to assess model performance, the hydrodynamic model used to generate the virtual environment, the framework and details of the IBM, and how model results were analyzed.

2.2.2 Juvenile Salmon Data

Every year, data are collected on the timing and survival of juvenile Chinook salmon as they pass through the hydropower system and Columbia River estuary. Passive integrated transponder (PIT) tags are implanted in a portion of juvenile salmonids to track migration timing and survival. As individual fish pass juvenile monitoring stations located at the dams, their tag code and the date and time of detection are recorded. The PIT tag data are then uploaded to the Columbia Basin PIT Tag Information System (PTAGIS, available at http://www.ptagis.org). The JSATS, developed by the Pacific Northwest National Laboratory and NOAA Fisheries for the U.S. Army Corps of Engineers, also monitors juvenile salmonid survival and travel times in the

Columbia River, lower estuary, and plume. The JSATS tags last for approximately 30 days, whereas the PIT tags last for years, remaining functional throughout the fish's lifespan. The detection range of 300 m in the JSATS system (McMichael et al. 2010) is greater than the detection range for PIT tags which typically must be within 10 – 100 cm of an antenna to be detected.

Downstream of Bonneville Dam, the last hydroelectric dam in the hydropower system, a pair-trawl is deployed from late March through early August in the lower estuary between Eagle Cliff (rkm 83) and Puget Island (rkm 61) (Figure 2.1). The pair-trawl study targets migrating juvenile Chinook salmon and steelhead, and data collected from this long-term study inform survival estimates of migrating juvenile salmonids and comparisons between in-river migrants and barged fish that are transported and released below Bonneville Dam (Ledgerwood et al. 2004). In 2010, there were more than 100,000 spring/summer (i.e. yearling) Chinook salmon and 28,698 fall (i.e. subyearling) Chinook salmon that were PIT-tagged and detected at Bonneville Dam. Of the Chinook salmon detected at Bonneville Dam, 3,632 spring/summer and 461 fall Chinook salmon were detected in the pair-trawl, representing detection rates of 3.6% and 1.6%.

As part of the 2010 JSATS study (Harnish et al. 2012), acoustic telemetry receivers were deployed in the navigation channel and off-channel areas from the estuary mouth to rkm 86 in depths of at least 4 m (Figure 2.1). Data were collected from these cross-channel arrays from late April to August and later analyzed to describe common migration pathways, travel times, and survival of migrating juvenile Chinook salmon and steelhead in the lower estuary. There were 3,880 yearling Chinook salmon and 4,449 subyearling Chinook salmon that were tagged and released in the 2010 JSATS study (Harnish et al. 2012). Subyearling Chinook salmon included in

the study were slightly larger than the general population, as only individuals greater than 95 mm in fork length were targeted (Harnish et al. 2012).

2.2.3 Hydrodynamic Model

Hindcast simulations using the unstructured grid, finite element model SELFE (Zhang and Baptista 2008) served as the virtual environment for the IBM. This 3-D hydrodynamic model has been benchmarked for the Columbia River estuary (Kärnä and Baptista 2016a; Kärnä et al. 2015), and data collected by numerous instruments throughout the estuary (Baptista et al. 2015) have been used to evaluate model skill. SELFE solves a set of nonlinear, baroclinic, shallow-water equations. The unstructured grid consists of triangular elements in the horizontal that extend in the vertical dimension to form 3-D prisms. The vertical grid in shallow regions is based on a hybrid terrain-following and free-surface adapted *S* grid (Song and Haidvogel 1994). Outside of the estuary, the surface grid transitions to an equipotential *z* grid starting at the 100 m isobath.

The model is driven by multiple forcings taken from larger-scale models. Atmospheric forcing is from the NOAA/NCEP North American Mesoscale Forecast System and includes wind velocities, shortwave and longwave radiation, air temperature, and pressure (Rogers et al. 2009). The tides come from a regional inverse model (Myers and Baptista 2001) and are applied along the ocean boundary. Temperature, salinity, and water elevations from the global Navy Coastal Ocean Model (NCOM) (Barron et al. 2006) are also imposed along the ocean boundary. Starting near the ocean boundary and extending approximately 50 km into the domain, temperature and salinity values computed by SELFE are nudged to NCOM values to prevent values from drifting significantly from NCOM. River discharge, elevations, and water

temperatures from USGS are used as riverine forcing from the Columbia and Willamette rivers, as well as smaller tributaries, the Lewis and Cowlitz rivers.

The horizontal mesh extends from northern California to Vancouver Island (39° N to 50° N) and from the Columbia River near Bonneville Dam (river kilometer 234) to 300 km offshore (Figure 2.1). There are 89,819 nodes, and 173,800 elements, and domain resolution is highest in the estuary, where resolution is typically between 100 - 200 m. The resolution becomes coarser past the estuary in the plume (200 – 1000 m) and is less resolved in the ocean (>1 km). The time step used in the circulation model is 36 seconds, and outputs are stored every fifteen minutes.

2.2.4 Individual-Based Model

Our IBM is described using the overview, design concepts, and details (ODD) protocol for IBMs outlined in Grimm et al. (2006). The purpose of the model as well as the structure and low-level entities are first described. This is followed by the design concepts that provide the framework for the IBM and the details that describe how the model is initialized, what inputs are used, and descriptions of the sub-models. A diagram of the model is shown in Figure 2.3.

2.2.4.1 Overview

2.2.4.1.1 Purpose

The purpose of the IBM is to investigate potential migration pathways and travel times of juvenile Chinook salmon in the Columbia River estuary. This was accomplished by simulating multiple swimming behaviors of varying complexity in addition to passive drift. Although there are long-term studies describing travel times to various reaches in the estuary, not enough is known about how environmental processes and swimming behavior influence estuarine residence and growth of juvenile Chinook salmon. The high spatiotemporal resolution of the

IBM provides an effective means for evaluating how environmental processes (e.g. river discharge and tides) and behavioral decisions affect migration pathways and residence times. Results from model simulations are compared against observational data on travel times and preferred estuarine migration pathways to evaluate the model's performance.

2.2.4.1.2 State Variables and Scales

The IBM is made up of multiple low-level entities that include environmental state variables and individual-based variables. The environmental state variables from the hydrodynamic model included water temperatures, 3-D flow velocities, and water depths. In addition, a habitat index that relates to the bioenergetics model was used. The temporal resolution of the environmental variables was fifteen minutes, with the exception of the habitat index that was constant over time. In some simulations, the estuary's hydrogeomorphic reach was considered, as well as geographic targets within these reaches that correspond with the downstream extent of that reach.

The variables describing individual fish included their initial location and size (defined by fork length and weight). Growth was simulated using a bioenergetics model, where growth rates were dependent on water temperatures, fish size, the proportion of maximum consumption (P-value), and prey energy density. Fish were initialized near Bonneville Dam and assigned a 3-D location and date of estuarine entry.

2.2.4.1.3 Process Overview and Scheduling

Simulations were conducted from March 13 to August 4 for yearling Chinook salmon and from April 25 to November 3 for subyearling Chinook salmon and correspond with statistics on run timing at Bonneville Dam. The last dates of initialization were July 5 for yearlings and

September 4 for subyearlings to ensure adequate time for individuals to exit the estuary. These dates and the number of individuals simulated over time were based on normal distributions of run timing data (see section 2.2.4.3.1.). Each model run commenced at 00:15 am (PST) on the first date of initialization. Environmental state variables were read in every fifteen minutes, and values at finer temporal resolutions corresponding with the IBM time step were linearly interpolated.

Movement due to advection, followed by movement due to active swimming, was calculated every 36 seconds, and the new location was stored every fifteen minutes. At the end of each fifteen-minute time step, individual growth was calculated using the bioenergetics model which factors in the temperature of the currently occupied position and the P-value assigned to the occupied element. Mortality, predation, and density-dependent interactions were not considered in the model. If all individuals exited the estuary prior to the end date of the simulation, the simulation ended early.

2.2.4.2 Design Concepts

2.2.4.2.1 Basic Principles

The IBM describes the migration of yearling and subyearling Chinook salmon through a heterogenous environment, where individuals go from narrow upstream reaches of the river to an increasingly tidally-influenced environment. As they move through this system, they can adopt a number of strategies that ultimately shape their migration pathways. Yearling Chinook salmon that are known to use the system as a migration corridor are more likely to occupy the main navigation channels, whereas subyearling Chinook salmon spend greater time in the estuary, particularly in shallow-water habitats. There are therefore two different strategies to explore

when it comes to simulating swimming behavior, one that optimizes efficient migration through the system, and one that optimizes growth in the estuary. The behavioral rules implemented for yearling Chinook salmon include directed migration optimizing timely estuarine exit, whereas the rules for subyearling Chinook salmon include reactive or directed movement to regions with high growth-rate potential.

Swim speeds are size-dependent (Ware 1978), and it is recognized that larger salmon migrate more quickly through estuaries (Dawley et al. 1986; Healey 1982). Therefore, it is necessary to track changes in fork length over time, as that affects travel times. The bioenergetics model computes growth over time based on the environmental conditions experienced, and as fish increase in length throughout the simulation, so too does their swim speed.

The bioenergetics model used a constant prey energy density and a P-value, the proportion of maximum daily consumption, that depended on habitat type. To factor differences in habitat quality into the bioenergetics model, P-values were based on the presence or proximity to wetland habitat. Elements classified as wetland habitat as well as the immediately neighboring elements had a P-value of 0.9, whereas outside of these regions, the P-value was 0.5. This allowed for a benefit to be factored in that considered preferred rearing habitats and relative feeding habits in these regions. This approach of classifying P-values based on habitat was similarly implemented in Brosnan (2014).

2.2.4.2.2 Sensing and Prediction

For simulated yearling Chinook salmon, under the more complex behavioral rules (e.g. negative rheotaxis and biased correlated random walk), individuals factored environmental states into their decisions. Under the negative rheotaxis behavior, fish oriented their movement to align

with the direction of prevailing flows, and could therefore sense their immediate flow environment. Under the biased correlated random walk behavior, fish movement was correlated with the movement calculated from the previous time step, and thus considered movement both due to advection and active swimming. In addition, the bias term directed fish to move downstream by orienting fish to move towards the downstream extent of each hydrogeomorphic reach. Thus, individuals simulated under this behavior had a predictive sense of what direction to swim in, based on the assumption that individuals optimize movement towards the ocean.

For simulated subyearling Chinook salmon, under the more complex behavioral rules (e.g. kinesis and restricted-area search), individuals sensed and/or predicted the growth rate potential of their environment. Individuals simulated using the kinesis behavior considered their immediate environment, and their swim speed and direction were based on the computed rate of consumption of the current position against an optimal rate of consumption. For individuals simulated using the restricted-area search behavior, they sensed their surrounding environment, and evaluated the growth rate potential of the immediately neighboring elements, where the average distance to neighbors was approximately 140 m. While the restricted-area search behavior accounted for both gains (i.e. consumption) and losses (e.g., respiration, egestion, and excretion) the kinesis behavior only considered gains.

2.2.4.2.3 Stochasticity

Simulations across the different behaviors were all started using the same random number seed. The random seed was used to initialize the starting location, initial lengths and weights, and date of entry for each of the different behaviors that were simulated. This means that all simulations started with the same initial conditions, but they varied in the swimming behavior

that was applied. Noise was also added to the model in the form of random noise that was added to individual swimming behavior.

2.2.4.2.4 Observation

After every fifteen-minute time step, the location and the length and weight of each fish were recorded. In addition, environmental variables were stored, including the temperature, water depth, and occupied element.

2.2.4.3 Details

2.2.4.3.1 Initialization

Individuals were initiated in the upstream region of the model domain near Bonneville Dam at 45°38’06’’N, 121°57’41’’W (Figure 2.1) using a normal distribution centered at this location with a standard deviation of 20 m in the horizontal. Vertical positions within the water column were initialized using a uniform distribution between 0 and 2 m below the surface. Initial fork lengths were based on daily fish condition fork length data collected at Bonneville Dam by the Fish Passage Center Smolt Monitoring Program. The fork length data for subyearling Chinook salmon showed an increasing trend over time. To reduce the bias of these longer fork lengths when creating the distribution of subyearling Chinook salmon starting lengths, only fork length data through the end of August were considered. The starting lengths were drawn from normal distributions for yearling Chinook salmon (μ = 142.5 mm, SD = 18.7 mm) and subyearling Chinook salmon (μ = 95.6 mm, SD = 13.3 mm). A truncated normal distribution with bounds at 61 mm and 140 mm was used for the subyearling Chinook salmon to prevent lengths at the tails of the distribution. This lower threshold also marks the difference between fingerlings and smaller emergent and resident frys.

Simulation timing was based on the smolt index at Bonneville Dam from the Fish Passage Center (Figure 2.4). The smolt index is based on PIT-tag detections at juvenile monitoring locations and factors in the flow magnitude to estimate the number of fish passing per day, as not all fish are detected at the monitoring locations. Passage dates for subyearling Chinook salmon prior to June were excluded when creating the run timing distribution as these detections are associated with juveniles from the previous year that were held over by hatcheries to be released as yearlings. In Figure 2.4, these larger individuals with earlier run timing are represented in the first two peaks.

Although it is recognized that the timing of detections for yearling and subyearling Chinook salmon do not follow normal distributions, this distribution was used to initialize times of simulated passage at Bonneville Dam in the IBM. Using the mean and standard deviation of run timing, normal distributions were generated for the yearling Chinook salmon simulation dates (μ = 133.5, SD = 13 days) and subyearling Chinook salmon simulation dates (μ=185.5, SD = 15 days) as indicated in Table 2.1. These distributions corresponded with initialization dates between March 13 – July 5 centered on May 13 for yearling Chinook salmon and April 25 – September 4 centered on July 4 for subyearling Chinook salmon. While individuals may be detected at Bonneville outside of these date ranges, these periods pertain to the period when most individuals migrate. The times of initialization were rounded to the nearest quarter hour to correspond with the fifteen-minute time step of the hydrodynamic model output.

2.2.4.3.2 Input

Environmental variables (e.g., water temperatures, velocities, water depths) from the hydrodynamic model were used as model inputs. Wetland habitat data from the 2010 High Resolution Land Cover Data from LCEP was used to generate P-values used in the bioenergetics

model, representing a proxy of habitat quality. This GIS dataset was first described in Simenstad et al. (2011) where it was applied to a particular hydrogeomorphic reach. The data include 26 different land cover classes, including tidal and non-tidal classes of coniferous, deciduous, shrub-scrub and herbaceous habitat as well as classes more representative of substrates or anthropogenic uses (e.g., agricultural, impervious surface, and developed). Juvenile salmon rely on food exported from emergent marsh habitat (Bottom et al. 2005), and macroinvertebrates associated with such habitats serve as a significant dietary source (Bottom et al. 2008). All wetland classes, with the exception of upland habitats were merged into one wetland class, and these data were then interpolated to the element centers.

2.2.4.3.3 Sub-models

2.2.4.3.3.1 Lagrangian Transport Sub-model

A Lagrangian method was used to simulate fish movement due to advection. The position at each time step was calculated from the previous time step according to:

$$x_{t+1} = x_t + u\delta t \quad (1)$$

$$y_{t+1} = y_t + v\delta t \quad (2)$$

$$z_{t+1} = z_t + w\delta t \quad (3)$$

Velocities due to advection (*u, v, w*) were computed from spatial and temporal interpolation of the flow fields, and the fish's location was updated using a Runge-Kutta fourth-order time integration method. Similar to the time step used in the hydrodynamic model, a 36-second time step was used for interpolation. This time step was preferred over the 15-minute time step of the hydrodynamic model output because it improved the particle tracking skill. In addition, it

reduced the frequency at which fish horizontally exit the domain or move to dry elements, which was a common occurrence, especially in narrower reaches of the river. If fish moved to a dry element or outside of the grid due to advection, the intersection between the individual's pathway and the intersected element edge was computed, and the tangential velocity was calculated to adjust the trajectory such that the individual maintained its position within the model domain.

2.2.4.3.3.2 Swimming Behavior Sub-model

Swimming behavior was simulated using different movement models that varied based on assumptions about how juvenile Chinook salmon use estuarine habitat. It was assumed that yearling Chinook salmon behaviors optimize efficient migration through the system, while subyearling Chinook salmon behaviors are more driven by the search for habitat where growth is optimized. The movement models varied in complexity from simple random walks to more sophisticated behaviors that depended on local environmental conditions. While predation is of concern in the system, field data were not available at a high enough spatial and temporal resolution to inform the model. In addition, not enough is known about juvenile salmon predator avoidance swimming behaviors in the estuary.

For both yearling and subyearling Chinook salmon, passive and random walk behaviors were simulated. Under the passive behavior, individual movement was driven by advection only and no active swimming was included. The simplest swimming behavior for both life-history types was an uncorrelated and unbiased random walk, where there was no behavioral response to external stimuli and the direction of movement was random (Codling et al. 2008; Willis 2011). This behavior was an effective null model allowing for comparisons against other swimming behaviors to assess whether or not more sophisticated models perform better than random

movement (Humston et al. 2004; Watkins and Rose 2013). Random swimming was simulated by drawing a random swimming angle in the horizontal plane from a von Mises distribution. This circular normal distribution depends on two parameters, μ and κ, where μ represents the mean direction and κ represents the concentration around this direction. To simulate uncorrelated and unbiased random movement, μ and κ were both set to zero. While fish move vertically based on flows, vertical swimming was not included in the random walk behavior or other movement models.

In addition to the uncorrelated and unbiased random walk, a biased correlated random walk (BCRW) was used for yearling Chinook salmon. It differed from the uncorrelated random walk because movement at each time step was correlated to the direction of movement in the previous time step, leading to a local directional bias (Codling et al. 2008). When correlation was high, an individual maintained its heading, whereas if correlation was near zero, pathways appeared random. Correlated random walks are a popular choice for movement models, as many animals tend to move forward in a persistent manner (Codling et al. 2008). In addition to the directional persistence term, this movement model included a directional bias such that movement was directed towards downstream locations. These downstream locations may not always be fixed, and instead can be adjusted based on an individual's location (Codling et al. 2004).

Movement in the BCRW was calculated from a weighted sum of a persistence term and a navigation term according to the following equations (Bailey et al. 2018; Benhamou and Bovet 1992):

$$\Delta x_{t+1} = x_t + \frac{BL_t}{10^3} \cdot \Delta t \cdot (w \cos(\Omega_T + \phi_n) + (1 - w) \cos(\theta_n + \delta_n)) \quad (4)$$

$$\Delta y_{t+1} = y_t + \frac{BL_t}{10^3} \cdot \Delta t \cdot (w \sin(\Omega_T + \phi_n) + (1 - w) \sin(\theta_n + \delta_n)) \quad (5)$$

where *x* and *y* are the locations, BL_t is the fork length (mm), *t* is time, *w* is a weighting term, Ω_T is the target direction, ϕ_n is the navigation error term, θ_n is the direction of movement in the previous step, and δ_n is a persistence error term.

Initial attempts to use the estuary mouth as a downstream target to orient fish towards when calculating the bias term were ineffective, especially in the upstream reaches of the system. Due to the sinuosity of the river as well as the system's geographic extent, multiple downstream locations were used to generate the bias term, and the specific location used was dependent on the occupied hydrogeomorphic reach (Simenstad et al. 2011). At each time step, the direction to orient for the bias term (i.e. angle between the current position and the reach's downstream location) was calculated. The persistence term was determined from the angle between the current position and the last position. The BCRW employed here therefore incorporates a rheotactic response, where the persistence term considers movement due to advection as well as powered swimming in addition to biased downstream movement. The weighting term (*w*) was set to 0.1 and was based on values used in Benhamou and Bovet (1992). The navigation error term and the persistence error term both used a von Mises distribution where κ, the measure of concentration around the angle of movement, equaled two.

The final movement model used for yearling Chinook salmon was a taxis behavioral response to ambient flow environments. This behavior was selected based on assumptions that yearlings time their migration to coincide with the spring freshet and typically spend less time in the estuary. Rheotaxis refers to a behavior where a fish aligns its swimming direction based on flows (Fraenkel and Gunn 1940), and this behavior has been suggested as a strategy used by

salmonids during their ocean migration (Booker et al. 2008; Burke et al. 2014; Mork et al. 2012; Royce et al. 1968) and return migrations (Hamilton and Mysak 1986; Healey et al. 2000). Negative rheotaxis has also been suggested as a behavioral response to changing light conditions that encourages downstream movement in smolts (Cooke et al. 2011).

Negative rheotaxis describes movement where fish orient themselves to swim in the direction of the prevailing current, and positive rheotaxis describes movement where fish orient themselves to move against the current. In this case, negative rheotaxis was simulated, such that yearling Chinook salmon optimized their movement to align with the currents. In upstream reaches of the system where river flows dominate, swimming directions were associated with riverine flows. In reaches where there is greater tidal forcing, movement was more closely tied to the phase of the tide as individuals swim in the same direction that they are displaced by advection. The angle of movement was computed from the horizontal velocity vectors at the currently occupied position with random noise added using a von Mises distribution where κ equals two.

For subyearling Chinook salmon, passive and random walk behaviors were simulated in addition to kinesis and restricted-area search swimming behaviors that depended on the expected consumption rate or growth rate. The growth rate depends on water temperatures and the P-value, where high values are associated with wetland habitat. The kinesis behavior entails movement that is responsive to ambient conditions but nondirectional, while the restricted-area search is more directional, with the individual assessing nearby habitat for optimal environmental conditions and moving there.

Kinesis behaviors result from an individual responding to environmental stimuli (e.g., temperature, salinity, flows) and either adjusting their speed (orthokinesis) or direction (klinokinesis) (Fraenkel and Gunn 1940). Kinesis behaviors are a popular choice in IBMs (see Fiechter et al. (2015b); Okunishi et al. (2012); Politikos et al. (2015); Rose et al. (2015); Watkins and Rose (2017)). Swimming velocities consist of an inertial component as well as a random component, defined as:

$$V_x(t) = f_x + g_x \tag{6}$$

$$V_y(t) = f_y + g_y \tag{7}$$

In this IBM, the inertial components (f_x and f_y) were calculated as:

$$f_x = V_x(t-1) \cdot H_1 \cdot I_H \tag{8}$$

$$f_y = V_y(t-1) \cdot H_1 \cdot I_H \tag{9}$$

The random components (g_x and g_y) were calculated as:

$$g_x(\theta) = \Phi \cdot \varepsilon(\theta) \cdot (1 - H_2 \cdot I_H) \tag{10}$$

$$g_y(\theta) = \Phi \cdot \varepsilon(\theta) \cdot (1 - H_2 \cdot I_H) \tag{11}$$

Variables in the above equations represent the following: $V_x(t-1)$ and $V_y(t-1)$ are the *x*- and *y*-velocities during the last time step, I_H represents an index of habitat quality, Φ is the maximum sustained swimming speed, and $\varepsilon(\theta)$ is a unit vector of a random angle generated using the von Mises distribution. H_1 and H_2 determine the height of the function, and values used in Humston et al. (2000) and Okunishi et al. (2012) were used ($H_1 = 0.75$, $H_2 = 0.9$). Whereas most other swimming behaviors used a standard swim speed based on the assumption of 1 BL s^{-1}, this

behavioral model had an evolving swim speed that depended on habitat quality. The maximum swimming speed used in this case was 4 BL s^{-1}. When the inertial component was dominant, the swimming velocities were reduced; however, when the random component was dominant, the swimming velocities were closer to the maximum swimming speed values.

The inertial and random component depended on the habitat quality (I_H) of the currently occupied element (Humston et al. 2004; Okunishi et al. 2012), which was calculated as the product of two terms:

$$I_H = I_T \cdot I_F \tag{12}$$

where I_T is a temperature dependence function used to calculate consumption in the bioenergetics model, and I_F is a metric representing prey availability. Since data on prey availability are limited for the entire estuary, I_F in this IBM was equal to the P-value of the occupied element that was based on the presence of wetland habitat. Both I_T and I_F had theoretical maximums of 1. When I_H was high, movement was dominated by the inertial component, and when I_H was low, movement was dominated by the random component.

The restricted-area search behavior was slightly more complex than the kinesis behavior and consisted of an individual assessing the growth rate potential of the currently occupied element and all neighboring elements and moving to the element with the highest value (Humston et al. 2004; Railsback et al. 1999; Watkins and Rose 2013). Other IBMs use metrics of habitat quality that are based on growth and mortality cues; however, this approach did not account for mortality. The growth rate potential for each element was calculated using the depth-averaged temperature at the element center. The direction of swimming was computed based on the angle between the fish's current position and the center of the neighboring element with the

highest growth rate potential. Stochastic noise was added using a von Mises distribution where κ equals two. Velocity was computed as:

$$V_x(t) = \frac{BL_i(t)}{10^3} \cdot \cos(\theta(t) + \varepsilon) \quad (13)$$

$$V_y(t) = \frac{BL_i(t)}{10^3} \cdot \sin(\theta(t) + \varepsilon) \quad (14)$$

where V is the velocity (m s^{-1}), BL is the body length (in mm) divided by 10^3 to convert to m, θ is the angle between the current position and destination element, and ε is stochastic noise.

For all movement models, if the trajectory computed by swimming resulted in the fish exiting the domain or getting stranded on land, the model continued to make attempts using different stochastic noise values until the trajectory resulted in the fish reaching a wet element. If fish movement resulted in vertical exit from the river, it was returned to the water surface (if exiting at surface) or to the bottom surface (if exiting at bottom). If an individual occupied an element that dried out at the next time step, it was nudged to the nearest wet element.

2.2.4.3.3.3 Growth Sub-model

The bioenergetics model relates the environmental conditions experienced during migration to individual growth, allowing for an assessment of how simulated behaviors and migration pathways influence size and condition. Growth in the IBM was simulated using the Wisconsin Bioenergetics model (Hanson 1997) with parameters for Chinook salmon defined in Table 2.2. Most of the original parameters described for adult Chinook salmon were used (Stewart and Ibarra 1991), with the exception of the temperature-dependent consumption parameters that were more recently defined for subyearling Chinook salmon (Plumb and Moffitt 2015).

Weight (W) was computed according to the following:

$$W_t = W_{t-1} + [C - (R + S + F + U)] \cdot \frac{e_p}{e_f} \cdot W_{t-1} \quad (15)$$

where C is consumption, R is respiration, S is specific dynamic action, F is egestion, and U is excretion, with C, F, and U in units of g prey g fish $^{-1}$ d^{-1}, and R in units of g O_2 g fish^{-1} d^{-1}. Variables e_p and e_f represent the prey energy density and the fish energy density. Each of these variables was computed from temperature- and mass-dependent functions. While reproduction is often included in this bioenergetics model, it was not considered in this application. The equations used in the Wisconsin Bioenergetics model were originally intended for a daily time step; however, growth in the IBM was computed every 15 minutes, thus the final growth term was divided by 96.

Consumption was calculated according to:

$$C = C_{max} \cdot p \cdot f(T) \quad (16)$$

$$C_{max} = a_c \cdot W^{b_c} \quad (17)$$

where C is the specific consumption rate (g g^{-1}d^{-1}), C_{max} is the maximum specific feeding rate (g g^{-1} d^{-1}), p is the proportion of maximum consumption, $f(T)$ is a temperature dependence function, T is water temperature (°C), W is fish mass (g), a_c is the intercept of the allometric mass function, and b_c is the slope of the allometric mass function. The temperature dependence function used in this application was equation 3, temperature dependence for cool- and cold-water species (Thornton and Lessem 1978). This function was also used in the kinesis model when calculating habitat quality.

Respiration, the energy used for routine metabolism, depends on the water temperature and the fish's size and activity. The total metabolism includes routine metabolism and digestion (i.e., specific dynamic action (SDA)). Energy lost to respiration was determined by multiplying the mass-dependent resting metabolism component by a temperature dependence function and activity component:

$$R = a_r \cdot W^{b_r} \cdot f(T) \cdot Activity \quad (18)$$

where R is respiration (g $g^{-1}d^{-1}$), a_r is the intercept of the allometric mass function, W is weight (g), b_r is the slope of the allometric function, $f(T)$ is a temperature dependence function, and *Activity* is an activity multiplier that depends on the swimming speed (cm $s^{-}1$) of the fish. The temperature dependence function used in the IBM was equation 1, exponential with swimming speed (Stewart et al. 1983). While the velocity used in the kinesis model was variable, an approach similar to that used in Humston et al. (2004) was used such that *vel* is set to 1 BL s^{-1}. Since the effect of swimming velocity on metabolism was less important than the effect of swimming behavior on simulated estuarine migration pathways and residence times, this helped to eliminate differences across the subyearling Chinook salmon movement models. SDA is equal to a proportion of energy consumed and was calculated according to:

$$S = SDA \cdot (C - F) \quad (19)$$

Egestion (F) and excretion (U) depend on mass, temperature, and ration (Elliott 1976) and were calculated as follows:

$$F = a_f \cdot T^{b_f} \cdot e^{(g_f \cdot p)} \cdot C \quad (20)$$

$$U = a_u \cdot T^{b_u} \cdot e^{(g_u \cdot p)} \cdot (C - F) \quad (21)$$

where a_f is the intercept of the proportion of consumed energy egested versus water temperature and ration, b_f is the coefficient of water temperature dependence of egestion, and g_f is the coefficient for feeding level dependence of egestion. Variables a_u, b_u, and g_u are similarly defined but for excretion.

Outputs from the bioenergetics equations were converted from units of g g^{-1} d^{-1} to units of J g^{-1} d^{-1} by multiplying consumption (*C*), egestion (*F*), and excretion (*U*) by the prey energy density. Prey energy densities were based on a common prey type of juvenile Chinook, chironomid pupae (Diptera), for which typical energy densities are 3400 J g^{-1} (Koehler et al. 2006). Respiration was also converted to units of (J $g^{-1}d^{-1}$) by applying the oxy-calorific coefficient (13,560 J g^{-1} O_2) to convert the oxygen consumed to energy consumed (Hanson 1997; Stewart et al. 1983). Once units were converted, growth in g d^{-1} was calculated by dividing by the fish energy density and multiplying by the mass of the fish. Energy density was calculated as:

$$e_f = \alpha + \beta \cdot W \tag{22}$$

where e_f is the fish energy density (J g^{-1}), α is the intercept of the allometric mass function, β is the slope of the allometric mass function, and W is the fish mass (g).

To obtain the weight of the fish at each time step, the computed growth was added to the weight at the previous time step. Depending on whether or not loss terms were greater than consumption terms, the fish either lost or gained weight. Data on subyearling and yearling Chinook salmon fork lengths from the lower estuary were used to generate a weight-length relationship equation, and this equation was then used to compute fork length from the new weight. Increases in length due to weight gain were calculated according to:

$$W = aL^b \tag{23}$$

where W is the mass of the fish (g), α is the intercept, L is the length (mm), and b is the slope. The slope and intercept were determined using observed length-weight data, and equation 23 was rearranged to solve for L:

$$L = \left(\frac{W}{e^{-12.27476}}\right)^{\frac{1}{3.18421}} \quad (24)$$

Although fish weight can fluctuate, their length cannot decrease as their weight decreases. Thus, a fish was only allowed to increase in length if it was greater or equal to the expected weight for a fish of its size. If the weight was greater or equal to this expected value, the fish increased in length; however, if the weight was less than this expected value, its length remained the same.

2.2.5 Analysis

To assess the skill of the passive particle tracking model, particles were simulated in a forward pattern during low and high flow periods for one, two, and three days. The tracks generated by the forward particle tracking were compared against backward tracks that were initialized from the final positions of the forward tracks. To evaluate skill, the distances between the starting positions from the forward tracking and final positions from the backward tracking were computed. The two periods simulated were a low flow period in April and a high flow period in June, corresponding with the freshet. Simulations were conducted for various lengths of time to explore how the simulation length and distances traveled impacted model skill.

Results from yearling and subyearling Chinook salmon simulations were analyzed by describing estuarine residence times, travel times to various locations throughout the estuary, and growth. Model results were compared against observed travel times from the pair trawl as well as travel times from JSATS data. The comparison between simulated migration timing and observed migration timing was done by comparing bulk statistics, and it should be noted that

direct comparisons between model results and observations were not achievable in this application. There were also temporal differences between the observations and the model results. The timing of the pair-trawl experiment (March 23 through August 4) differed from the timing of individual initializations at Bonneville for yearling Chinook salmon (March 13 – July 5) and subyearling Chinook salmon (April 25 – September 4), but despite this, all individuals were considered as there was not significant variability in travel times to Jones Beach over time. JSATS data collection did not commence until late April. Since the observed detections at the JSATS arrays occurred from April 29 – June 15 for yearling Chinook salmon and June 14 – August 5 for subyearling Chinook salmon, only simulated fish that were active in the estuary during these periods were considered in model-data comparisons with the JSATS data. Lastly, the subyearling Chinook salmon targeted in the JSATS study were larger than simulated subyearling Chinook salmon, but this size difference was not accounted for in the analysis.

In addition, results from simulations were analyzed by visualizing common migration pathways and comparing against migration pathways described in Harnish et al. (2012). The impacts of environmental conditions on potential estuarine migration pathways were explored by analyzing the estuarine residence times against river flows at initialization and the tides at the time of marine entry. The effects of swimming behaviors were explored with a greater emphasis on how behaviors of varying complexity influence migration patterns and travel rates and how they compare with observations and less on identifying the correct mechanisms that control behavioral decision-making. The IBM was intended to be used as an exploratory tool to assess the efficiency of behavioral mechanisms on simulating potential migration pathways of different life-history types. Comparisons of more sophisticated movement models against passive and random walk simulations made it possible to determine if simple swimming behaviors and/or

passive drift adequately simulated migration histories or if more complex behaviors were appropriate.

Data from the 2010 pair-trawl study as well as PIT-tag detections from Bonneville Dam were downloaded from PTAGIS. As there were often multiple detections of a single tag at one monitoring location, the last record was used, such that each tag only had one unique result at each location. Data from Bonneville Dam juvenile stations and the pair trawl (TWX) were joined using the tag code identification number, and the travel time to Jones Beach was computed by subtracting the time of detection at Bonneville from the time of detection by the pair trawl. Travel times to Jones Beach for simulated fish were determined by calculating the time at which individuals passed -123°16’ 50.541”, the approximate longitudinal location of Jones Beach (Figure 2.1).

JSATS data were downloaded from JSITE, and travel times between cross-channel arrays were computed for rkm 86-50, rkm 50-37, rkm 37-22, and rkm 22-8. At each upstream array, the time of last detection was computed for all individuals, and at each downstream array, the time of first detection was calculated. In instances where individuals were detected by both the navigation channel array and peripheral channel array in the same general longitudinal location (e.g., rkm 50, rkm 37, rkm, 22, rkm 8), individuals were assigned to the upstream array where the last detection occurred. When computing the time of first detection at the downstream array, it was therefore necessary to factor in the time of last detection at the upstream array to ensure that all travel times reflected downstream movement. Prior to this consideration, some of the travel times between downstream and upstream arrays were negative because the tides would transport fish near the estuary mouth back into the estuary and past the upstream array where it was already detected. Since a fish may have passed an upstream array multiple times due to the

tides, it was necessary to account for this pattern of movement when computing first and last detection times. In addition, the time of detection at the downstream array considered all detections for that unique rkm (e.g., rkm 50, 37, 22, and 8), and did not distinguish between the main or navigation channel. This method was implemented for both the JSATS data and simulated fish. For a more detailed description of how JSATS travel times and pathways were calculated, see Harnish et al. (2012).

2.3 Results

2.3.1 Particle Tracking Skill

Errors in particle tracking can potentially distort simulated migration pathways in significant ways. To assess tracking skill, we used a closure approach, where once a forward track was concluded, we backward track from the end position to reconstruct the starting position at the starting time. The distance between the original and reconstructed starting positions should be zero. The larger the distance is, the lesser the skill.

During low flow periods, the particle tracking skill was high, especially when only one or two days were simulated (Table 2.3). The mean skill was 0.16 ± 0.38 (0.39) m for the one-day and two-day low flow simulations. Model skill decreased as the simulation length increased, with the mean distance between the starting forward positions and final backward positions increasing to 153.29 ± 1,377.06 m. The particle tracking skill was also less during the high flow period, where error was several orders of magnitude greater than the error during low flow periods with mean values ranging from 1,122.28 m for the one-day simulation up to 11,367.60 m for the three-day simulation. Distances traveled were much greater during the high flow periods, and were often twice as much as the distances traveled during low flow periods, especially in the upper reaches of the river. With the increases in flows and distances traveled, the likelihood of

particles exiting the domain was higher during the high flow period, which could allow small errors in trajectories to be propagated over time when conducting backtracking. In addition, during the high flow period, there were more particles that entered the ocean, and backtracking from these initial positions could further introduce large errors, especially if the particles did not return to the estuary.

2.3.2 Travel Times, Residence, and Migration Pathways

2.3.2.1 Travel Times

Travel times were considered for multiple regions, including the upper estuary between Bonneville Dam and Jones Beach, the region sampled by the pair trawl. Travel times and migration pathways were also described for the lower estuary, between rkm 86, and various locations in the main channel and peripheral channels at rkm 50, 37, 22, and 8.

Travel times to the pair-trawl and between JSATS arrays were right-skewed and not normally distributed, so median values are described. In addition, means and standard deviations are reported in Table 2.4 for reference. The median travel time for yearling Chinook salmon observed in the pair-trawl experiment was 2.00 days (n = 3,632). Across all yearling Chinook salmon simulations, median travel times to Jones Beach ranged from 2.10 to 2.49 days (Table 2.4, Figure 2.5), with values of 2.40 days for the passive particle simulation, and 2.49 for the random walk simulation. The more complex yearling Chinook salmon behaviors, including negative rheotaxis and biased correlated random walk resulted in reduced median travel times of 2.17 and 2.10 days.

Median travel time from the pair trawl experiment for subyearling Chinook salmon detected from March 23 through August 4 was 2.07 days (n = 461). The simulated travel times to

Jones Beach for subyearling Chinook salmon were slightly longer than observed values and were fairly similar to those of yearling Chinook salmon (Table 2.4, Figure 2.5). Median travel times from the passive and random walk simulations were 2.23 and 2.27 days. Fish simulated using the kinesis behavior had a median travel time of 2.39 days. Travel times for the restricted-area search behavior were longer than the other movement model travel times, with a median value of 3.04 days. This behavior was also much more right-tailed than the others. While there was a discrepancy in the temporal overlap between observed and simulated data, overall, there was very little difference between the observed yearling Chinook salmon travel times and subyearling Chinook salmon travel times from the pair trawl. It's also important to note that the sample sizes between the two were not equivalent and that yearling Chinook salmon were the life-history type of interest during the pair-trawl experiments.

In general, the median travel times to Jones Beach from the IBM were consistently greater than median observed travel times to Jones Beach; however, this difference in travel times was on the scale of hours. For both the yearling and subyearling Chinook salmon passive simulations, travel times due to passive drift were fairly close to the median observed travel times. This suggests that passive drift alone could be largely responsible for travel times through upstream reaches of the system, and that swimming behavior, while important, may not be as important of a driver. However, it's also important to note that the passive behavior was not as right-skewed as the observations, suggesting that passive drift does not capture the variability in travel times that is more evident in the observations and active swimming behaviors.

Travel times for yearling and subyearling Chinook salmon from Harnish et al. (2012) as well as simulated travel times across behaviors are described for various segments of the lower estuary in Table 2.5 and shown in Figures 2.6 and 2.7, with the array locations shown in Figure

2.1. In general, travel times for simulated yearling and subyearling Chinook salmon were within several hours of the observed travel times. Most simulated travel times were several hours longer than the observed travel times, with the exception of the travel times between the navigation channel at rkm 50 to rkm 37 and the north channel near the Washington shoreline between rkm 22 and rkm 8. Travel times from Clifton Channel (CC50) to rkm 37 were much greater for simulated yearling and subyearling Chinook salmon, with the exception of the biased correlated random walk behavior.

The median observed travel times between the navigation channel at rkm 86 and rkm 50 for yearling and subyearling Chinook salmon were 12.4 and 12.2 hours. Simulated median travel times for yearling and subyearling Chinook salmon between these points ranged from 14.9 – 17.4 hours and 15.2 – 17.2 hours. Median observed travel times for yearling and subyearling Chinook from the navigation channel at rkm 50 to rkm 37 were 4.5 and 5.1 hours, while simulated median travel times ranged from 3.0 – 3.6 hours for yearling Chinook salmon and 3.3 – 7.9 hours for subyearling Chinook salmon. The travel times from Clifton Channel (CC 50) to rkm 37 were often twice as long for simulated Chinook salmon. In addition, the proportion of simulated fish detected in Clifton Channel was much less than the proportion of observed juvenile Chinook salmon detected in this peripheral channel.

From the navigation channel at rkm 37 to rkm 22, the median observed travel times for yearling and subyearling Chinook salmon were 11.9 hours and 12.7 hours. For the passive and random walk yearling behaviors, simulated travel times in this reach were nearly twice as long as observed values, while the travel times for the negative taxis and biased correlated random walk behaviors were approximately three hours longer. The simulated travel times for subyearling Chinook salmon were up to four hours longer in this reach, with the exception of the area search

behavior that was over twice the observed rate. From Cathlamet Bay at rkm 37 to rkm 22, observed travel times were 9.3 and 10.3 hours, and most simulated behaviors for yearling and subyearling Chinook salmon were approximately three hours longer, except the area search behavior.

Median travel times from the navigation channel from rkm 22 to rkm 8 were 2.8 and 4.0 hours for observed yearling Chinook salmon and subyearling Chinook salmon. The simulated travel times for the passive and random walk yearling Chinook salmon behaviors through this reach were several hours longer, while those of the negative taxis and biased correlated random walk behaviors were just over an hour longer. For simulated subyearling Chinook salmon in this reach, the median travel times for the passive, random walk, and area search behaviors were within minutes to an hour of the observed travel times, while the time of the kinesis behavior was over twice as long. The median travel times between rkm 22 along the Washington side (WA 22) to rkm 8 were 2.2 and 2.1 hours for observed yearling and subyearling Chinook salmon, and median simulated times ranged from 1.9 – 2.0 hours for yearling and subyearling Chinook salmon. Within this region, median simulated travel times were nearly identical to the median observed times, and there was very little variation across the behaviors, suggesting that behavioral effects in this region were minimal and that physical processes dominate.

In general, the travel times for simulated yearling Chinook salmon were consistently reduced for the negative rheotaxis and biased correlated random walk behaviors compared to the passive and random walk behaviors. In the rkm 50 to rkm 37 reach, the simulated travel times for both yearling and subyearling Chinook salmon were less than observed travel times. The behavior that stood out as the most variable from observations was the restricted-area search because of the longer travel times between arrays.

2.3.2.2 Estuarine Residence Times

Estuarine residence times for yearling Chinook salmon did not vary significantly across the different swimming behaviors (Table 2.4, Figure 2.8). In the passive particle simulation, the median time to estuarine exit was 5.11 days, and the median distance traveled per day was 55.87 km. The random walk behavior resulted in slightly longer estuarine residence times of 5.38 days and a slightly decreased rate of travel of 53.48 km d^{-1}. The median estuarine residence times of the negative rheotaxis and biased correlated random walk were slightly decreased at 4.92 and 4.78 days respectively, with median travel rates of 61.11 and 61.27 km d^{-1}. This difference in distances traveled between the passive and random walk simulations and the more sophisticated behaviors was due to the behavioral response of orienting movement based on the direction of prevailing currents and resulting directional biases.

Median estuarine residence times for simulated subyearling Chinook salmon were close to simulated yearling Chinook salmon estuarine residence times, and with the exception of the restricted-area search behavior, did not differ significantly across swimming behaviors (Table 2.4, Figure 2.8). Median estuarine residence times were 4.83 days for the passive behavior, 4.96 days for the random walk behavior, 5.24 days for the kinesis behavior, and 9.34 days for the restricted-area search behavior. The median distance traveled per day in the restricted-area search behavior (33.51 km d^{-1}) was significantly less than the distances traveled in the simpler behavioral models and kinesis model (54.86 – 58.83 km d^{-1}). While the medians were more appropriate to report as the data were not normally distributed, the variability in subyearling Chinook salmon estuarine residence times was especially evident when comparing the means and standard deviations. The restricted-area search behavior mean residence time and standard deviation were between 3-4 times greater than the other behaviors, with values of 22.51 ± 25.98

days. Longer estuarine residence times are typical for subyearling Chinook salmon, so longer estuarine residence times observed in the restricted-area search behavior suggest that swimming behavior can have an important influence on residence times.

Flow magnitude largely influenced simulated estuarine residence times for both yearling and subyearling Chinook salmon (Figure 2.9), and this was especially evident for the yearling Chinook salmon behaviors, passive particle simulations for both yearling and subyearling Chinook salmon, and the random walk and kinesis behaviors for subyearling Chinook salmon. For the restricted-area search behavior, estuarine residence times were mostly reduced when river discharge at the time of release was greater than ~8,000 m^3 s^{-1}, and when flows were less than this threshold, residence times were much longer. The phase of the tide also impacted the timing of marine entry, as most yearling and subyearling Chinook salmon exited the estuary during the ebb phase (Figure 2.10). For several of the behaviors (e.g., negative rheotaxis, and biased correlated random walk), this behavior was built in, as fish oriented their swimming direction to move in the direction of prevailing currents. However, even for behaviors where swimming was not based on the flow direction, most fish exited during the ebb phase. Since flow velocities in the lower estuary were high when both river discharge and tidal velocities directed flows seaward, fish movement would be largely driven by advection and behavioral effects would likely be insignificant.

2.3.2.3 Migration Pathways

Migration pathways were analyzed across simulated yearling and subyearling Chinook salmon behaviors by examining the common routes used, with a particular emphasis on the lower estuary. In general, yearling Chinook salmon migration pathways were concentrated in the navigation channel, before passing through the tidal flats into the north channel (Figure 2.11).

There was minimal transport into the lateral bays in the passive simulation, with the exception of Baker Bay. Migration pathways for the random walk simulation did not differ much from the passive particle pathways, although there were slightly greater concentrations in the lateral bays.

In the more complex yearling Chinook salmon behaviors, negative rheotaxis and the biased correlated random walk, individuals were concentrated in the navigation channel and the north channel. While patterns were fairly similar to those seen in the passive and random walk simulations, there was less concentration in the tidal flats and accumulation in Baker Bay, and greater presence in Cathlamet Bay. Lastly, most individuals near the estuary mouth traveled from the north channel as opposed to the navigation channel at rkm 22, suggesting that fish move from the navigation channel across the tidal flats to the north channel.

Migration pathways for the subyearling Chinook salmon passive and random walk behaviors showed similar patterns to the yearling Chinook salmon behaviors, with pathways concentrated in the navigation channel, across the tidal flats, and in the north channel (Figure 2.12). The kinesis behavior also showed concentrated migration pathways in these regions in addition to Cathlamet Bay. There were some regions in Youngs Bay and Cathlamet Bay where individuals simulated using the kinesis behavior accumulated, suggesting that flows in these regions were minimal, and the connectivity across wet elements was reduced.

Migration pathways for the restricted-area search behavior differed drastically from the other subyearling Chinook salmon behaviors. Since individuals were directed to regions with high growth rate potential, pathways for this behavior were predominantly in shallow regions of the lower estuary and the lateral bays in particular. These habitats were used more extensively than the navigation channel, which helps to explain the longer residence times using this

behavior as well as the minimal distances traveled on average, when compared to other subyearling Chinook salmon behaviors.

2.3.2.4 Growth

Daily growth was similar across the different yearling Chinook salmon swimming behaviors with median values of 0.20 mm d^{-1} (Table 2.4). While most individuals grew throughout the simulation, some simulated yearling Chinook salmon did not increase in fork length at all. Minimal differences in simulated growth rates across these behaviors were likely due to the similar temperatures experienced by migrating individuals, especially since most simulated yearling Chinook salmon remained in the main channel regions and had similar travel times through the lower estuary. Even though the estuarine residence times for some of the subyearling Chinook salmon behaviors (e.g., random walk, kinesis) were fairly similar to the yearling Chinook salmon estuarine residence times, daily growth was often greater, with median values ranging from 0.30 – 0.33 mm d^{-1} (Table 2.4). This was most likely due to differences in temperatures based on the timing of the simulations, where subyearling Chinook salmon experienced warmer temperatures throughout their migration.

The restricted-area search behavior simulated for subyearling Chinook salmon resulted in the highest median growth rate of 0.48 mm d^{-1}. Individuals simulated under the kinesis behavior had slightly greater growth rates than the random behavior; however, growth rates were still less than the area search behavior. Although both the kinesis and restricted-area search behavior were designed to optimize growth, the kinesis behavior was more reactive to environmental conditions experienced, while the restricted-area search behavior had a directional bias to move to regions with the highest growth rate potential. This directional bias resulted in greater time spent in optimal temperatures and habitats, resulting in greater growth.

2.4 Discussion

Results from the simulations indicate that estuarine residence times are strongly influenced by riverine flow. Previous work that quantified nursery habitat for the Columbia River estuary found river forcing to be a dominant driver, while the tides were a predominant force in lower reaches (Rostaminia 2017). Across all simulated behaviors for yearling and subyearling Chinook salmon, estuarine residence times were less when flows were greater (~> 8000 m^3/s). During periods of high discharge, estuarine residence times were mostly on the order of days. These results are consistent with those of Kärnä and Baptista (2016b), that show residence times being on the order of days in the system.

The different simulated yearling Chinook salmon behaviors did not show significant variability in travel times to Jones Beach or estuarine residence times. However, the more complex swimming behaviors that factored in directional and navigational biases and/or the direction of the prevailing currents resulted in reduced travel times and estuarine residence. This highlights the influence of swimming behavior for yearling Chinook salmon, in that some behaviors optimize movement to remain in the main channels and outside of peripheral channels. Evidence of simulated yearling Chinook salmon present in Cathlamet Bay across the movement models suggests that once juveniles enter the lower estuary, they are no longer confined to main channels and instead may move into lateral bays, both due to environmental forcing and swimming behavior. The presence of yearling Chinook salmon in Cathlamet Bay also suggests that they may utilize wetland habitats and may be directed to these regions both through advective processes and swimming behavior. This supports recent work that has challenged the existing paradigm that yearling Chinook salmon do not utilize wetland habitats.

Across the subyearling Chinook salmon swimming behaviors, there was little variability across the passive, random walk, and kinesis behaviors. However, the restricted-area search behavior differed significantly from those behaviors, leading to longer estuarine residence, increased growth, and decreased daily travel rates. The longer residence times, increased growth, and shorter distances traveled were likely associated with the occupation of peripheral habitats and lateral bays (e.g. Cathlamet Bay), where waters tend to be older (Kärnä and Baptista 2016b). By occupying waters where flows are reduced, individuals are less likely to be rapidly flushed, and thus their estuarine residence times may be extended. In addition, individuals were more likely to occupy shallower habitats where temperatures and the availability of food resources derived from wetland habitat were more optimal for growth.

Although the restricted-area search behavior was effective at directing individuals to productive shallow habitats, it often resulted in aggregation in regions of local optima. While this positively contributed to growth, once individuals occupied an area where potential growth rates were high, there was no incentive to search for new habitat. In most cases, flow velocities and randomness in the swimming behavior would limit long-term aggregation; however, in regions with frequent wetting and drying, where flows were minimal, fish could easily be artificially retained.

Previous attempts at developing a restricted-area search behavior used different criteria based on nursery habitat that was computed from depth, velocity, salinity, and temperature criteria, but these habitats were extremely patchy. Directing individuals to these regions without secondary cues resulted in minimal occupation of optimal habitats. Using a secondary cue of searching for shallow habitat was effective in directing individuals to regions with good nursery habitat, but frequently resulted in significant stranding because once fish encountered shallow

habitat, they tended to stay there. In these regions, water velocities were reduced, and therefore fish moved less due to advection. Their swimming behavior became more of a driving force. When the behavior directs individuals to local optima, there is nothing to prompt movement outside of the optima, especially if flows remain low. This was also an issue when using the growth-rate potential; however, there were a lot fewer fish that got stuck in extremely shallow habitats under this method. Additional behaviors were attempted to keep individuals from getting stuck, yet they remained ineffective in leading individuals to exit the estuary.

There are several large-scale drivers that influence migration behavior, including some genetic component that entices individuals to move. While individuals may spend various amounts of time in good habitat, eventually they will be prompted to exit the estuary. Although the restricted-area search behavior was effective at reproducing expected distributions of subyearling Chinook salmon in shallow habitats, it was not effective for simulating departure from these optimal habitats, and thus may be limited when simulating a migratory species that exits the system. Future attempts should consider using a size-dependent, time-dependent, or duration-dependent behavior within the restricted-area search behavior to avoid accumulation in certain regions. While it was expected that the kinesis simulations might increase the likelihood of fish encountering wetland habitat, the reduced residence times for this simulation suggest that was not the case.

With regards to observed estuarine residence times, there have not been many studies that have documented travel times between Bonneville Dam and the estuary mouth, as most studies have focused on particular reaches of the estuary (e.g., Bonneville Dam to Jones Beach). Carter et al. (2009) found that smolts pass through the estuary more quickly during periods of high discharge and later in the migration season and that yearling Chinook salmon migrate at rates of

~60 km/day between Vancouver, Washington and the estuary mouth. These results correspond with results for simulated yearling Chinook salmon, where individuals that migrate later and during periods of high discharge have shorter estuarine residence times, and average distances traveled are on the order of 55 – 65 km d^{-1}. McComas et al. (2008) found that acoustic-tagged subyearling Chinook salmon moved quickly through the system to the river mouth with a mean travel time of 4.1 days. This is fairly close to the estuarine residence times of the simpler simulated subyearling Chinook salmon behaviors (e.g., passive, random walk, and kinesis).

When comparing the observed travel times against simulated travel times to Jones Beach, there was fairly close agreement between observed and modeled values for the yearling Chinook salmon, especially in the negative rheotaxis and biased correlated random walk. Although the sample size for subyearling Chinook salmon in the pair trawl was small, there was also fairly close agreement between observed values and simulated values for the passive, random walk, and kinesis behaviors. In addition, the simulated travel times were within range of observed travel times described from the JSATS data, and the preferred migration pathways from simulations (i.e., greater occupation of navigation channel and WA 22) were also seen in the observations. Although direct comparisons with observed data were not possible in this application, the proximity of simulated travel times against observed travel times is a promising result and suggests that an IBM can be an effective tool for exploring migratory behavior of juvenile Chinook salmon in an estuarine environment.

Simulated growth rates in the IBM for subyearling Chinook salmon were within the range of growth rates reported from field observations, while those for yearling Chinook salmon were typically less than observed rates. Rich (1920) estimated growth rates of 0.44 mm d^{-1} from rkm 261 to the river mouth, while other studies have identified growth rates of 0.25 and 0.31 mm

d^{-1} (McCabe et al. 1986; Roegner et al. 2012). Campbell (2010) studied otolith-derived growth estimates and determined mean daily growth rates of 0.41 mm d^{-1} for juvenile salmon in saline portions of the estuary. McNatt et al. (2016) documented mean growth rates of 0.49 – 0.58 mm d^{-1} for juveniles residing in wetlands, with length increases by as much as 10 – 20 mm for juveniles remaining in wetland areas longer than 15 days. Additional growth rates estimated from otolith analysis were on average 0.5 mm d^{-1} (Bottom et al. 2008). While it may be challenging to validate growth rates from the IBM, the growth rates were within the range of observed values, which lends support to the IBM being an effective tool for exploring how the estuary supports growth of juvenile Chinook salmon during their migration.

2.4.1 Limitations

IBMs have become an increasingly popular approach for simulating animal behavior and for exploring ecological questions. They offer a means by which we can test hypotheses and investigate how environmental processes and individual behavior influence population-level dynamics. Despite advances in modeling techniques and computing power, IBMs continue to be limited. Since modeling relies on assumptions and simplification of behaviors, IBMs should not be expected to exactly mimic nature; however, they can be effective in answering questions that might be difficult to investigate using observations or Eulerian modeling techniques. This paper highlights the functionality of an IBM to investigate estuarine migration patterns of juvenile Chinook salmon, but it is important to note the limitations of our model and IBMs in general.

As juvenile Chinook salmon migrate from freshwater to brackish and increasingly marine waters, their behavior changes in response to ambient conditions. While the IBM effectively approximates movement, it is not a realistic representation of actual swimming behaviors through an evolving environment. The IBM is certainly an improvement from Eulerian-based

methods that quantify salmon habitat for juvenile Chinook salmon, but there are still limits on its utility. Furthermore, juvenile Chinook salmon likely employ multiple strategies as they migrate through the system and rely on multiple cues simultaneously when making movement decisions. Their needs change over time, and they switch modes multiple times during their migration, from focusing on downstream movement to feeding and predator avoidance. In addition, there are larger-scale processes that influence their behavior, as well as their genetically-driven urge to migrate to the ocean. These environmental and behavioral drivers are constantly at play in different degrees. Since models are designed to simplify behavior to help us understand some of these dynamics, they will never accurately capture all of the more complex processes at play.

While including the bioenergetics model was a necessary component, especially as it influenced the swim speeds, there were limitations in how it was implemented. All of the standard equations used in the model worked well; however, the way in which prey energy density was approximated was overly simple. A constant prey energy density was used, and the P-value, which controls the amount of energy was based on proximity to wetland habitat. These methods of oversimplifying the bioenergetics model were somewhat necessary, as high-resolution data on salmon prey in the Columbia River estuary are limited. However, this oversimplification likely influenced results for individual growth and may explain why yearling Chinook salmon growth showed such little variation and why the restricted-area search behavior led to such high growth rates.

Although simulated behaviors produced results that were within the range of observed travel times, model results should be interpreted with caution because predator avoidance was not considered as a behavioral response, and the cumulative effects of predation on migration patterns were not represented. Predation and mortality were not included in this version of the

model due to the lack of high-resolution spatial and temporal observations on these top-down drivers. In addition, not enough is known about how juvenile Chinook salmon swimming behavior is influenced by predator avoidance, particularly in a system where flow velocities are so high. Even though information may be lacking, we acknowledge that predator avoidance could play a role in residence times and preferred migration pathways.

The hydrodynamic model used as the virtual environment for the IBM had some limitations, including the lack of freshwater flows imposed in the model that limited circulation in the smaller tributaries in the lateral bays. This led to the accumulation of passive particles or simulated fish in the shallowest upstream reaches of these tributaries. Kärnä and Baptista (2016b) mention that hydrodynamic model results in the lateral bays may not be reliable due to the lack of freshwater input and because of issues with the wetting-drying method, which is consistent with issues encountered in this work. In addition, most of the model skill validation for the circulation model focused on the main channels or deeper locations in the lateral bays. Thus, it is difficult to assess the skill of the circulation model in shallow regions. Lastly, the resolution of the bathymetry and size of the grid in shallow regions was limited, which affected migration pathways in shallow regions.

With regards to model-data comparisons, the pair-trawl and JSATS data were very valuable; however, the fish targeted in these studies were often not representative of the full diversity of sizes and life histories present in the estuary. Instead, they primarily targeted larger juveniles that remained in the main channels. In general, acoustic telemetry studies are rare in shallow habitats; however, there are some exceptions (Johnson et al. 2015; McNatt et al. 2016). Data describing travel times are likely inappropriate to apply to smaller subyearling Chinook salmon as they have longer residence times and are less likely to be tagged (see Bottom et al.

2005). Similarly, many of these tagging studies target fish from hatcheries and thus are not necessarily representative of behaviors associated with wild-type Chinook salmon.

2.5 Conclusions

An IBM was developed to explore estuarine migration pathways, residence times, and growth of juvenile Chinook salmon migrating through the Columbia River estuary. Multiple behaviors were implemented, ranging from random behaviors to more sophisticated behaviors that either optimized efficient migration through the system or opportunities for growth. Simulated behaviors for juvenile yearling Chinook salmon that optimized rapid migration outperformed the passive drift and random walk simulation due to reduced residence times. Similarly, the behaviors implemented for subyearling Chinook salmon that optimized increased growth resulted in higher growth rates when compared to the random walk behavior. In most simulations, residence times were on the order of days. River discharge had a strong influence on residence times, and during periods of high discharge, residence times were reduced.

While the model does have many limitations in its current implementation, it was effective for investigating how juvenile Chinook salmon respond to environmental forcing and behavioral controls. River discharge was a strong driver of residence times; however, active swimming and behavioral decisions made by individuals were also important in driving potential migratory pathways. The availability of PIT tag and JSATS tag data allowed for an in-depth model-data comparison. Consistent patterns in migration pathways and travel times between the simulated individuals and observed individuals suggest that this IBM could be used to inform management decisions by evaluating various scenarios.

Tables

Table 2.1. Run timing distributions for yearling and subyearling Chinook salmon, as well as the dates the runs commenced and ended, and the starting lengths.

Life-History Type	Run Timing	Start Date	End Date	Starting Length
Yearling	133.5 ± 13 days	March 13	August 4	142.5 ± 18.7 mm
Subyearling	185.5 ± 15 days	April 25	November 3	95.6 ± 13.3 mm

Table 2.2. Parameters, descriptions, and values used in bioenergetics sub-model based on the Wisconsin bioenergetics model. Adult parameters were used, with the exception of juvenile parameters (*) used to calculate consumption.

Parameter	Description	Value	Reference
W	Fish mass (g)	-	-
α	Allometric mass function intercept	5764.0	1
β	Allometric mass function slope	0.5266	1
	Consumption		
a_c	Allometric mass function intercept	0.303	1
b_c	Allometric mass function slope	-0.275	1
CQ	Lower temperature (°C) for C_{max}	4.97*	2
CTO	Optimum temperature (°C) for C_{max}	20.93*	2
CTM	Maximum temperature (°C) for C_{max}	20.93*	2
CTL	Upper temperature (°C) for C_{max}	24.05*	2
CK_1	Proportion of C_{max} at CQ	0.09*	2
CK_4	Proportion of C_{max} at CTL	0.53*	2
	Respiration		
a_r	Allometric mass function intercept	0.00264	1
b_r	Allometric mass function slope	-0.217	1
RQ	Approximates Q_{10}	0.06818	1
RTO	Coefficient of swimming speed	0.0234	1
SDA	Specific dynamic action	0.172	1
	Egestion (F) and Excretion (U)		
a_f	Intercept of the proportion of consumed energy egested versus water temperature and ration	0.212	1
b_f	Coefficient of water temperature dependence of egestion	-0.222	1
g_f	Coefficient for feeding level dependence (P-value) of egestion	0.631	1
a_u	Intercept of the proportion of consumed energy excreted versus water temperature and ration	0.0314	1
b_u	Coefficient of water temperature dependence of excretion	0.58	1
g_u	Coefficient for feeding level dependence (P-value) of excretion	-0.299	1

[1]Stewart and Ibarra (1991)
[2]Plumb and Moffitt (2015)

Table 2.3. Mean and standard deviation of passive particle tracking skill and mean distances traveled during low and high flow periods.

Metric	Flows	Simulation Length		
		1 day	2 days	3 days
Model skill (m)	Low	0.16 ± 0.38	0.16 ± 0.39	153.29 ±1377.06
	High	1,122.28 ± 1455.12	9,045.68 ± 8542.73	11,367.60 ± 19,003.91
Mean distance traveled (km)	Low	54.4	96.0	142.4
	High	104.6	191.8	239.0

Table 2.4. Results of model simulations for yearling and subyearling Chinook salmon swimming behaviors, including the mean (μ), standard deviation (σ), and median ($\tilde{x}$) values for various run metrics. Values reported include the travel time to Jones Beach (days), estuarine residence time (days), the daily distance traveled (km d^{-1}), and the daily growth (mm d^{-1}) for all individuals that successfully exited the estuary.

	Travel time to Jones Beach (days)		Estuarine Residence Time (days)		Daily Distance Traveled (km d^{-1})		Daily Growth (mm d^{-1})	
Yearling	μ ± σ	$\tilde{x}$	μ ± σ	$\tilde{x}$	μ ± σ	$\tilde{x}$	μ ± σ	$\tilde{x}$
Passive	2.37 ± 0.53	2.40	5.37 ± 1.95	5.11	56.08 ± 9.26	55.87	-	-
Random walk	2.54 ± 1.34	2.49	5.80 ± 2.78	5.38	53.54 ± 9.83	53.48	0.19 ± 0.07	0.20
Taxis	2.21 ± 1.18	2.17	5.18 ± 1.93	4.92	61.19 ± 9.97	61.11	0.19 ± 0.07	0.20
BCRW	2.12 ± 0.92	2.10	5.09 ± 2.02	4.78	61.24 ± 10.37	61.27	0.19 ± 0.07	0.20
Subyearling								
Passive	2.26 ± 1.80	2.23	5.56 ± 6.30	4.83	59.53 ± 12.48	58.83	-	-
Random walk	2.33 ± 1.13	2.27	5.90 ± 7.11	4.96	58.12 ± 13.30	57.08	0.30 ± 0.06	0.30
Kinesis	2.48 ± 1.05	2.39	6.65 ± 8.55	5.24	55.12 ± 13.52	54.86	0.33 ± 0.07	0.33
Area Search	7.35 ± 15.49	3.04	22.51 ± 25.98	9.34	32.33 ± 17.95	33.51	0.52 ± 0.14	0.48

Table 2.5. Median travel times (hours) in the lower estuary between cross-channel JSATS arrays located in main and peripheral channels. Main channels are denoted with the Nav prefix, and peripheral channels are denoted with acronyms CC (Clifton Channel), CB (Cathlamet Bay) and WA (Washington shoreline).

	Nav86 to rkm50	Nav50 to rkm37	CC50 to rkm37	Nav 37 to rkm 22	CB37 to rkm 22	Nav 22 to rkm 8	WA 22 to rkm 8
	Yearling Chinook Salmon						
Literature[1]	12.4	4.5	12.1	11.9	9.3	2.8	2.2
Observed[2]	12.5	4.5	12.1	11.9	9.3	2.8	2.2
Passive	16.2	3.5	24.3	21.3	12.7	6.4	2.0
RW	17.4	3.6	26.9	21.9	13.4	7.0	2.0
Taxis	14.9	3.0	25.0	15.0	12.4	3.9	2.0
BCRW	14.9	3.0	16.2	14.7	12.6	3.7	1.9
	Subyearling Chinook Salmon						
Literature[1]	-	5.1	11.9	12.7	10.3	4.0	2.1
Observed[2]	12.2	5.1	11.9	12.7	10.3	4.0	2.1
Passive	15.2	3.3	-	16.9	13.2	3.6	1.9
RW	15.4	3.4	29.4	17.0	13.3	4.4	1.9
Kinesis	15.8	3.6	28.4	16.9	13.5	9.4	2.0
Area search	17.2	7.9	27.6	26.1	22.8	4.9	2.0

[1] Values reported in (Harnish et al. 2012) study.

[2] Observed values are calculated from JSATS data downloaded from JSITE. These same values are portrayed in Figures 2.6 and 2.7

Figures

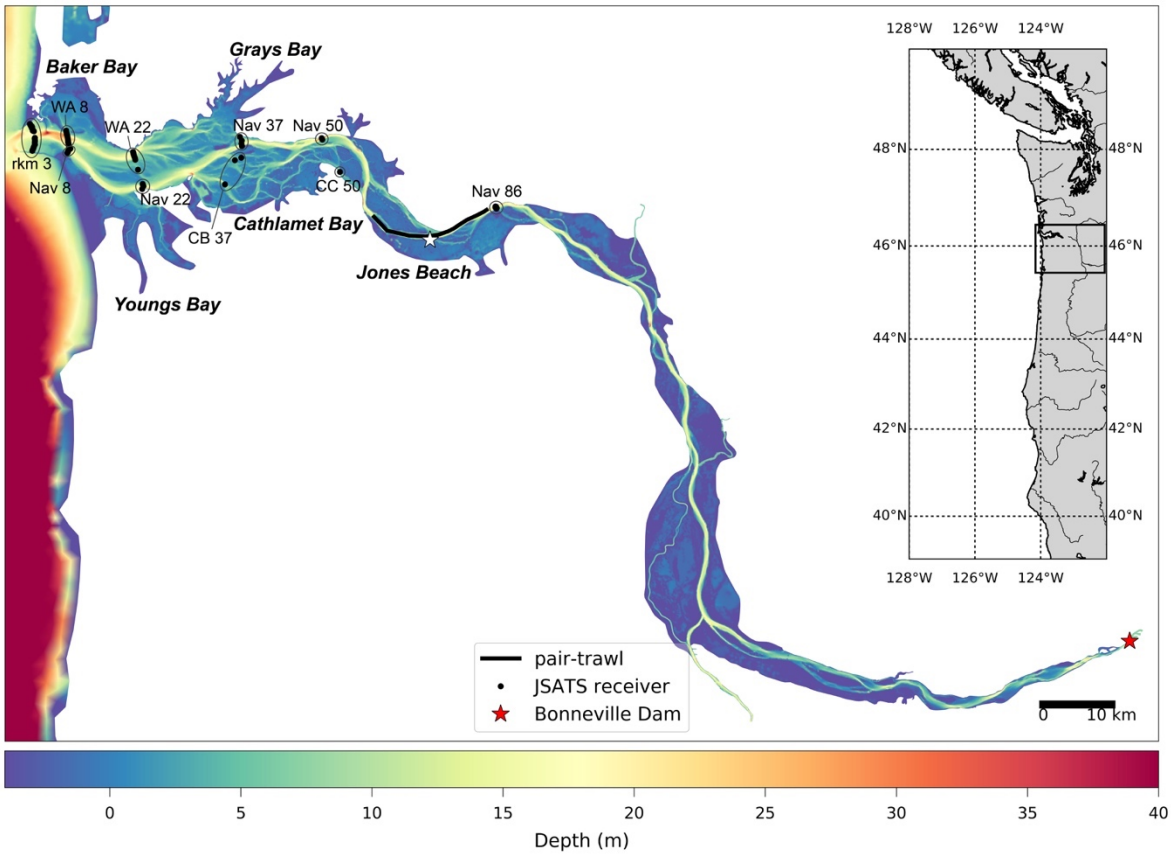

Figure 2.1. Map of the simulated virtual environment. The inset represents the entire region simulated in the hydrodynamic model, with the outlined region representing the Columbia River estuary. The bathymetry of the estuary is represented as well as locations of specific interest, including Bonneville Dam, where fish were initialized, the region sampled by the pair-trawl near Jones Beach, the lateral bays, and the locations of JSATS nodes that constitute cross-channel arrays in the lower estuary. Array locations with the Nav prefix are located in the navigation channel, while those with different prefixes are located in peripheral or secondary channels (e.g., CC = Clifton Channel, CB = Cathlamet Bay, WA = Washington shoreline).

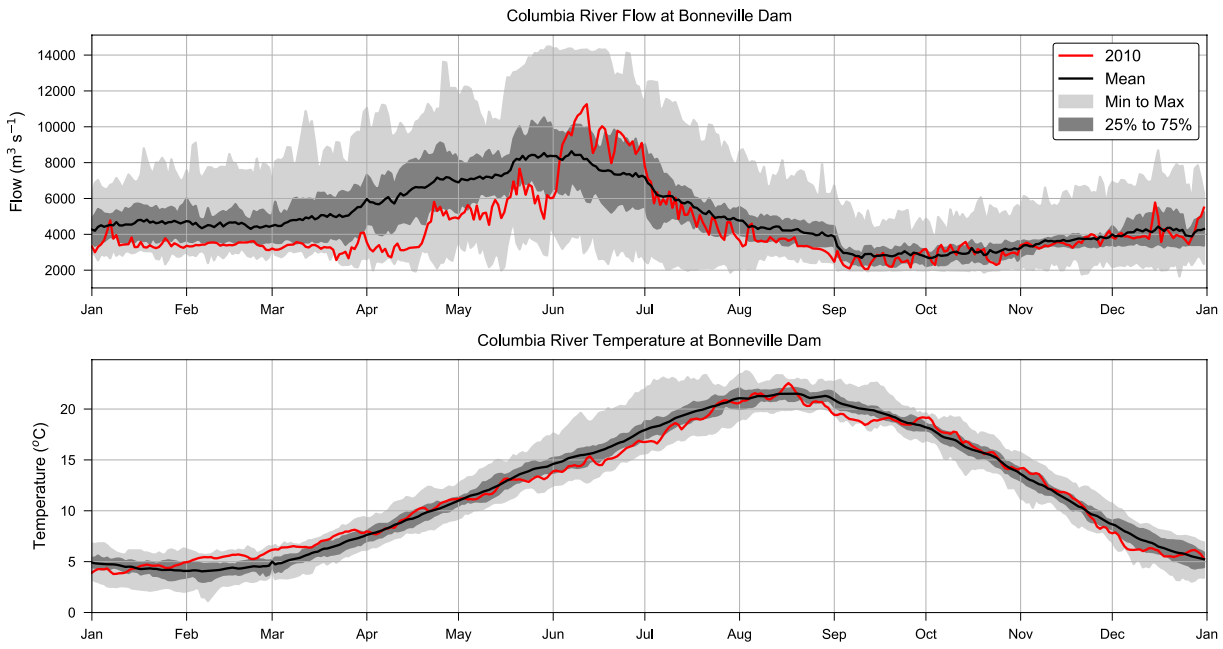

Figure 2.2. Daily Columbia River flows ($m^3 s^{-1}$) (*top*) and daily temperatures (°C) (*bottom*) at Bonneville Dam in 2010 (red), in addition to mean, 25% - 75% percentiles, and minimum and maximum values from 1999 - 2016.

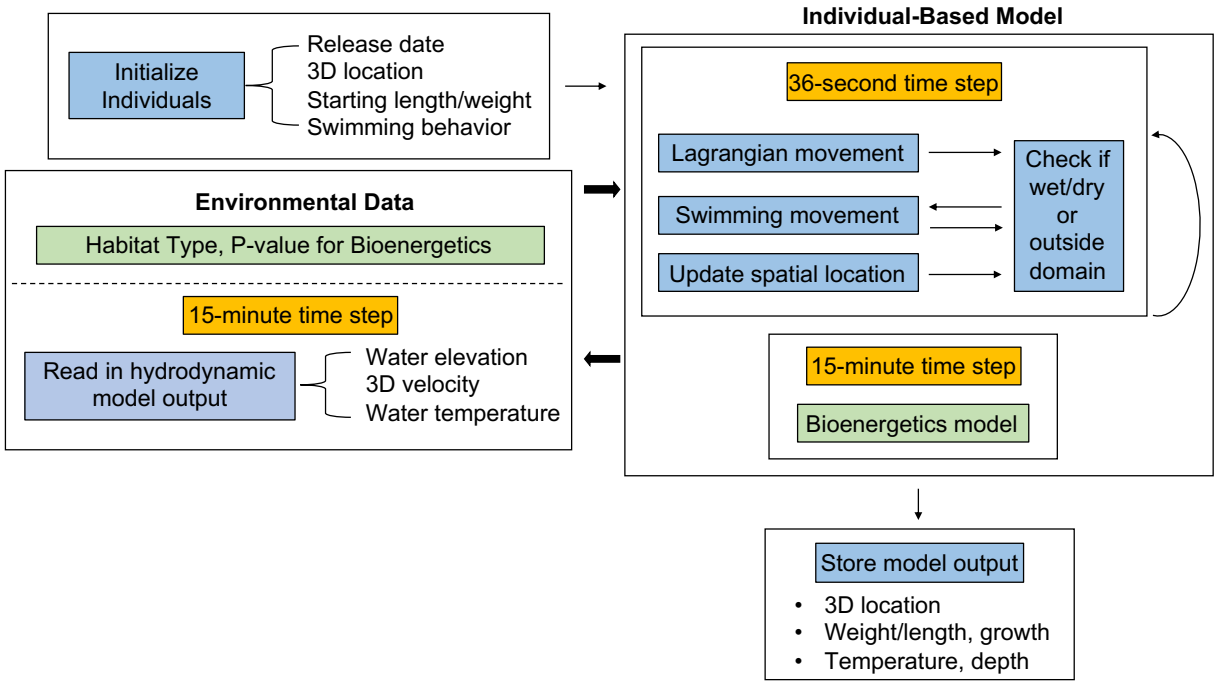

Figure 2.3. Conceptual diagram of the IBM. Individuals are initialized and environmental data are read in, including global variables relating to the bioenergetics model and output from a hydrodynamic model with a 15-minute time step. At every 15-minute time step, individual movement is simulated using a 36-second time step and loops through until the end of that period. Following that, growth is computed using the bioenergetics model, and output is stored for that time step before proceeding to the next time step.

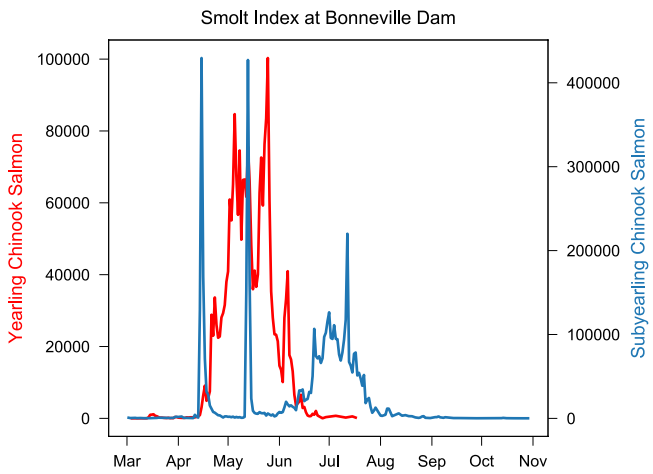

Figure 2.4. Smolt index (fish day^{-1}) for yearling Chinook salmon and subyearling Chinook salmon at Bonneville Dam in 2010.

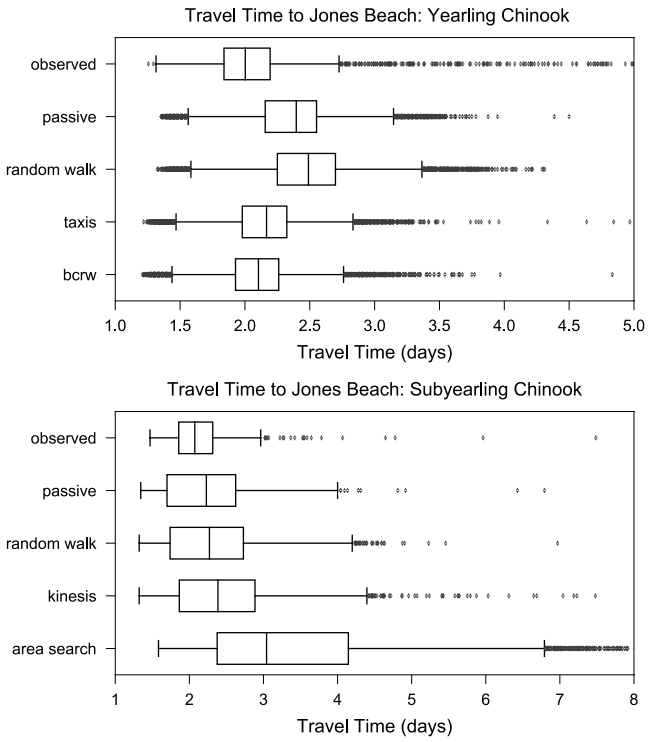

Figure 2.5. Yearling Chinook salmon (*top*) and subyearling Chinook salmon (*bottom*) travel times to Jones Beach, including observations from the pair-trawl experiment and simulated fish employing different movement models.

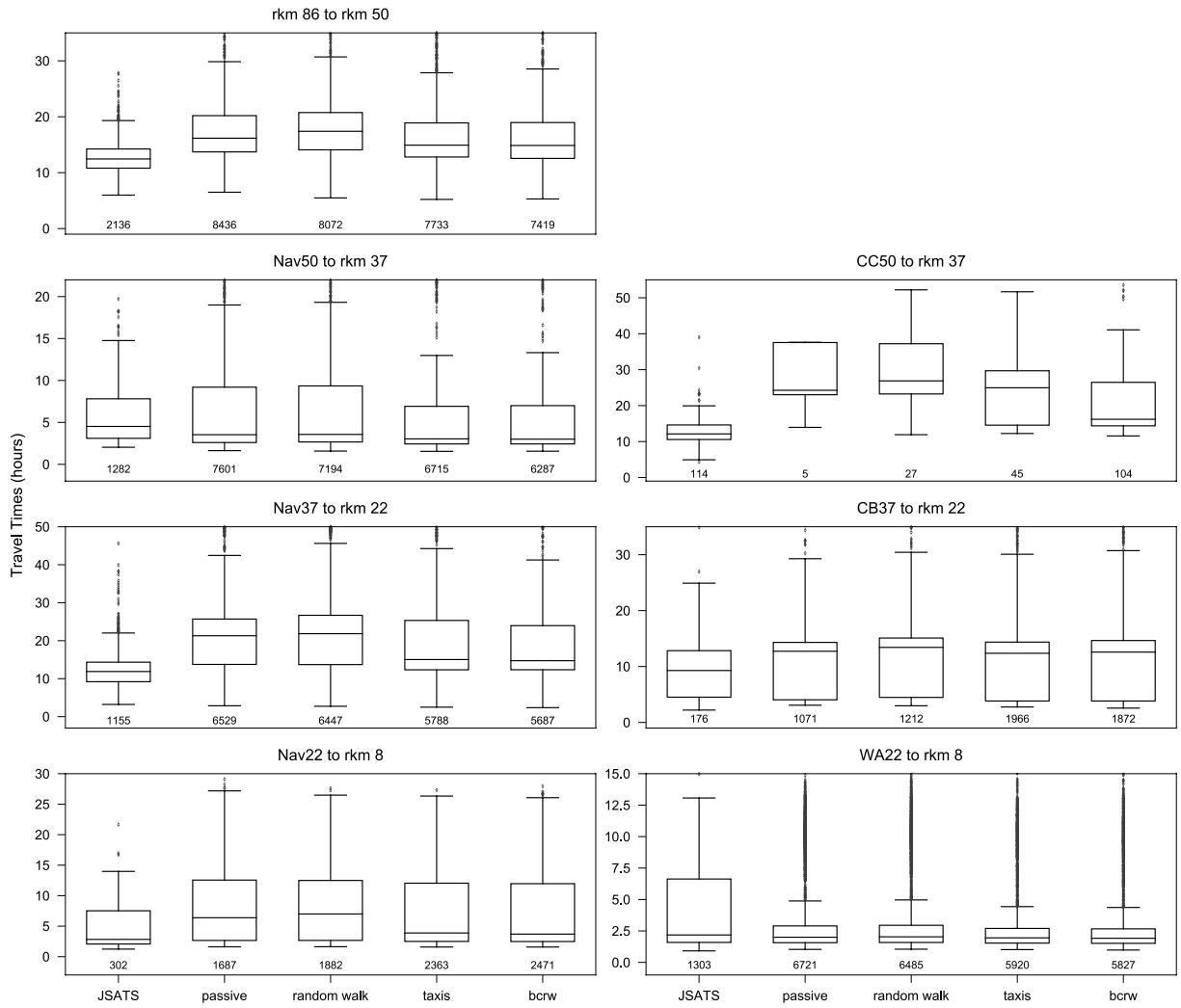

Figure 2.6. Yearling Chinook salmon travel times (hours) between the JSATS arrays for observed and simulated fish. Only simulated fish detected from April 29 – June 15, 2010 are represented to correspond with observed dates. The number of individuals described is indicated in the boxplots.

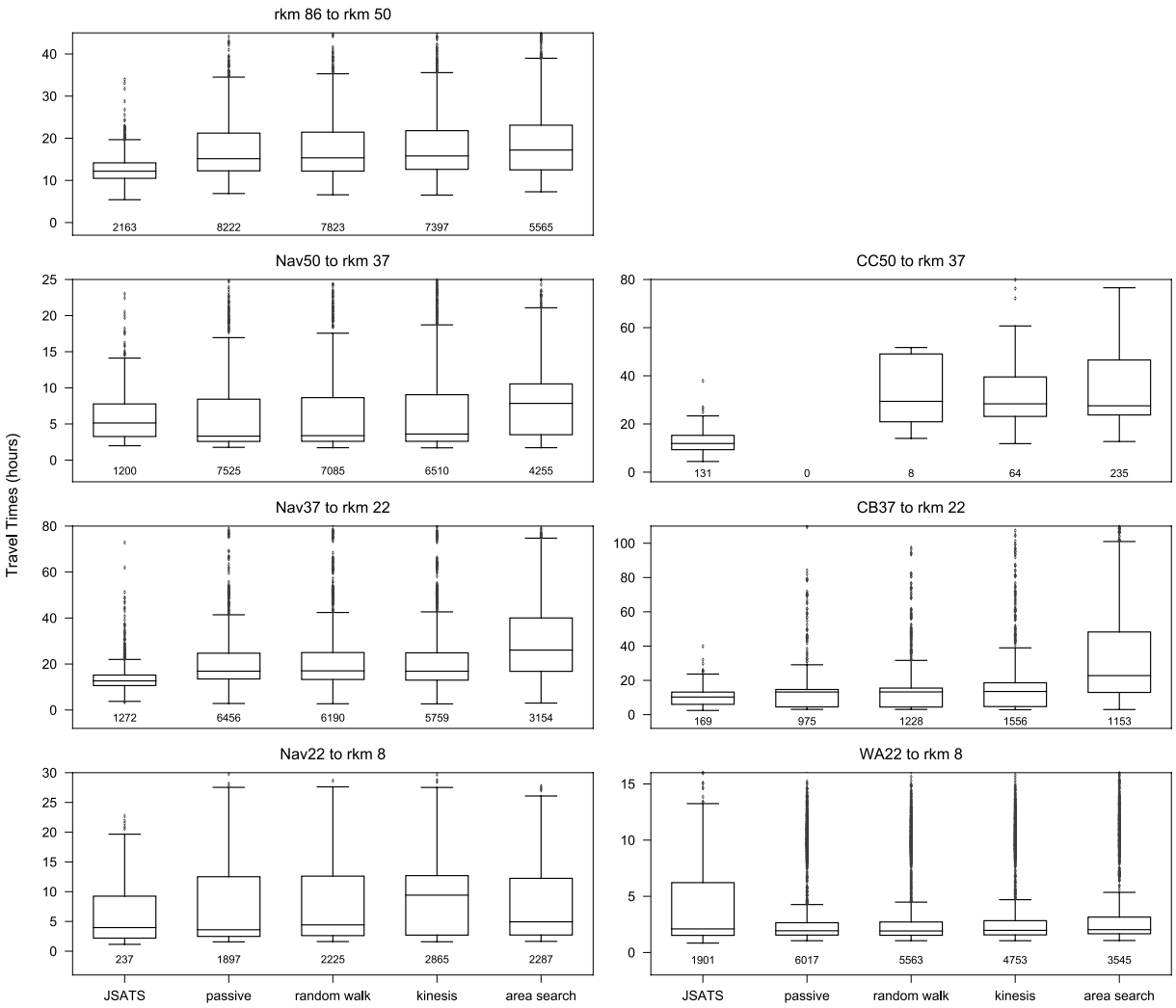

Figure 2.7. Subyearling Chinook salmon travel times (hours) between the JSATS arrays for observed and modeled fish. Only simulated fish detected from June 14 – August 5, 2010 are represented to correspond with observed dates. The number of individuals described is indicated in the boxplots.

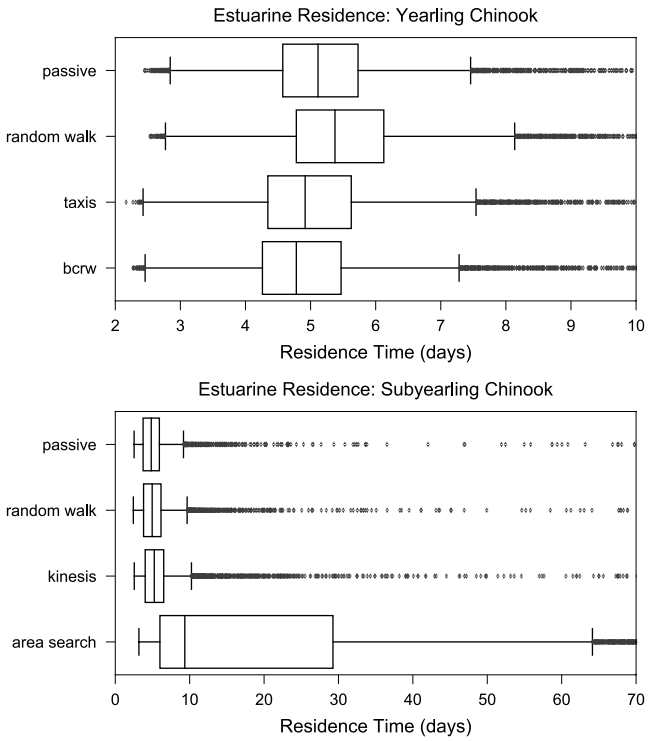

Figure 2.8. Yearling Chinook salmon (*top*) and subyearling Chinook salmon (*bottom*) estuarine residence times (days) for all simulated behaviors.

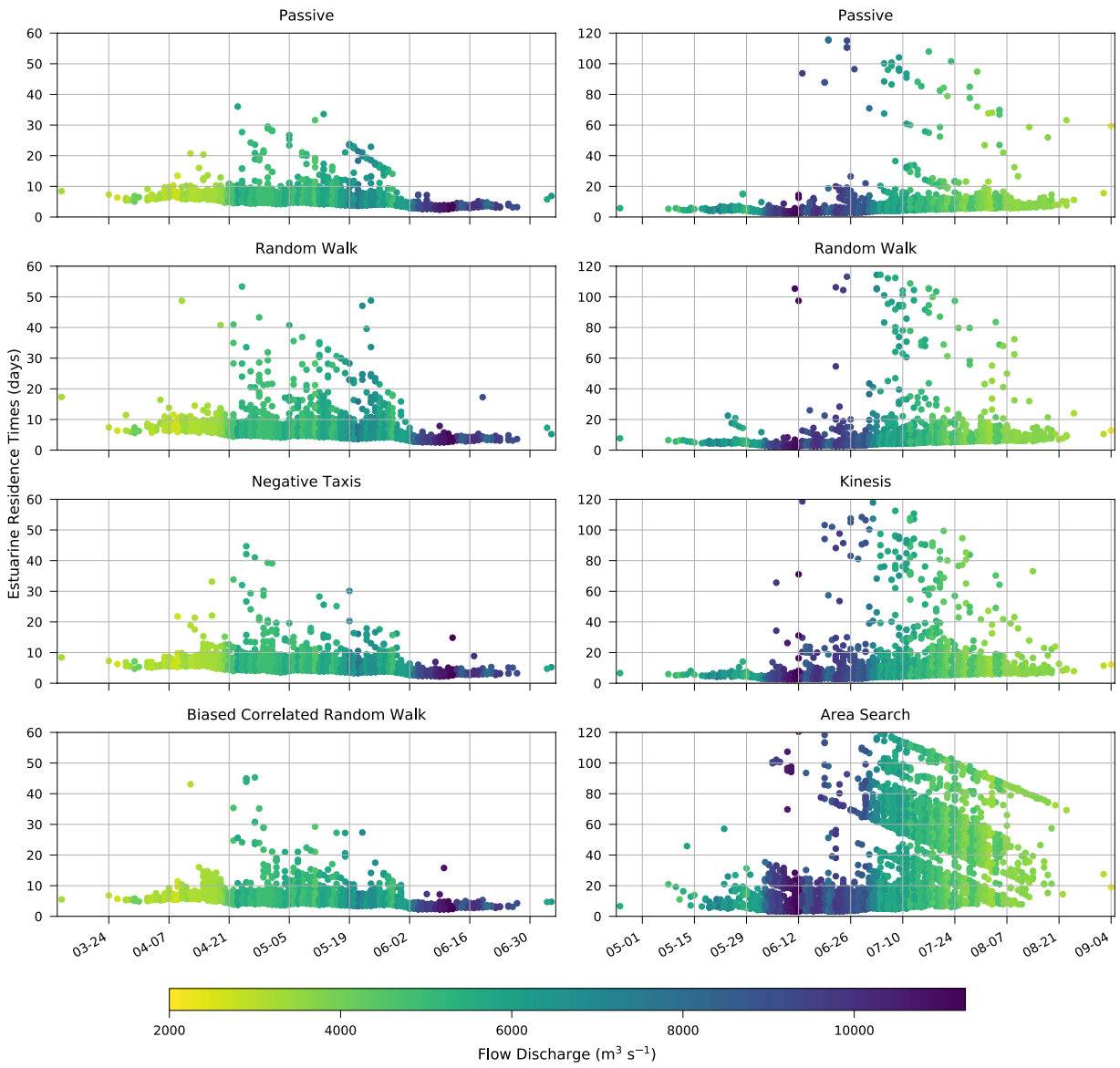

Figure 2.9. Estuarine residence times (days) for simulated yearling Chinook salmon behaviors (*left*) and simulated subyearling Chinook salmon behaviors (*right*). Dates correspond with the date when fish were released at Bonneville Dam. Points are colored by the corresponding daily mean discharge on the day of release.

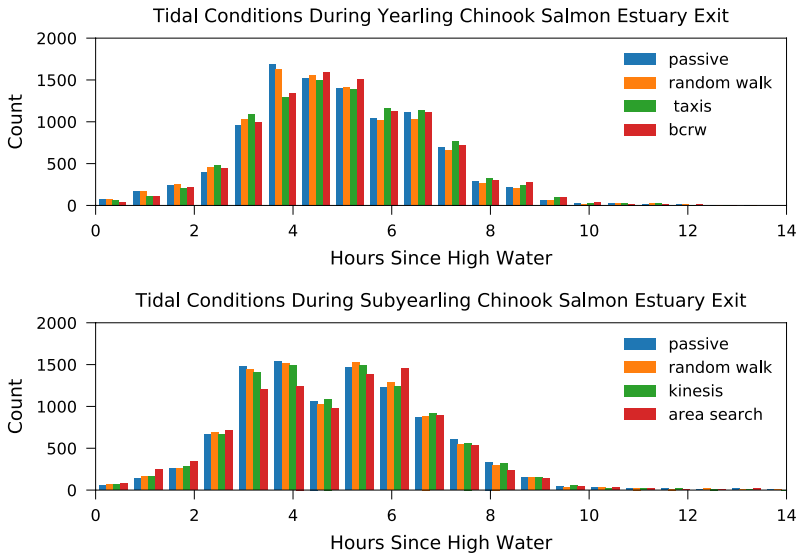

Figure 2.10. Hours since high water at time of estuary exit for simulated yearling Chinook salmon (*top*) and simulated subyearling Chinook salmon (*bottom*).

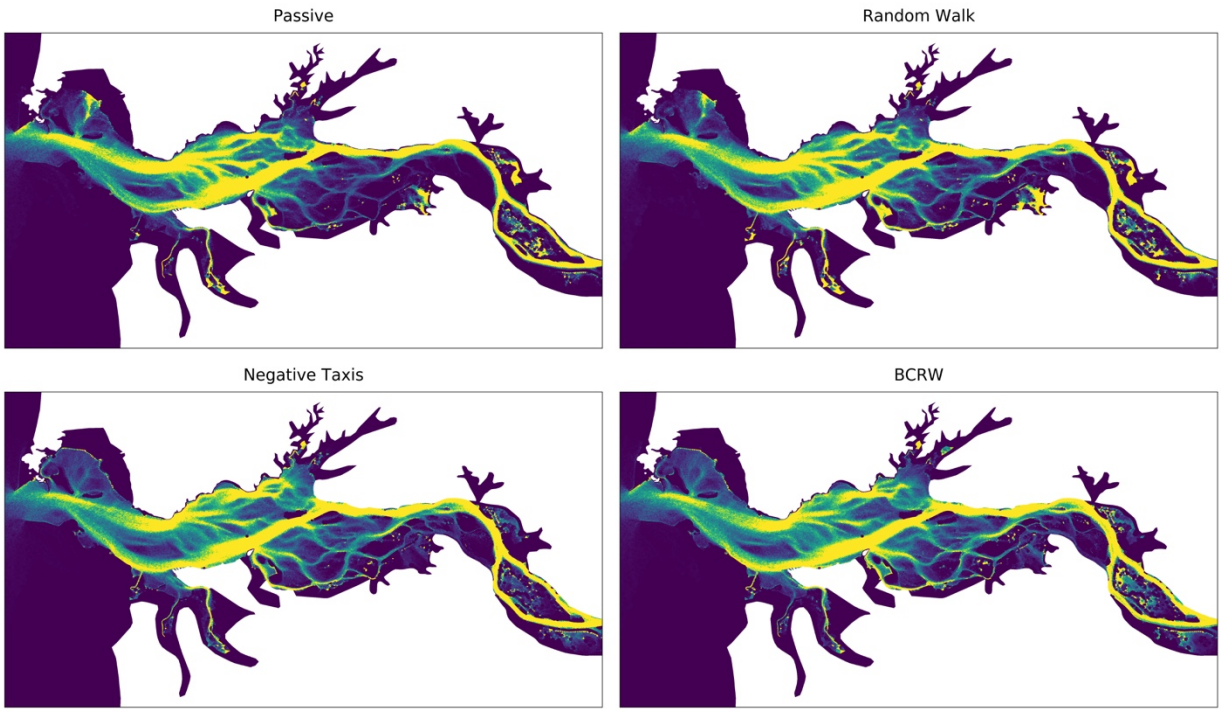

Figure 2.11. Simulated migration pathways for yearling Chinook salmon, showing the number of times an element is occupied over time normalized by the element area for passive drift, random walk, negative rheotaxis, and biased correlated random walk behaviors. Yellow regions highlight common pathways.

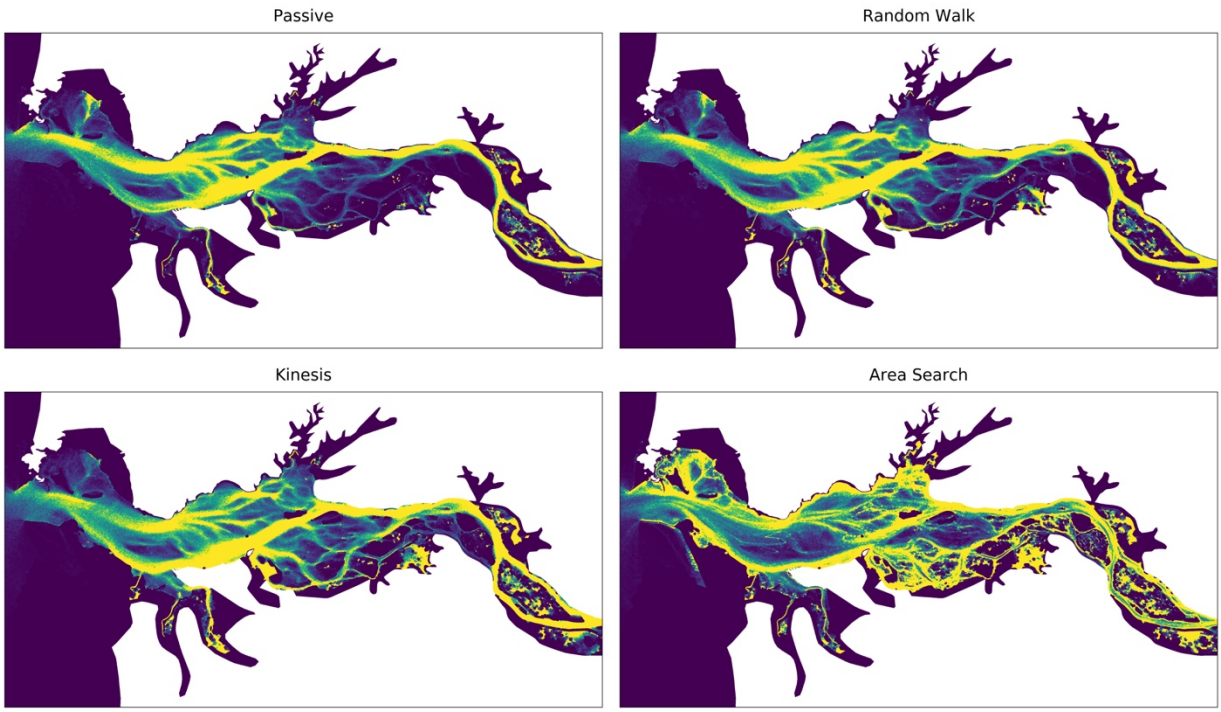

Figure 2.12. Simulated migration pathways for subyearling Chinook salmon, showing the number of times an element is occupied over time normalized by the element area for passive drift, random walk, kinesis, and restricted-area search behaviors. Yellow regions highlight common migration pathways.

3 Interannual variability in juvenile Chinook salmon estuarine migration and growth in the Columbia River

Abstract

An individual-based model was used to explore interannual variability in juvenile Chinook salmon estuarine migration patterns, and how those patterns varied across the estuarine continuum. Migration rates and growth were described for the entire estuary from Bonneville Dam to the estuary mouth, as well as across eight hydrogeomorphic reaches that differ based on their geomorphological characteristics and fluvial and tidal hydrology. Several swimming behaviors and passive drift were simulated for yearling and subyearling Chinook salmon, including random walks and more complex swimming behaviors. Growth was simulated using the Wisconsin bioenergetics model. Variability in migration patterns over time showed that flow conditions were the primary driver of migration rates and residence times. River temperatures, which were related to flow intensity, as well as ocean temperatures and large-scale ocean indices largely influenced simulated growth. Years with below-average flows and warmer temperatures were associated with increased growth for yearling Chinook salmon. However, growth rates for subyearling Chinook salmon were reduced in low flow years due to warmer summer temperatures, especially when positive PDO and ENSO phases contributed to warmer than average conditions. Trends across the estuary's hydrogeomorphic reaches showed decreased migration rates and growth rates in the lower estuary across both life-history types and swimming behaviors. During high flow years, migration rates were greater in reaches C – H; however, migration rates were decreased throughout the lower estuary regardless of flow intensities.

3.1 Introduction

In the Columbia River basin, salmonids experience a range of environmental conditions and habitats throughout their migration from freshwater spawning habitats to the marine environment. While the freshwater and estuarine juvenile stages are formative, Pacific salmonids spend one to five years in the northern Pacific Ocean taking advantage of abundant food resources and increasing their biomass by > 90% before returning to their natal streams to reproduce (Groot and Margolis 1991; Quinn 2005). Multiple studies have found significant relationships between adult survival and post-Federal Columbia River Hydropower System (FCRPS) experiences (Haeseker et al. 2012; Petrosky and Schaller 2010; Schaller and Petrosky 2007; Schaller et al. 2014). However, post-FCRPS experiences are challenging to quantify and describe as they include the entire time between juvenile passage and adult return at Bonneville Dam. While juvenile salmonids only spend a small amount of time in the Columbia River estuary, their experiences in freshwater habitats and the estuary influence their size and condition as well as their timing of marine entry which have been suggested to influence survival (Duffy and Beauchamp 2011; Scheuerell et al. 2009; Zabel and Williams 2002). Therefore, understanding how salmonids utilize and benefit from estuarine habitat and how their migration patterns are impacted by interannual variability in hydrological and marine conditions is of value. In addition to investigating the effects of physical drivers, characterizing spatial differences across the estuarine continuum serves to identify regions of the estuary that provide beneficial habitat.

Estuarine habitat and habitat usage by juvenile Chinook salmon (*Oncorhynchus tshawytscha*), the most estuarine-dependent salmonid in the system (Healey 1982), have often been described as the product of three major elements: habitat opportunity, habitat capacity, and

life history structure (Bottom et al. 2011; Bottom et al. 2005; Simenstad and Cordell 2000). Together, these components shape the juvenile stages of salmonids as they migrate from freshwater to marine habitats. The physical habitat characteristics (e.g., water depths, temperatures, salinities, and flow velocities) and the ability of juvenile salmonids to access and benefit from these habitats constitute habitat opportunity. While habitat opportunity emphasizes physical features, habitat capacity describes habitat quality and how it affects biological interactions and bioenergetic processes (Simenstad and Cordell 2000).

Chinook salmon life-history types have adapted to use freshwater and estuarine habitats differently, varying in their juvenile migration timing, estuarine residence, and habitat usage (Bottom et al. 2005; Roegner et al. 2012). This life history variation is likewise expressed in the timing of adult returns, and a seasonal designation is used to differentiate subgroups of Chinook salmon. Stream-type stocks (i.e. spring and summer) spend up to a year rearing in freshwater environments before migrating to the ocean, while ocean-type stocks (i.e. fall) spend less time rearing in freshwater and instead spend greater time rearing in estuarine environments (Healey 1982; Quinn 2005; Simenstad et al. 1982; Weitkamp et al. 2014).

Juvenile Chinook salmon may be detected in the estuary year-round; however, there are seasonal patterns in their abundance (Dawley et al. 1986; McCabe et al. 1986). Stream-type Chinook salmon often peak in abundance between April and June (Weitkamp et al. 2012), with their main migration period coinciding with the timing of the spring freshet. Ocean-type Chinook salmon peak in abundance between May and July and usually exit the estuary in mid to late summer (Emmett et al. 2006). These life-history strategies may be attributed to genetic differences (Waples et al. 2004); however, these patterns are also affected by environmental conditions (Clarke et al. 1992).

Individual characteristics likewise influence migration rates and estuarine residence times. Migrating juveniles seeking growth opportunities often select habitats in relation to their body size (Burke 2004). Whereas small fry and fingerlings occupy shallow intertidal habitats, larger juveniles prefer deeper subtidal channels (Reimers 1973; Congleton et al. 1981; Meyer and Horton 1982; Levings et al. 1986). Furthermore, larger juveniles spend less time rearing in the estuary and instead migrate more quickly through the system, often using it as a migration corridor. Overall life-history types may be differentiated by patterns of estuarine habitat use, fish size, and migration timing.

Aside from individual characteristics that influence habitat preferences, migration patterns are also impacted by physical and anthropogenic drivers, including river discharge (Scheuerell et al. 2009), ocean conditions, and hydroelectric dams (Raymond 1988; Williams et al. 2005). Periods of high discharge are associated with faster migration rates (Dawley et al. 1986). Similarly, the tides influence migration patterns in the lower estuary, particularly in the lower 50 km of the river, with downstream movement during the ebb phase and upstream movement during the flood phase (Schreck and Stahl 1998). The time of year also influences migration rates, with faster rates later in the migration season (Ledgerwood et al. 2004; McMichael et al 2006; McComas et al. 2008).

Methods for assessing salmon habitat in the Columbia River estuary have included time series analysis methods that informed river stage and tidal models (Kukulka and Jay 2003a; Kukulka and Jay 2003b) as well as habitat association models that use outputs from long-term hydrodynamic model simulations. Outcomes of these approaches have focused on evaluating shallow-water habitat and/or quantifying salmon habitat opportunity, an area-based metric (Bottom et al. 2005; Burla 2009), or salmon habitat, a volume-based metric (Rostaminia 2017),

where the latter two depend on multiple temperature, water depth, salinity, and water velocity criteria. These methods have proven useful for describing habitat opportunity and variations in physical habitat over space and time; however, these techniques do not characterize juvenile salmonid migratory behavior or habitat usage under varying hydrological and marine conditions.

An individual-based model is developed to address the need for a model that tracks how juvenile salmonids respond to environmental conditions. This type of model simulates the movement and growth of individuals allowing for an investigation into how interannual variability impacts migration rates, growth, and habitat use and how these patterns vary across distinct hydrogeomorphic reaches under different flow regimes. The IBM is spatially-explicit and leverages output from a hydrodynamic model of the Columbia River estuary.

In this work, the following questions are addressed:

1. How does interannual variability impact estuarine migration pathways, residence times, and growth?
2. How do migration characteristics differ across the estuarine continuum?

3.2 Methods

3.2.1 Model Overview

IBM simulations were conducted from 2000 – 2015 to investigate how interannual variability influences juvenile Chinook salmon estuarine migration and growth. This time span captures a range of conditions, including low and high flow years (Figure 3.1) as well as varying large-scale climate indices (Figure 3.2). The initial conditions for yearling and subyearling Chinook salmon at the start of simulations were based on smolt indices and fork length data collected at Bonneville Dam. Individual fish movement and growth were tracked from

initialization near Bonneville Dam until ocean entry. Movement was simulated based on a Lagrangian particle tracking method and assigned swimming behaviors, and growth was simulated using the Wisconsin bioenergetics model.

3.2.2 Salmon Data

Data collected by the Smolt Monitoring Program were used to inform simulation design and included the daily smolt index and fish condition at Bonneville Dam. The smolt index represents the number of juvenile salmonids passing Bonneville Dam every day and is adjusted for flows to account for individuals that were not detected at the PIT-tag monitoring station (i.e., fish that bypassed through the turbines or in the spill). This index is not ESU-specific but rather a more general estimate of life-history type, such as subyearling and yearling Chinook salmon. The smolt indices and daily fork length data for both subyearling and yearling Chinook salmon were downloaded from the Fish Passage Center for years 2000 – 2015, and averages were computed for individual years to generate a normal distribution used for run timing in the model for both life-history types (Figure 3.3). In addition to the run timing data, fork-length data from Bonneville Dam were used to inform the starting fork lengths. Unlike the smolt index data, these data were not available until 2009, so only years 2009 – 2015 were considered when generating distributions used in simulations.

3.2.3 Hydrodynamic Model

Environmental variables, including water temperatures, depths, and velocities, that comprised the IBM's virtual environment were provided by the hindcast database 33 (db33) generated from the finite element hydrodynamic model, SELFE (Zhang and Baptista 2008) . Multiple external forcings were used in the generation of this database, including atmospheric forcing from the NOAA/NCEP North American Mesoscale Forecast System (Rogers et al.

2009), tides from a regional inverse model (Myers and Baptista 2001), and temperature, salinity, and water elevations from the Navy Coastal Ocean Model (NCOM) (Barron et al. 2006). River forcing, including discharge and temperatures for the Columbia River at Bonneville Dam and the Willamette River at Morrison Bridge in Portland, Oregon were imposed at the riverine boundary of the grid using US Geological Survey (USGS) data. While the coastal ocean out to ~300 km offshore from northern California to southern Canada were simulated by the hydrodynamic model, the IBM focused exclusively on the Columbia River estuary from Bonneville Dam to the estuary mouth.

3.2.4 Individual-Based Model

3.2.4.1 Overview

3.2.4.1.1 Purpose

The IBM was used to explore how interannual variability of flow regimes and estuarine conditions influences estuarine habitat use, travel rates, and growth of outmigrating yearling and subyearling Chinook salmon in the Columbia River estuary. In addition to interannual comparisons for both life-history types, simulation results were analyzed across the estuary's hydrogeomorphic reaches to better understand how specific regions of the estuary support juvenile Chinook salmon.

3.2.4.1.2 State Variables and Scales

Individual attributes followed over time included the 3D location and occupied element computed from the combined Lagrangian movement and active swimming sub-models as well as the fork length and weight calculated from the bioenergetics model. Growth was simulated using equations from the Wisconsin bioenergetics model and was dependent on the water temperature

from the hydrodynamic model, the fish size, the prey energy density, and the proportion of maximum consumption (P-value). A constant prey energy density was used for each life-history type, and the P-value depended on the proximity of the occupied element to wetland habitat.

Aside from water temperatures, additional environmental variables used in the IBM included water depth and 3-D flow velocities from the hydrodynamic model. These environmental variables had horizontal resolutions of 100 – 200 m and vertical resolutions ranging from centimeters to meters. The temporal resolution of the environmental variables was fifteen minutes.

3.2.4.1.3 Process Overview and Scheduling

Simulation timing for yearling and subyearling Chinook salmon was based on the smolt indices from the Smolt Monitoring Program from years 2000 – 2015, with dates described in Table 3.1. For yearling Chinook salmon, simulations started on March 7 and ended on August 6, with the last date of initialization on July 8. For subyearling Chinook salmon, simulations commenced on April 20 and ended on November 6, with individuals initialized no later than September 7. This difference between the last release date and the end of the simulation was to ensure that all individuals had adequate time to exit the system.

While the IBM relied on environmental variables with a temporal resolution of fifteen minutes, a smaller time step corresponding to the original time step used in the hydrodynamic model of 36 seconds was used. Therefore, as movement was calculated, both due to advection followed by movement due to active swimming, flow velocities were interpolated to the smaller time step. At the end of each fifteen-minute step, growth was calculated based on the temperature of the individual's 3-D position and the P-value of the occupied element. Once

individuals exited the estuary, their movement and growth were no longer tracked, and they were considered to have successfully migrated from the system. In instances where all individuals had exited the estuary prior to the date when simulations were designed to end, the simulation was stopped. Mortality was not considered in this application.

3.2.4.2 Design Concepts

3.2.4.2.1 Basic principles

Animal behavior is complex and reflects individual decision-making that factors in both short-term and long-term goals. Examples of short-term goals include feeding, predator avoidance, and optimizing environmental conditions. A significant long-term goal is to maximize fecundity, and this often relies on optimizing growth and minimizing mortality. For salmonids, an additional long-term goal is successful migration to productive marine habitats and the return to freshwater spawning habitats to reproduce. While it would be ideal to consider both short- and long-term goals in the IBM design, different life stages utilize habitat differently, and this impacts how they prioritize growth, feeding, and efficient migration.

This IBM simulates yearling and subyearling Chinook salmon migration from Bonneville Dam to the estuary mouth using simple random walk behaviors in addition to more complex swimming behaviors. For yearling Chinook salmon, a biased correlated random walk was implemented based on the assumption that they utilize the estuary as a migration corridor and optimize efficient downstream movement. For subyearling Chinook salmon, a restricted-area search behavior was implemented based on the assumption that they spend longer periods rearing in estuarine environments seeking opportunities for growth. For all active swimming behaviors, a swim speed of 1 BL s^{-1} was assumed since swim speeds are size-dependent (Ware

1978). This assumption necessitated that growth be computed over time to simulate realistic swimming behaviors as. Aside from active swimming, passive drift was also simulated based on the run timing for both life-history types.

3.2.4.2.2 Sensing and prediction

For the simpler random walk behaviors, simulated individuals did not have predictive or sensory abilities that influenced movement. However, the more complex behaviors did assume that individuals could adapt their movement based on their current experiences and/or their nearby environment. The biased correlated random walk behavior included sensory components that directed downstream movement. This included a bias term and a correlated movement pattern that led individuals to move forward in a persistent manner based on the direction of flows and swimming velocities from the previous time step. Predictive abilities associated with the restricted-area search behavior allowed individuals to sense the potential growth rates of the immediately neighboring elements and make habitat selection decisions that optimized movement towards regions of higher growth.

3.2.4.2.3 Stochasticity

Simulations across years and behaviors were initialized with the same random number seed. Randomly drawn variables included the starting location, initial fork length, and timing of entry into the domain. All individuals for each year were therefore initialized with identical conditions, but varied in the behavior and/or year simulated. In addition, random noise was included in the swimming direction to impart randomness in individual movement.

3.2.4.2.4 Observation

Model output from the IBM was saved every fifteen minutes. The 3-D location and the length and weight of each fish were recorded, as well as variables pertaining to the environmental conditions experienced by individual fish, including the water temperature, water depth, and occupied element.

3.2.4.3 Details

3.2.4.3.1 Initialization

Each year, 10,000 individuals were simulated using the run timing distributions described in Table 3.1. Yearling Chinook salmon were initialized near Bonneville Dam using a normal distribution centered on May 11 with a standard deviation of 14 days. Similarly, subyearling Chinook salmon run timing was based on a normal distribution centered on July 3 with a standard deviation of 16 days. These run timing distributions were based on the averaged smolt indices from 2000 – 2015 from the Fish Passage Center Smolt Monitoring Program. For the subyearling Chinook salmon run timing, peaks in abundance prior to June were ignored as these were associated with larger individuals that are held over by hatcheries and released as yearlings.

Entrance into the domain occurred near Bonneville Dam using a normal distribution centered at 45°38’06’’N, 121°57’41’’W with a standard deviation of 20 m. Vertical distributions were generated from a uniform distribution between 0 and 2 m below the surface. Fork lengths assigned to individuals at the start of the simulation were based on normal distributions generated from fork length data for yearling and subyearling Chinook salmon of 141 ± 15 mm and 95 ± 13 mm respectively. For subyearling Chinook salmon, a truncated distribution bounding the minimum length at 61 mm and the maximum length at 140 mm was used.

3.2.4.3.2 Input

Input provided by a 3-D circulation model hindcast database served as the IBM's virtual environment, and variables included water temperatures, depths, and 3-D velocities. Additional environmental input included wetland habitat data from the 2010 High Resolution Land Cover Data from the Lower Columbia Estuary Partnership. These data were used to approximate P-values, the proportion of maximum consumption, in the bioenergetics model. P-values were defined at the element centers based on their distance to the nearest neighboring element classified as wetland habitat. Wetland habitat classes were merged from multiple tidal and non-tidal classes of wetlands (e.g., coniferous, deciduous, shrub-scrub, and herbaceous) to one tidal class, and the data were interpolated to the element centers of the circulation model mesh.

Juvenile Chinook salmon diets depend on food derived from marsh habitats (Bottom et al. 2005) and macroinvertebrates (e.g., chironomids) associated with these habitats constitute a large portion of their diet (Bottom et al. 2008). While food sources may be commonly found in wetland habitats, studies also suggest that these food sources may be exported from wetlands into nearby channels and into the water column (Thom et al. 2018). To represent this flux of food from wetland habitats, P-values were defined based on their distance to wetland habitat according to the values described in Table 3.2 and shown in Figure 3.4. Elements in closest proximity (< 100 m) to wetland habitat had maximum P-values of 0.9, whereas elements greater than 1000 m from wetland habitat had minimum values of 0.4.

3.2.4.3.3 Sub-models

3.2.4.3.3.1 Movement model

Individual movement was simulated in two parts. First 3-D advective transport was calculated using a Lagrangian particle tracking method, where velocities were spatially and temporally interpolated. Locations were updated using a Runge-Kutta fourth-order time integration method and a 36-second time step. If a particle trajectory resulted in movement into a dry element or outside of the mesh, the tangential velocity was calculated, and the trajectory was adjusted accordingly so that the pathway remained within the domain and in wet elements. Similarly, if the trajectory extended past the bottom water depth or surface, it was nudged back into the water column, just above the bottom or below the surface.

For both subyearling and yearling Chinook salmon, passive and random walk behaviors were simulated to investigate the pathways of particles without behavior and individuals with random undirected swimming (Table 3.3). Random swimming was simulated using an uncorrelated and unbiased random walk, where movement did not rely on external cues or reactions to environmental stimuli (Codling et al. 2008; Willis 2011). The swimming direction of this behavior was generated from a von Mises distribution ($\mu = 0$, $\kappa = 0$). Vertical movement occurred solely by advection for this behavior as well as subsequent behaviors.

A biased correlated random walk was also simulated for yearling Chinook salmon using the equations and parameters outlined in Chapter 2. The bias term encouraged seaward migration by directing fish towards geographic targets at the downstream boundary of each hydrogeomorphic reach. In addition, the direction of movement at each time step was correlated with the direction of fish movement, due to both advection and swimming behavior, at the prior

time step. This behavior resulted in individuals moving forward in a persistent pattern. Both the bias term and correlated term were relevant to this life-history type which is associated with efficient migration through the lower estuary and short residence times.

A restricted-area search behavior was simulated for subyearling Chinook salmon and equations and parameters are likewise defined in Chapter 2. This behavior involved individuals assessing the immediately neighboring elements' growth rates and moving to the element with the highest value, with random noise added. The growth rate for each neighboring element was computed using the Wisconsin bioenergetics model and was based on the depth-averaged temperature at the element center.

In Chapter 2, there were limitations identified with this behavior, where fish were artificially retained in local optima, particularly in low flow environments. Once an individual moved to an area associated with a high growth rate, it tended to remain there. To reduce the occurrence of artificially inflated residence times, this behavior was modified by restricting the length of time an individual could spend in a general location. If after a period of 24 hours, an individual had not occupied more than four unique elements, its behavior switched to move to the element with the greatest depth-averaged velocity. This behavior of leaving an area of high growth and moving to an area with increased flows emulates observed behaviors where fish move from shallow-channel habitats to deeper peripheral channels. In addition, once an individual's fork length increased by 25%, their behavior was switched to simulate efficient outmigration by adapting the area search to identify the neighboring element with the greatest depth-averaged velocities. Without including this modification, a significant portion of the individuals never exited the estuary.

3.2.4.3.3.2 Bioenergetics

At each fifteen-minute time step, growth was calculated using the Wisconsin bioenergetics model (Hanson 1997) from energy gain and loss terms, according to:

$$G = C - ((R + A + S) + (F + U))$$

Energy gains are represented by consumption (*C*), while loss terms include respiration (*R*), egestion (*F*), and excretion (*U*), with all terms having a mass and temperature dependence. Each of these parameters were separately computed using equations defined in Hanson (1997). All of these components were computed based on values defined by Stewart and Ibarra (1991), with the exception of some of the consumption parameters that utilized values from Plumb and Moffitt (2015). For further details on the equations and variables used, see Chapter 2. While Chapter 2 used a uniform prey energy density, this work used different densities based on the life-history type. For subyearling Chinook salmon, the prey energy density for chironomid pupae of 3400 J g^{-1} was used (Koehler et al. 2006), and for yearling Chinook salmon a prey energy density of 4000 J g^{-1} was used. Originally, both life-history types used a value of 3400 J g-1; however, preliminary results for yearling Chinook salmon growth were below average (~0.2 mm d^{-1}), so the imposed prey energy density was increased. The P-values used in the bioenergetics model depended on the proximity to wetland habitat as defined in 3.2.5.3.2.

3.2.5 Analysis

Results from simulations were analyzed to assess interannual trends in residence times, migration rates, and growth rates for all individuals that successfully exited the system. Rates were calculated based on the time between marine entry and initialization near Bonneville Dam. While the focus was on variability in environmental conditions over time, within-year

comparisons were likewise conducted to understand how pathways of passive particles, random swimming, and more complex behavioral rules differed. Median travel times to Jones Beach for yearling Chinook salmon were also calculated. There were few observations from 2000 – 2015 for which model-data comparisons could be made; however, annual travel times to Jones Beach were provided by the long-term annual pair-trawl surveys (Ledgerwood et al. 2004).

To understand the effect of environmental conditions on residence times and growth rates, the mean flows at initialization and the mean temperatures and P-values experienced by each individual during their entire migration were analyzed. This provided context on how trends in river conditions and habitats experienced shaped estuarine residence times and potential growth. Aside from river conditions, large-scale indices were evaluated to assess the impacts of the Pacific Decadal Oscillation (PDO) and El Nino Southern Oscillation (ENSO) on migration rates, residence times, and growth rates. Both of these indices are associated with basin-scale oceanic and atmospheric processes that occur over large spatial scales. The PDO has been shown to correlate with salmon population dynamics in the Northeast Pacific (Mantua et al. 1997). ENSO cycles affect precipitation patterns and snowpack which can impact spring freshet flows that juvenile salmon use as an environmental cue. Impacts from ENSO, especially during warm, low flow years could also negatively impact the development of smolts during their freshwater phase.

PDO and ENSO indices were originally represented as monthly anomalies, and these monthly values were averaged over the relative periods simulated for yearling Chinook salmon (March through July) and subyearling Chinook salmon (April through September). Similarly, anomalies were computed for river discharge, ocean temperatures, and river temperatures by calculating the z-score for each year. The mean and standard deviation across 2000 – 2015 for

the two defined periods mentioned above were first calculated. To obtain a z-score for each year, the mean from years 2000 – 2015 was subtracted from the mean for each year, and this was then divided by the standard deviation for years 2000 – 2015.

Z-scores were also calculated for the residence times, migration rates, and growth rates for each year and for each behavior. Using these metrics to identify positive and negative anomalies provided a means by which to evaluate how variations in river conditions and large-scale indices impacted simulated individuals. Simulation results were also evaluated across the estuary's hydrogeomorphic reaches to assess how migration pathways, habitat use, and growth differed across the freshwater to marine continuum.

3.3 Results

3.3.1 Migration Rates and Estuarine Residence

As previously mentioned, the Jones Beach pair-trawl study provided the only observations through which model-data comparisons could be made from 2000 – 2015. For yearling Chinook salmon, observed travel times of run-of-river fish ranged from 1.5 to 2.3 days, while simulated travel times ranged from 1.6 to 3.2 days for passive particles, 1.6 to 3.4 days for the random walk behavior, and 1.4 to 2.9 days for the biased correlated random walk behavior (Table 3.4). Median simulated travel times tended to be greater than observed travel times to Jones Beach, and differences between observed and simulated times increased with decreasing flows (Figure 3.5).

Estuarine residence times and migration rates varied across years and swimming behaviors for both yearling and subyearling Chinook salmon. Yearling Chinook salmon median residence times ranged from 3.2 to 6.9 days for passive particles, 3.3 to 7.3 days for the random

walk behavior, and 3.0 to 6.5 days for the biased correlated random walk (Table 3.5, Figure 3.6). Median migration rates, defined as the total distance traveled by individuals divided by the residence time ranged from 46.9 to 78.5 km d^{-1} for passive particles, 44.8 to 74.8 km d^{-1} for the random walk behavior, and 50.5 to 83.8 km d^{-1} for the biased correlated random walk behavior. Across all years simulated, the residence times and migration rates simulated using the random walk behavior were greater than the times and rates for the passive particles, while those of the biased correlated random walk were less. Considering the results across years and behaviors, there was greater variability across time for a given behavior than variability within the same simulated year across behaviors.

Simulated median residence times for subyearling Chinook salmon ranged from 3.1 to 9.6 days for passive particles, 3.2 to 9.9 days for the random walk behavior, and 6.3 to 31.6 days for the restricted-area search behavior (Table 3.6, Figure 3.7). Median migration rates ranged from 41.9 to 80.0 km d^{-1} for passive particles, 40.6 to 77.9 km d^{-1} for the random walk behavior, and 17.2 to 48.2 km d^{-1} for the restricted-area search behavior. For a specific year, there was little variability between the passive particle and random walk simulations; however, the restricted-area search behavior was associated with much longer residence times and reduced migration rates. While there were changes over time in migration patterns for each behavior, results across behaviors for a simulated year exhibited a much greater degree of variability than was seen for yearling Chinook salmon.

Overall, the flow conditions at initialization were a major driver of estuarine residence times and migration rates for both yearling and subyearling Chinook (Figure 3.8). In addition, the variability in residence times for a given behavior was associated with flow magnitude. During high flow conditions, particles and simulated individuals tended to migrate at similar

rates, often above 80 km d^{-1} and exited the estuary within days. However, as flows at initialization decreased, there was a wider range of estuarine migration patterns as evidenced by the spread in residence times.

3.3.2 Estuarine Growth

Median growth rates for yearling Chinook salmon ranged from 0.30 to 0.46 mm d^{-1} for the random walk behavior and from 0.31 to 0.48 mm d^{-1} for the biased correlated random walk behavior (Table 3.5). There were minimal differences in growth rates between the simulated behaviors for a given year (Figure 3.9). Variability in growth rates over time was reflected in the differences in temperatures across years. Figure 3.9 shows the distributions of mean temperatures and mean P-values experienced by all simulated individuals that successfully exited the estuary. The mean temperatures for a specific year varied little between the two behaviors which explains why there were minimal differences in growth rates for specific years. Looking at the interannual variability in mean temperatures and mean P-values across individuals, it is evident that the growth rate differences across years were associated with differences in temperatures, as the mean P-values over this time range varied little.

Median growth rates for subyearling Chinook salmon ranged from 0.19 to 0.41 mm d^{-1} for the random walk behavior, and 0.52 to 0.65 mm d^{-1} for the restricted-area search behavior (Table 3.6). For the random walk behavior, median growth rates were relatively constant over time. The exception was 2015, when median growth rates were nearly half the value of other years and the mean temperature experienced by all individuals was greatest (Figure 3.10). Mean temperatures in 2015 were warmer than other years, particularly for the random walk behavior, and this resulted in decreased growth rates for that year (Figure 3.10). While mean P-values for yearling Chinook salmon differed little across the years simulated, P-values for subyearling

Chinook salmon were much greater for the restricted-area search behavior than the random walk behavior. Mean values for the random walk behavior were similar to those seen in the yearling Chinook simulations. Although mean temperatures differed to a greater degree across behaviors for the subyearling Chinook salmon, the difference in growth rates between the two behaviors were mostly a result of the P-values, relating to the habitats occupied by individuals over time.

Considering the effects of flows at initialization and mean temperatures experienced by simulated individuals, low growth rates for subyearling Chinook salmon were associated with low flow periods and above average temperatures (Figure 3.11). Growth rates for yearling Chinook salmon were reduced when temperatures were colder than average and were greater when temperatures were above average. During low flow years, temperatures were elevated. This led to anomalously warm temperatures during the subyearling Chinook salmon migration period that were much warmer than the mean water temperatures experienced during the earlier yearling Chinook salmon migration period. Whereas the much warmer summer temperatures experienced by subyearling Chinook salmon during a low flow year limited their growth, the warm temperatures for yearling Chinook salmon (that were comparatively cooler in the spring) resulted in increased growth.

3.3.3 Interannual Variability: Environmental Conditions, Migration, and Growth

To explore the effect of environmental conditions on residence times, migration rates, and growth rates, anomalies associated with large-scale indices (e.g., PDO and ENSO), ocean temperature, river discharge, and river temperature were analyzed. During periods when yearling Chinook salmon were simulated (March through July), positive anomalies for PDO were observed in 2003 – 2006 and 2014 – 2015, while positive ENSO anomalies were observed in 2002-2005, 2009 – 2010, 2012, and 2014 – 2015 (Figure 3.12). Ocean temperature anomalies

followed similar trends as PDO anomalies. Anomalies in river flow did not deviate significantly from the mean, with the exception of low flow years (e.g., 2001 and 2015) and high flow years (2011, 2012). River temperatures showed less variability over time than the other environmental indicators. There were negative temperature anomalies in 2011 and 2012, associated with high flow years, and a positive anomaly in 2015 when flows were reduced. While 2001 flows were also reduced, river temperatures were not below average, and this difference between the two low flow years was likely due to the increased PDO and ENSO anomalies in 2015 that would have contributed to warmer temperatures. Overall, river temperature anomalies were mostly inversely related to the river flow anomalies.

Anomalies in yearling Chinook salmon residence times followed trends in anomalies for flow conditions, with the greatest positive anomaly in residence times associated with the year where the river discharge anomaly was most negative in 2001. In general, positive anomalies in residence times were associated with years when there were negative anomalies in mean flow. Similarly, negative anomalies in residence times were associated with positive anomalies in river discharge (e.g., 2006, 2011 and 2012). Migration rates, which were inversely related to residence times, were also closely related to trends in river discharge anomalies, with positive anomalies observed during years where positive anomalies in river discharge occurred.

Growth rates for yearling Chinook salmon were typically greater during low flow years when temperature anomalies were positive. In contrast, growth rate anomalies were negative in 2002, 2008 – 2011 when temperature anomalies were likewise negative. While river temperatures had a strong influence on growth rates, growth rate anomalies also trended similarly to the PDO and ENSO anomalies. In 2015, when PDO and ENSO anomalies were greater than 1.0, growth rates were much greater. In 2004, growth rates were higher than

average; however, this positive anomaly was more associated with river temperatures than the PDO or ENSO.

Anomalies for ocean indices, river flows, and river and ocean temperatures, as well as subyearling Chinook salmon residence times, migration rates, and growth rates are shown in Figure 3.13. Trends in large-scale indices followed similar patterns as those seen from 2000 – 2015 for the yearling Chinook salmon simulations, with some slight differences as it highlighted a different period of time (April through September). PDO anomalies were negative in 2000, 2001, and 2008 – 2013 and were positive in 2003 – 2005 and 2014-2015. Years 2002, 2006, and 2007 did not deviate significantly from the mean. ENSO anomalies differed slightly, with years 2002 – 2006, 2009, 2012, and 2014 – 2015 having positive anomalies, and negative anomalies in 2007 – 2008 and 2010 – 2011. Ocean temperature anomalies of note were years 2004 and 2015 when temperatures were above average and 2008 and 2012 when temperatures were below average. Years with river flows that differed substantially from the mean included years 2001 and 2015 when flows were below average and years 2011 – 2012 when flows were well above average. Negative river temperature anomalies were observed in 2002, 2008, and 2010 – 2012, while positive temperature anomalies occurred in 2001, 2003 – 2005, and 2013 – 2015.

Similar to yearling Chinook salmon, anomalies in subyearling Chinook salmon residence times and migration rates were associated with river discharge anomalies, with longer residence times and reduced migration rates in low flow years, and shorter residence times and increased migration rates during high flow years. Positive temperature anomalies, and 2015 in particular, were associated with decreased growth rates for subyearling Chinook salmon. When temperatures were above average, growth rates were below average, with the exception of 2001. Although 2001 and 2015 were both low flow years, different temperature anomalies during these

years, which were associated with different patterns in PDO and ENSO in 2001 and 2015, may be responsible for the diverging patterns in growth rates, despite having similar residence times.

3.3.4 Variability Across the Hydrogeomorphic Reaches

To understand how migration patterns varied across the estuarine continuum over time, migration rates were calculated for each specific hydrogeomorphic reach (Figures 3.14, 3.15). Across the passive particles and yearling Chinook salmon behaviors, migration rates for each year were greatest in reach G (rkm 165 – 204), likely due to increased velocities throughout this reach that would transport fish more quickly through this upstream region. Migration rates were reduced in reach B (rkm 23 – 61), and this was true across behaviors. Reduced migration rates in this reach were likely due to this region having greater tidal influence which could act to reduce downstream flow velocities. In addition, the upstream extent of reach B was the region where the river became less channelized and increased in width, which could impact flows in this region. Since this reach also covered a large portion of the lower estuary, the low migration rates impacted the amount of time individuals spent in this part of the estuary.

Migration rates for subyearling Chinook salmon exhibited similar patterns, with faster migration rates in reach G and reduced migration rates in reach B (Figure 3.15). Migration rates for the restricted-area search were even more reduced for reach B, with mean migration rates typically less than 30 km d^{-1}. For both life-history types, migration rates throughout all reaches were reduced in 2001 and 2015 when flows were less. Migration rates in 2011 and 2012 were much greater than other years. However, even in the high flow years, migration rates were reduced through reach B, and there was less variability over time in this reach than in other reach.

Patterns in mean growth rates across time for hydrogeomorphic reaches showed increased growth rates in reaches C – F for yearling Chinook Salmon, and decreased growth rates in reaches A and B in the lower estuary and near the estuary mouth (Figure 3.16). There was greater variability in growth rates across specific reaches than there was variability over time. Subyearling Chinook salmon growth rates for the random walk behavior were reduced in reaches G, B, and A. While most years had similar growth rates in upstream reaches, growth rates were reduced across all reaches in 2015, particularly in reaches A and B for the random walk behavior and reaches A and G for the restricted-area search behavior. In 2001, when flows were similarly reduced, growth rates were slightly greater in these lower estuary reaches for the random walk behavior. For the restricted-area search behavior, growth rates were less in reaches G and A. Unlike the other subyearling behavior and the yearling behaviors, growth rates were not as reduced in reach B, likely due to the directed swimming behavior towards regions of increased growth, which in the case of reach B, would be associated with the lateral bay habitats such as Cathlamet Bay.

3.4 Discussion

3.4.1 Model Performance

As there were limitations in conducting model-data comparisons to assess the skill of the IBM, it was challenging to assess the effectiveness of this IBM in simulating juvenile Chinook salmon migration. Nevertheless, the Jones Beach pair-trawl study provided an opportunity to assess median travel rates from Bonneville Dam to ~rkm 75, a distance of nearly 159 rkm for yearling Chinook salmon from 2000 – 2015. When mean river flows were elevated (> 8,000 m^3 s^{-1}), the median simulated travel times were usually within several hours of median observed travel times, for both the passive particles and simulated yearling behaviors. Median travel rates

for the biased correlated random walk behavior remained within several hours of observed times at most flow conditions, except in 2001. During both 2001 and 2015, there was a greater difference between observed and simulated travel times.

While the IBM performed well at higher flow conditions, its skill decreased at lower flow conditions. This difference across flow conditions suggests that flows may have been underrepresented by the hydrodynamic model or that the IBM did not adequately simulate swimming behaviors during low flow conditions. Since the relative skill during high flow years was decent across the passive drift and simulated behaviors, this suggests that advective transport was the primary driver for downstream movement, and that individual swimming may have been less important in directing downstream migration in high flow years. During lower flows, it's possible that individuals may compensate for reduced flows by increasing their swim speed to optimize downstream migration, but the IBM did not account for this, instead keeping swim speeds constant at 1 BL s^{-1}. It is also important to note that the simulated travel times to Jones Beach were described for fish passing that longitudinal location, including fish in both the main channel and along the shallow river edges. This contrasts with the observed fish travel times that were detected by a trawl net deployed in the main channel that did not account for fish swimming along the channel peripheries where flow velocities would be reduced.

3.4.2 Trends in Estuarine Migration and the Role of Environmental Variability

For both yearling and subyearling Chinook salmon, residence times and migration rates were driven by river flows. Positive anomalies in migration rates matched positive anomalies in river flow anomalies, while residence times were inversely related to flow anomalies. There was less variability in migration rates and residence times for individuals simulated at higher flows, whereas during lower flow conditions, there was a greater variability expressed in migration

patterns. This suggests that above a certain flow threshold, most outmigrating salmonids move rapidly through the system and are less likely to occupy habitats outside of the main channels. When flows were reduced, there was an increased likelihood of individuals occupying peripheral habitats outside of the main channels, as evidenced by their longer residence times.

Assessing the role of behavior and environmental conditions on residence times and migration rates revealed contrasting patterns for yearling and subyearling Chinook salmon when looking at patterns within a year and across years. While the biased correlated random walk behavior which directed downstream movement had the fastest migration rates and reduced residence times, there was typically greater variability across years for a specific behavior than there was variability across behaviors within a year. In this instance, the behavioral component may either increase or decrease migration rates, but overall, the river flows were largely responsible for dictating the length of time juvenile Chinook salmon spend in the estuary.

During low flow years, median residence time for the biased correlated random walk was nine hours less than passive drift. When flows were higher, the median residence time for this behavior was just 4 to 6 hours less than passive drift. Differences in median migration rates between the optimized migration behavior and passive drift were usually between 5 to 7 km d^{-1}, and were fairly consistent over time. However, differences in median migration rates for the same behavior, such as the biased correlated random walk varied by as much as 33 km d^{-1} across years. Overall, these results confirm that interannual differences in environmental conditions are more influential on migration pattern variability than behavioral differences

Behaviors simulated for subyearling Chinook salmon on the other hand exhibited the opposite pattern. While there were still interannual differences for specific behaviors, there was

greater variance across behaviors within a year. In this case, the simulated behavior had a significant impact on the migration rates and simulated residence times. Individuals simulated using the restricted-area search behavior had residence times that were two to three times greater than residence times of passive drift. Similarly, migration rates for this behavior were significantly reduced compared to passive drift migration rates. These differences were especially evident during low flow years, and tended to be less drastic during high flow years. In general, the behavioral rules that directed individuals to regions where growth rates were high resulted in slower migration rates due to the greater occupation of habitats outside the main channel. By occupying shallower habitats where there was more wetland habitat, individuals inhabited areas where flows were reduced, and their search for habitats with high growth rates resulted in longer occupation of these habitats.

Overall, this work confirms that flows are the main driver with regards to migration rates and residence times. With the exception of the subyearling Chinook salmon behavior that directed individuals to shallow peripheral wetland habitats, juvenile Chinook salmon residence times were clearly driven by flow magnitudes, and when flows are above a certain threshold, most individuals exited the system in a matter of days. This has important implications for hydropower management if the magnitude in flows may be used to roughly estimate the amount of time outmigrating juvenile salmon may spend in the estuary, particularly if trying to take advantage of estuarine or coastal conditions that are sub-optimal or optimal.

3.4.3 Trends in Estuarine Growth and the Role of Environmental Variability

Patterns in estuarine growth for yearling Chinook salmon showed little variability between the random walk and biased correlated random walk behaviors in a given year. This suggests that individuals simulated under the two behaviors experienced similar temperature

conditions and occupied similar habitats. There was greater difference across time in growth rates within behaviors, and these trends in estuarine growth were driven primarily by changes in mean temperatures experienced by yearling Chinook salmon from 2000 – 2015. Since there were minimal differences in the distributions of mean P-values experienced by individuals over time, this suggests that individuals simulated under the two yearling Chinook salmon behaviors occupied similar habitats during their downstream migration. Overall, during years when temperatures were above average, growth rates for yearling Chinook salmon were greater, and when temperatures were below average, growth rates were reduced.

Variability in growth rates for subyearling Chinook salmon swimming behaviors was mostly attributed to differences in P-values. Greater P-values seen in the restricted-area search behavior were due to this behavior directing fish to habitats closer to wetland habitat where temperatures were more optimal. In 2015, growth rates were particularly low, especially for the random walk behavior, when temperatures were anomalously high and positive PDO and ENSO phases occurred. Whereas 2011 was associated with reduced growth rates for yearling Chinook salmon, this year was associated with increased subyearling Chinook salmon growth.

While there appeared to be clear trends in flow regimes and river temperatures that dictated growth rates, large-scale indices were likewise important. This was evident when comparing the low flow years of 2001 and 2015, when migration rates were less and residence times were greater. While growth rates were elevated during both years for yearling Chinook salmon, subyearling Chinook salmon growth rates, especially for the random walk behavior, were not. Positive temperature anomalies in 2015 were associated with positive anomalies in the PDO and ENSO. While these indices were positive in 2015, it was likely the blob that contributed to the unusually warm conditions. Although flows in 2001 were also low, river

temperatures were not nearly as high as they were in 2015. Whereas growth rates in the low flow year of 2015 were reduced, the low flow year of 2001 exhibited the greatest growth rates for subyearling Chinook salmon. Therefore, the trend that low flow years were disadvantageous for subyearling Chinook salmon was not necessarily true. Instead, anomalously warm river temperatures and unusually warm ocean conditions limited growth. When considering the impacts of changing flow regimes and the changes in temperature conditions, both due to warming temperatures and reduced flows, it's important to consider the larger-scale ocean indices as these may act to amplify or decrease the effects of warming temperatures on juvenile Chinook salmon bioenergetics during their estuarine phase.

3.4.4 Spatial Variability Across Estuarine Continuum

Studies that have described migration rates throughout the estuary found rates to vary through specific reaches (Carter et al. 2009; Harnish et al. 2012). JSATS studies from 2004 – 2008 that investigated travel times in the estuary found that yearling Chinook salmon traveled at rates of ~80 km d^{-1} between Bonneville Dam and Vancouver, WA, and at rates of ~60 km d^{-1} between Vancouver, WA and the mouth of the Columbia River. At the estuary mouth between rkm 8.3 and 2.8, yearling Chinook salmon migrated at rates of 100 – 150 km d^{-1}. In 2007 when arrays were placed throughout the lower estuary, yearling and subyearling Chinook were found to migrate more slowly in the last 50 km of the system.

Results from this IBM followed similar trends of increased migration rates in the upstream reaches followed by slower migration rates in the lower estuary, specifically in reach B. Although there were trends across time in migration rates throughout specific hydrogeomorphic reaches, similar spatial trends were observed over time. Reduced migration

rates in the lower estuary suggest where in the estuary juvenile Chinook salmon spend more time which could help inform where in the estuary field studies should be concentrated.

Spatial trends in growth rates for yearling Chinook salmon showed similar patterns for the two simulated behaviors, with increased growth through reaches C – F and decreased growth in reaches A and B. For subyearling Chinook salmon, growth rates were likewise elevated through these reaches for the random walk behavior, in addition to reach H. While the restricted-area search behavior also had greater growth occurring in reaches C – F and H, growth rates are also high in reach B. Since growth rates were dependent on P-values which were based on the proximity to wetland habitat, growth rates were largely a reflection of the influence of wetland habitat in each reach. Since there was a lot more open water in reaches A and B near the mouth, individuals were less likely to come into close contact with productive wetland habitats. The restricted-area search behavior was unique in this case as individuals were directed to regions with high growth rates. Thus, while migrating through reach B, these individuals were more likely to move through the lateral bays where there was more wetland habitat available. Their increased contact with these habitats was evident in the higher growth rates in this reach.

3.4.5 Model Weaknesses

This IBM was effective for exploring trends in migration and growth patterns and the relationship with environmental drivers, including river flow, river and ocean temperatures, and large-scale indices. However, there were many simplifying assumptions that likely influenced model behavior, and it is important to account for these. Some of the limitations of the IBM include how swimming behaviors were parameterized, the exclusion of important drivers, and how P-values and prey energy densities were approximated. While the IBM was a useful

exploratory tool for understanding juvenile Chinook salmon estuarine migration, limitations in the design of the IBM require that results be interpreted with caution.

Swimming behaviors were modeled based on the current understanding of how yearling and subyearling Chinook salmon utilize estuarine habitat. It is generally accepted that yearling Chinook salmon spend less time in the estuary and migrate more quickly through the system, which justifies the use of a swimming behavior that optimizes downstream migration. Similarly, it is recognized that subyearling Chinook salmon spend greater amounts of time in the estuary, so a behavior that directs individuals to take advantage of growth opportunities in the system during their outmigration is defensible. However, animal behavior is constantly changing, and it is naïve to assume that a fish employs strict rules as are necessary in an IBM to migrate through a dynamic habitat. To simplify across all swimming behaviors, a constant swim speed of 1 BL s^{-1} was used; however, it's highly unlikely that individuals maintain a constant swimming speed. In addition, the methods used to encourage subyearling Chinook salmon movement away from local optima and outmigration were likely inappropriate. However, without these additional behavioral rules to keep individual fish moving on to the next habitat or to exit the estuary, simulated individuals would not be prompted to ever leave the estuary.

An additional limitation of the IBM was that it did not consider competition or the impacts of predation. Since this study was primarily interested in investigating the influence of interannual variability on migration patterns, including predation was deemed unnecessary; however, future iterations of this work will consider predation as it would likely influence the outcomes of the IBM with regards to migration rates, residence times, survival, and growth rates. Similarly, competition and density-dependent interactions were not accounted for in this IBM as the process for implementing competition and density dependence was deemed overly

complicated. However, competition for resources related to the density of fish in a given area would likely impact swimming behaviors, particularly for the restricted-area search behavior that was based on optimizing growth. Including competition would have likely reduced residence times in areas of high growth since competition amongst an increasing number of individuals would limit prey resources. In general, it is highly likely that the presence and behaviors of other individuals occupying similar or nearby habitats would influence the behaviors and decision-making of others if density-dependent interactions were considered.

Although the way P-values were parameterized in this chapter were slightly more complex than what was used in Chapter 2, there were still drawbacks and simplifications associated with the constant prey energy density used and how P-values were assigned to elements. Bioenergetics models are strongly influenced by prey quality (Beauchamp et al. 1989). By using a constant prey energy density, this model did not account for how prey types vary throughout the estuary and how their abundance varies over time, thereby limiting the impact of these results from the bioenergetics model. Similarly, basing P-values on the proximity to wetland habitat does not accurately reflect how productive certain parts of the estuary are and instead assumes that all wetland habitats and the neighboring area are sufficiently productive. By not including a feedback process with the bioenergetics model, there was no competition for food resources by individuals occupying the same area, nor was there a drawdown of food resources which would happen in a real system. While it would be ideal to attempt to mimic processes and food availability in the IBM, this would be challenging to implement, and instead, many simplifying assumptions are used.

3.5 Conclusions

Despite limitations in its implementation, this IBM proved effective for exploring how interannual variability influences juvenile Chinook salmon migration in the Columbia River estuary and how migration behaviors and growth differ along the estuarine continuum. Simulations were conducted for two life-history types to identify how environmental forcing and potential swimming behaviors differentially impact migration histories. Flow regimes were the primary drivers of estuarine migratory behavior, where high flows were associated with faster migration rates and reduced residence times, and low flows were associated with longer residence times and reduced migration rates. Above average water temperatures were often associated with years when flows were reduced, and this impacted yearling and subyearling Chinook salmon differently. While yearling Chinook salmon benefited from lower flows associated with warm spring temperatures in terms of growth, subyearling Chinook salmon were negatively impacted during low flow years when summer temperatures were abnormally warm.

Although it did not factor in management decisions on juvenile salmon migration in the estuary, this model could prove useful for anticipating migration and growth rates under different flow management scenarios. This IBM builds upon previous work that characterized physical habitat and how that varied across the hydrogeomorphic reaches. However, this work improves upon that technique and instead highlights how migration rates differ throughout the system which has implications for the amount of time individuals are spending in various parts of the estuary. By accounting for residence times and regions where juvenile Chinook salmon spend their estuarine migration, using models that characterize habitat availability can be more effectively interpreted based on the duration of residence described by an IBM.

Tables

Table 3.1. Run timing, including the range of release dates and the days that simulations ended, as well as starting lengths used across yearling and subyearling Chinook salmon populations.

Life-History	Run Timing	Release Dates		Simulation Ends	Starting Length (mm)
		First	Last		
Yearling	May 11 ± 14	March 7	July 8	August 6	141 ± 15
Subyearling	July 3 ± 16	April 20	September 7	November 6	95 ± 13

Table 3.2. Proportion of maximum consumption (P-values) assigned to elements based on the distance from the nearest neighboring wetland habitat.

Distance (m)	P-Value
<= 100	0.9
100 < *d* <= 300	0.8
300 < *d* <= 500	0.7
500 < d <= 750	0.6
750 < d <= 1000	0.5
1000 < d	0.4

Table 3.3. Simulated behaviors for subyearling (CH0) and yearling (CH1) Chinook salmon.

Behavior	Life Stage	Description
Passive particle	CH0, CH1	No active swimming
Random walk	CH0, CH1	Random swimming angles
Biased correlated random walk	CH1	Swimming direction correlated to previous time step and biased towards target
Restricted-area search	CH1	Nearest-neighbor search using growth rate based on depth-averaged temperature

Table 3.4. Median travel times (days) to Jones Beach for observed and simulated yearling Chinook salmon from 2000 – 2015.

Year	Observed	Passive	Random walk	Biased Correlated Random Walk
2000	1.7	1.8	1.9	1.7
2001	2.3	3.2	3.4	2.9
2002	1.8	2.1	2.2	1.8
2003	1.8	2.0	2.1	1.8
2004	1.9	2.2	2.3	2.0
2005	1.8	2.2	2.3	2.0
2006	1.7	1.6	1.7	1.5
2007	1.7	2.0	2.1	1.8
2008	1.7	1.8	1.9	1.7
2009	1.7	1.9	1.9	1.7
2010	2.0	2.4	2.5	2.1
2011	1.5	1.7	1.7	1.5
2012	1.6	1.5	1.6	1.4
2013	1.6	1.7	2.0	1.7
2014	1.6	1.7	1.8	1.6
2015	2.1	2.6	2.8	2.3

Table 3.5. Mean river flows, median residence times, and median migration rates from 2000 – 2015 for passive particles and simulated yearling Chinook salmon behaviors (RW = random walk, BCRW = biased correlated random walk). Median growth rates for simulated yearling Chinook salmon are also included. Values represent rates from Bonneville Dam to the estuary mouth.

Year	Mean Flow ($1000\ m^3\ s^{-1}$)	Residence Time (d)			Migration Rate ($km\ d^{-1}$)			Growth Rate ($mm\ d^{-1}$)	
	March 7 – July 8	Passive	RW	BCRW	Passive	RW	BCRW	RW	BCRW
2000	6.7	4.14	4.32	3.83	64.8	62.5	71.2	0.39	0.40
2001	3.7	6.91	7.26	6.52	46.9	44.8	50.5	0.44	0.47
2002	6.8	4.53	4.70	4.19	60.3	58.2	66.1	0.34	0.35
2003	6.4	4.41	4.65	4.13	62.0	59.0	67.5	0.36	0.37
2004	5.8	4.99	5.23	4.68	57.2	54.7	62.9	0.46	0.47
2005	5.1	4.84	5.06	4.51	58.2	55.2	63.4	0.44	0.45
2006	8.0	3.53	3.68	3.29	71.5	69.1	78.2	0.41	0.43
2007	6.6	4.34	4.53	4.06	62.1	59.5	67.6	0.42	0.43
2008	7.3	3.91	4.14	3.67	65.6	63.0	71.9	0.35	0.36
2009	6.6	3.96	4.19	3.73	65.3	62.3	70.2	0.30	0.31
2010	5.7	5.20	5.44	4.87	55.3	53.0	60.6	0.37	0.39
2011	10.1	3.50	3.60	3.25	73.2	71.1	79.7	0.31	0.31
2012	9.2	3.16	3.33	2.98	78.5	74.8	83.8	0.38	0.40
2013	6.7	3.86	4.30	3.85	70.8	62.6	70.8	0.44	0.45
2014	7.8	3.66	3.87	3.47	70.7	67.1	75.8	0.41	0.42
2015	5.1	5.74	6.03	5.47	53.3	50.9	57.7	0.46	0.48

Table 3.6. Mean river flows, residence times, and migration rates from 2000 – 2015 for passive particles and simulated subyearling Chinook salmon (RW = random walk, RAS = restricted-area search). Growth rates for simulated subyearling Chinook salmon are also included. Values represent rates from Bonneville Dam to the estuary mouth.

Year	Mean Flow ($1000\ m^3\ s^{-1}$)	Residence Time (d)			Migration Rate ($km\ d^{-1}$)			Growth Rate ($mm\ d^{-1}$)	
	Apr. 20 – Sep. 7	Passive	RW	RAS	Passive	RW	RAS	RW	RAS
2000	5.9	5.65	5.83	16.02	52.6	51.3	23.1	0.38	0.62
2001	3.3	9.58	9.93	31.55	41.9	40.6	17.2	0.41	0.65
2002	6.6	4.25	4.38	7.10	63.6	62.0	41.5	0.38	0.54
2003	5.8	6.17	6.34	16.90	50.8	49.7	22.8	0.37	0.61
2004	5.6	5.88	6.14	17.33	51.2	49.8	22.0	0.35	0.58
2005	5.1	5.67	5.88	14.85	51.7	50.3	23.1	0.37	0.61
2006	7.0	5.20	5.32	13.02	55.2	54.2	25.2	0.36	0.59
2007	5.6	5.81	5.96	15.35	51.4	50.1	22.6	0.37	0.62
2008	6.9	3.95	4.11	9.32	65.8	63.4	32.8	0.38	0.56
2009	5.9	5.60	5.77	13.57	52.4	51.1	25.4	0.38	0.57
2010	5.7	4.72	4.86	10.27	59.4	57.7	30.6	0.39	0.58
2011	9.3	3.11	3.21	6.27	80.0	77.9	43.5	0.40	0.59
2012	8.6	3.40	3.51	5.58	74.2	72.2	48.2	0.38	0.52
2013	6.2	4.92	5.01	9.06	58.4	57.1	35.1	0.36	0.54
2014	6.7	4.59	4.68	7.51	61.3	59.9	39.6	0.35	0.52
2015	4.3	6.79	7.00	28.45	48.1	46.8	15.6	0.19	0.55

Figures

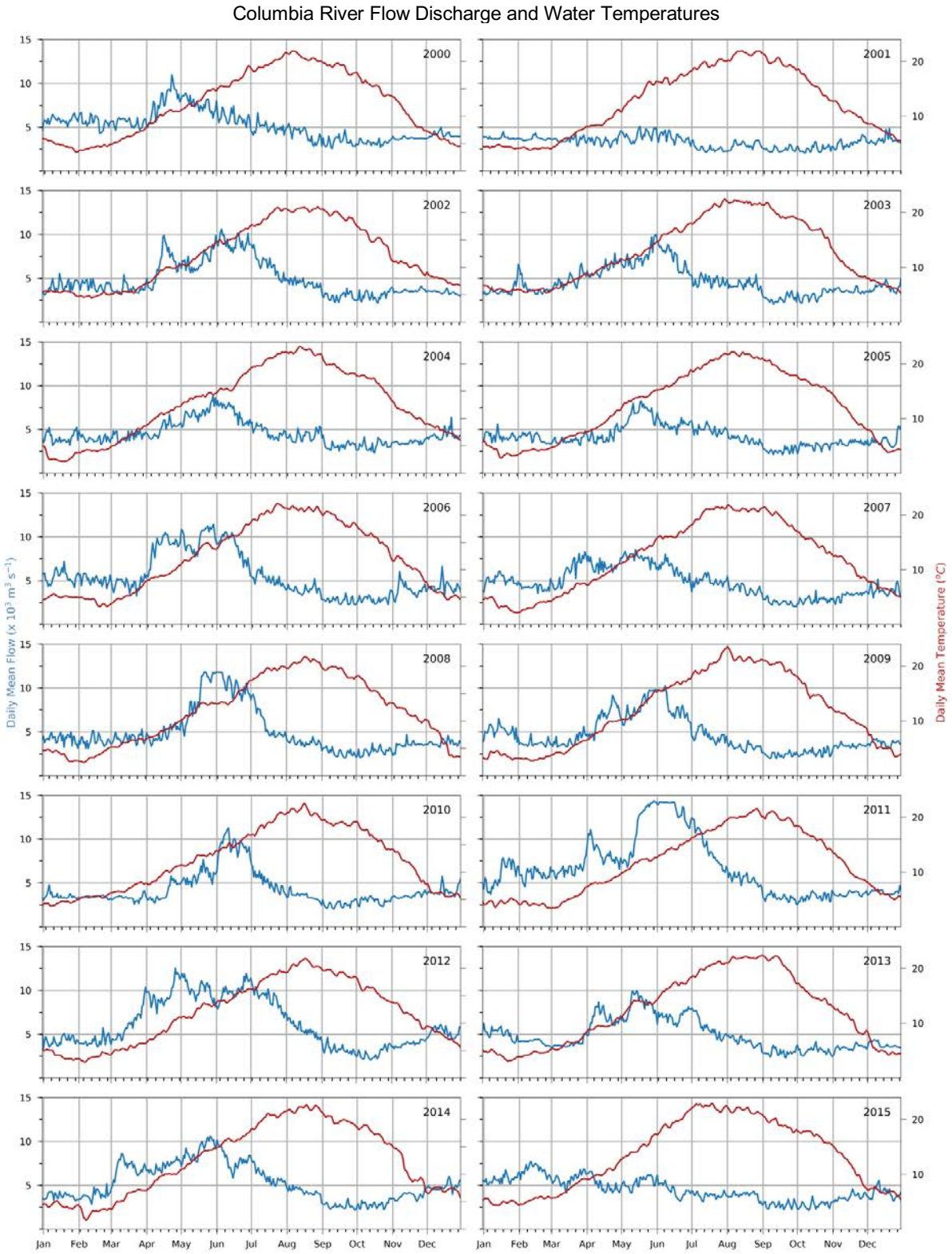

Figure 3.1. Daily mean flows ($m^3 s^{-1}$) and daily mean temperatures (°C) from 2000 – 2015.

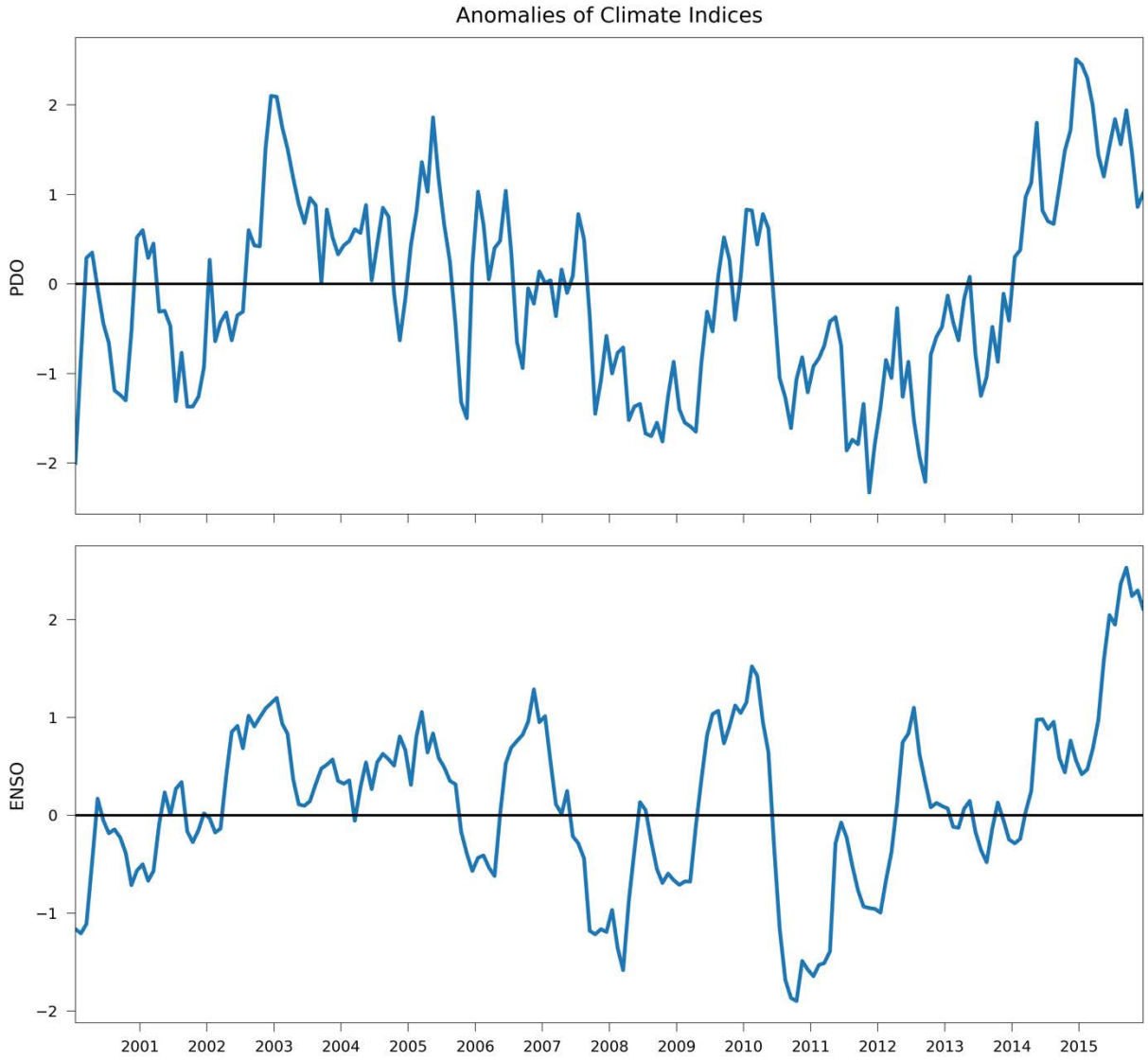

Figure 3.2. Monthly anomalies for the Pacific Decadal Oscillation (PDO) and El Niño-Southern Oscillation (ENSO) for 2000 – 2015.

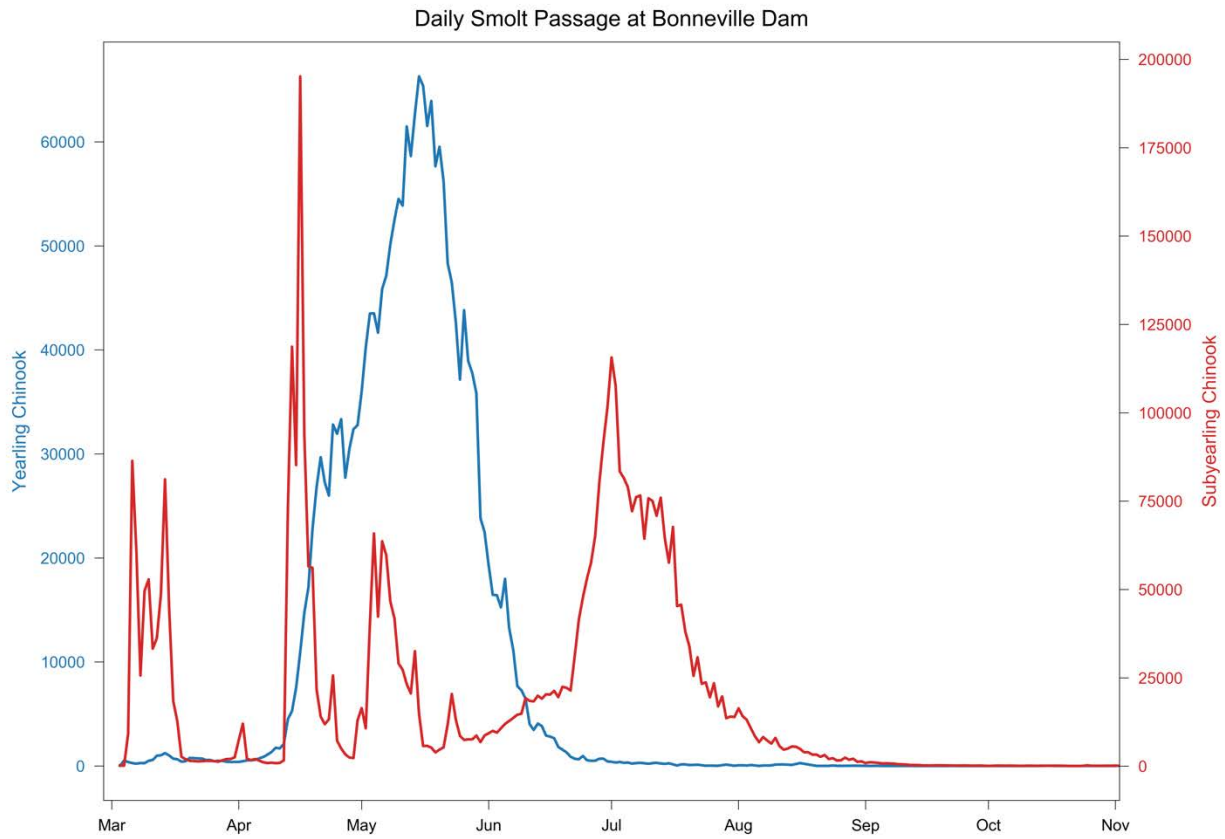

Figure 3.3. Daily smolt passage at Bonneville Dam for yearling and subyearling Chinook salmon, averaged over 2000 – 2015.

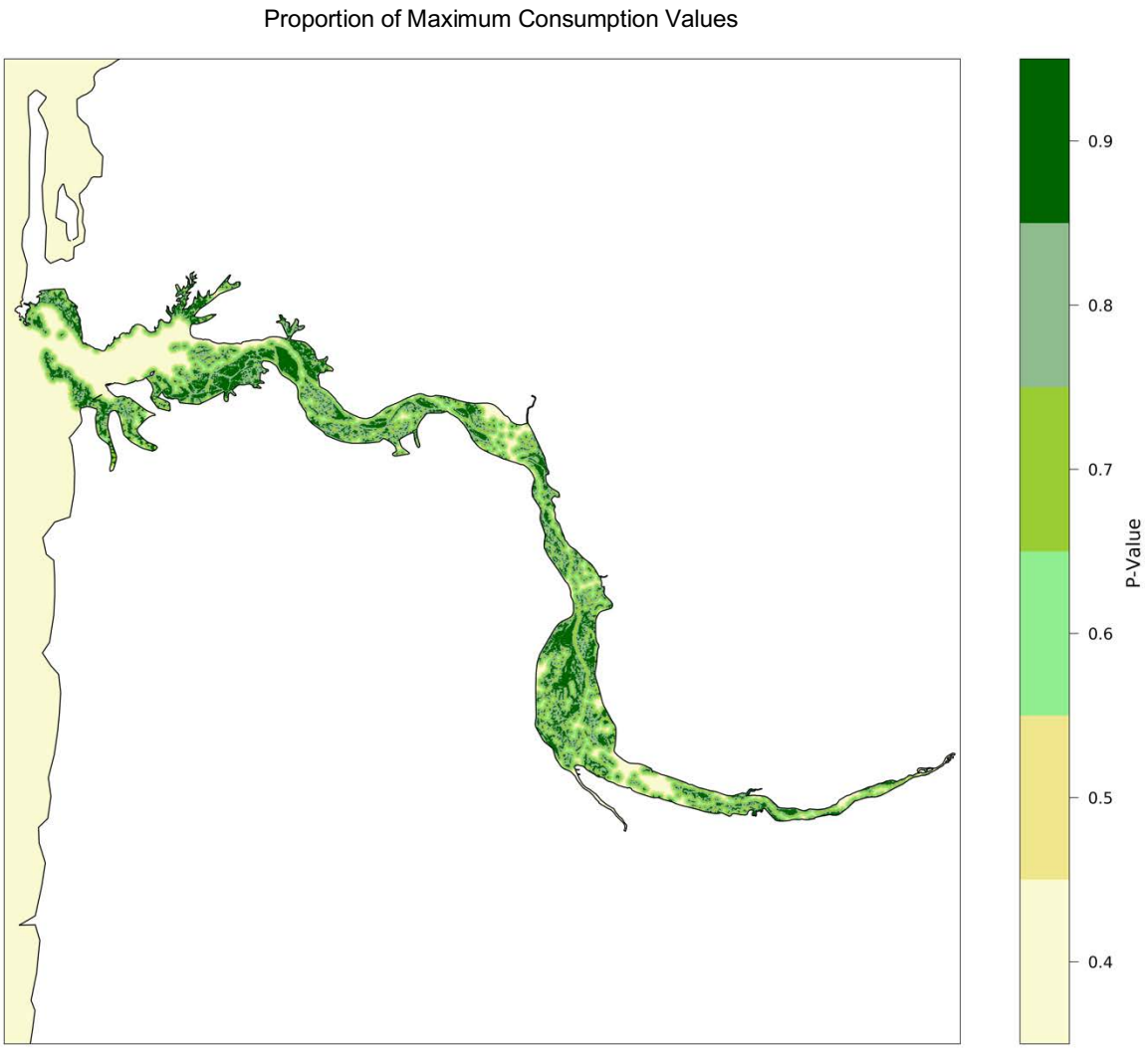

Figure 3.4. Proportion of maximum consumption values (P-values) used in the bioenergetics model based on proximity to wetland habitat.

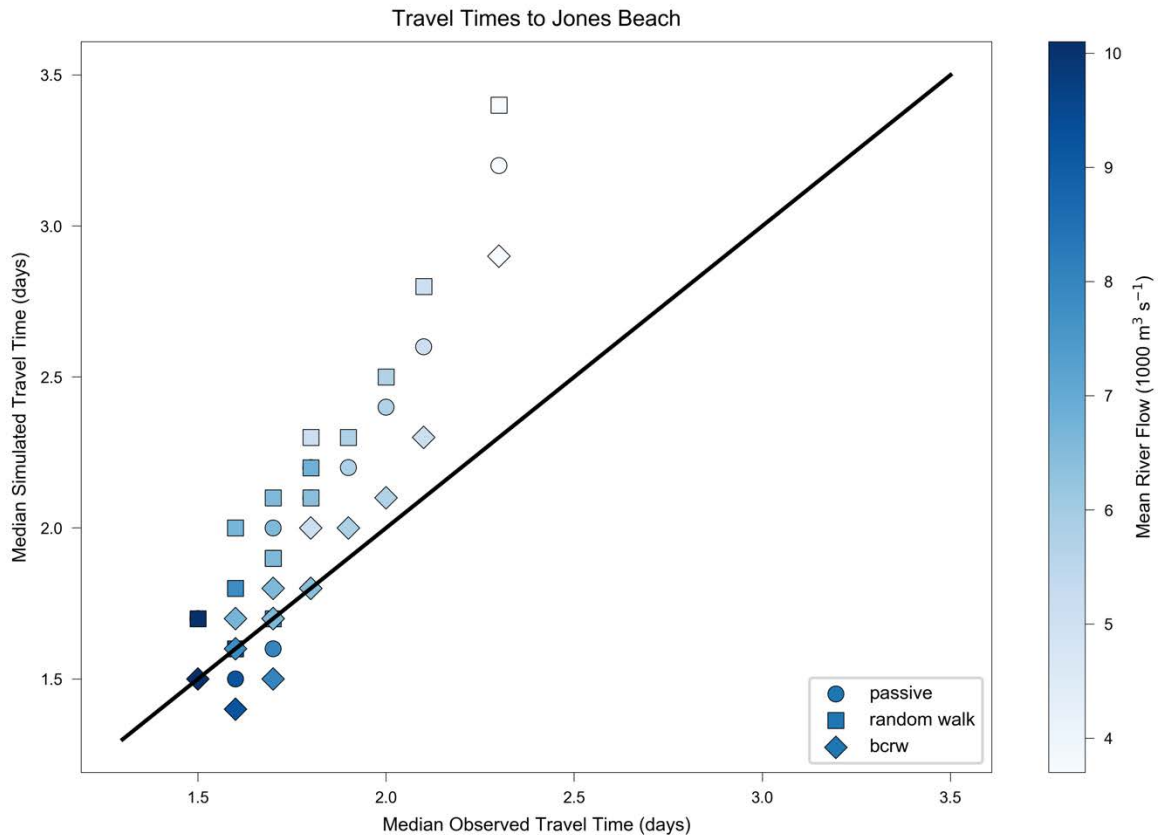

Figure 3.5. Median travel times to Jones Beach for yearling Chinook salmon from 2000 – 2015, including observed times (*x-axis*) and simulated travel times (*y-axis*) for passive, random walk, and biased correlated random walk behaviors. Points are colored by the mean flow rates at Bonneville Dam from March 7 – July 8, associated with the simulated release dates.

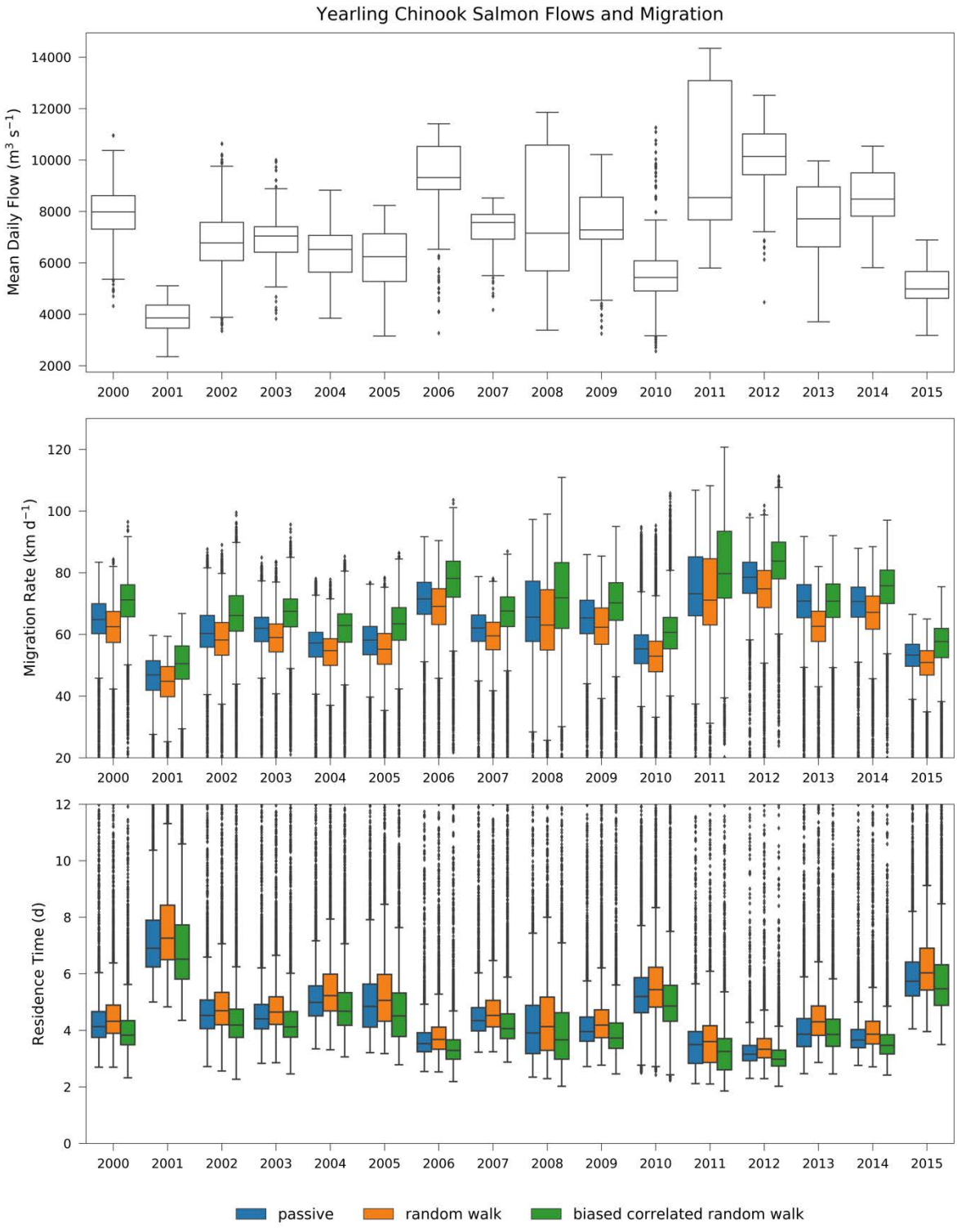

Figure 3.6. (*top*) Mean daily flows (m^3 s^{-1}) at the time of initialization near Bonneville Dam for yearling Chinook salmon simulations, as well as migration rates (km d^{-1}) (*middle*), and estuarine residence times (d) (*bottom*) for passive, random walk, and biased correlated random walk behaviors.

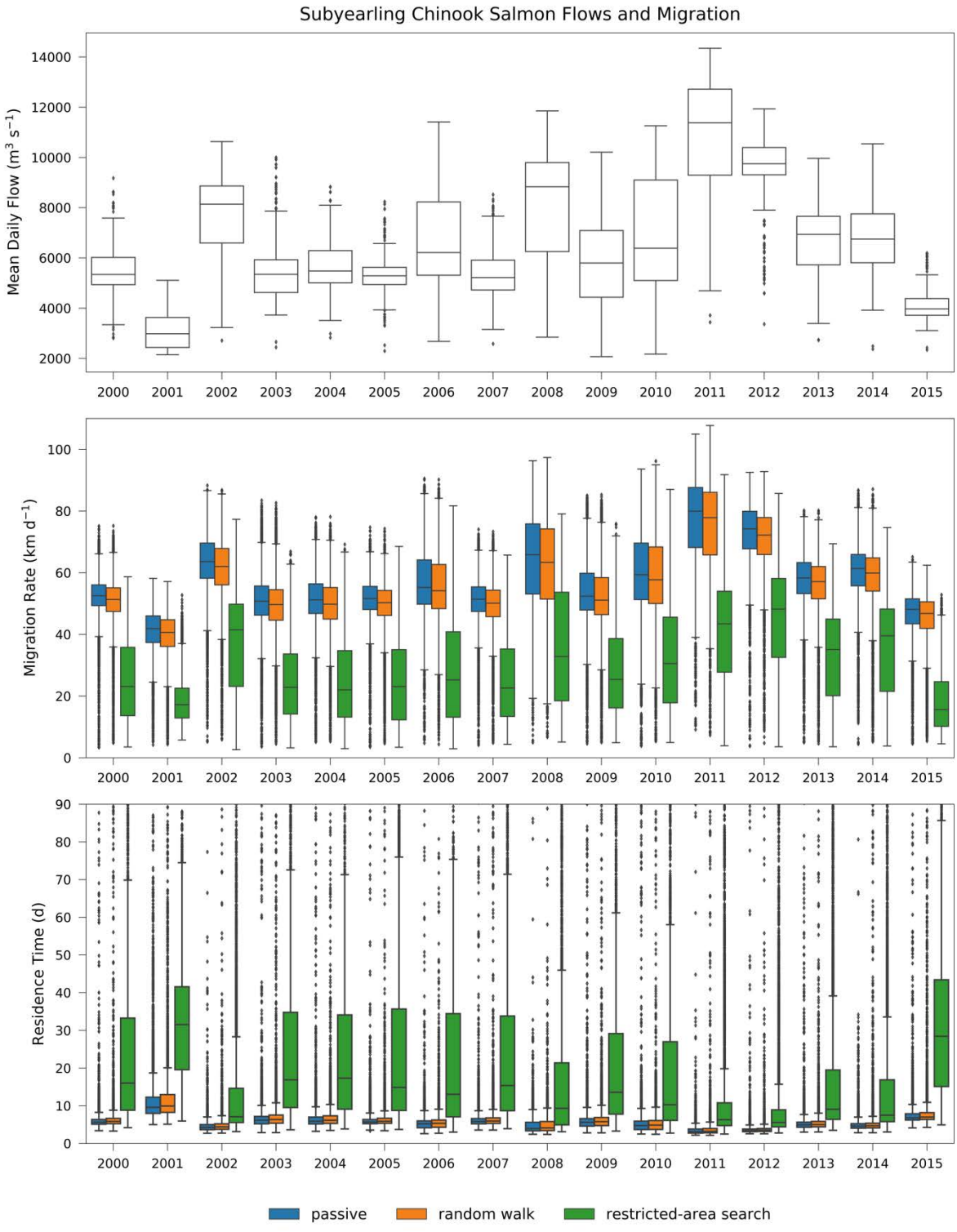

Figure 3.7. (*top*) Mean daily flows ($m^3 s^{-1}$) at the time of initialization near Bonneville Dam for subyearling Chinook salmon simulations, as well as migration rates (km d^{-1}) (*middle*) and estuarine residence times (d) (*bottom*) for passive, random walk, and restricted-area search behaviors.

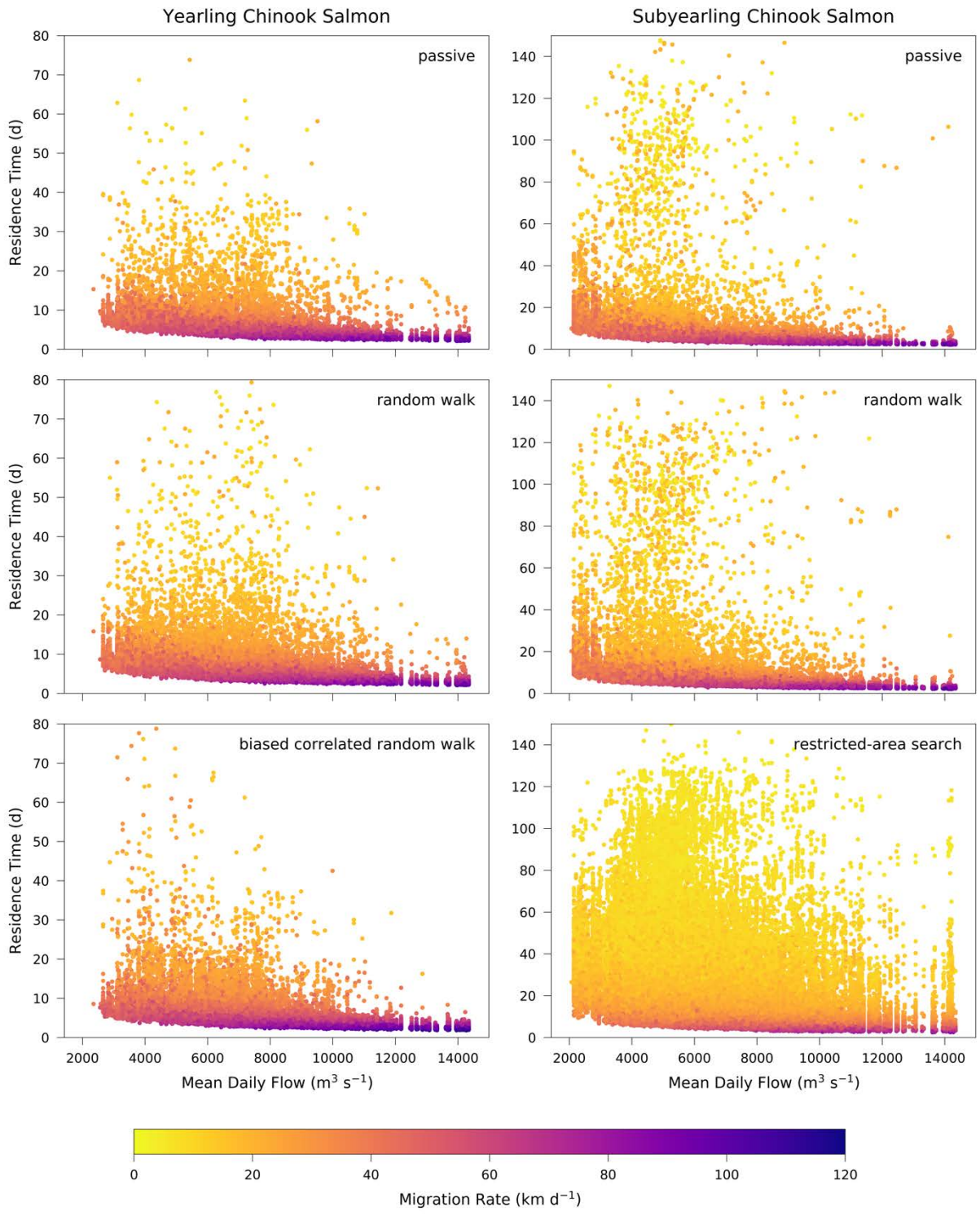

Figure 3.8. Yearling (*left*) and subyearling (*right*) Chinook salmon daily mean flow at initialization (m^3 s^{-1}) and estuarine residence times (d) colored by migration rates (km d^{-1}).

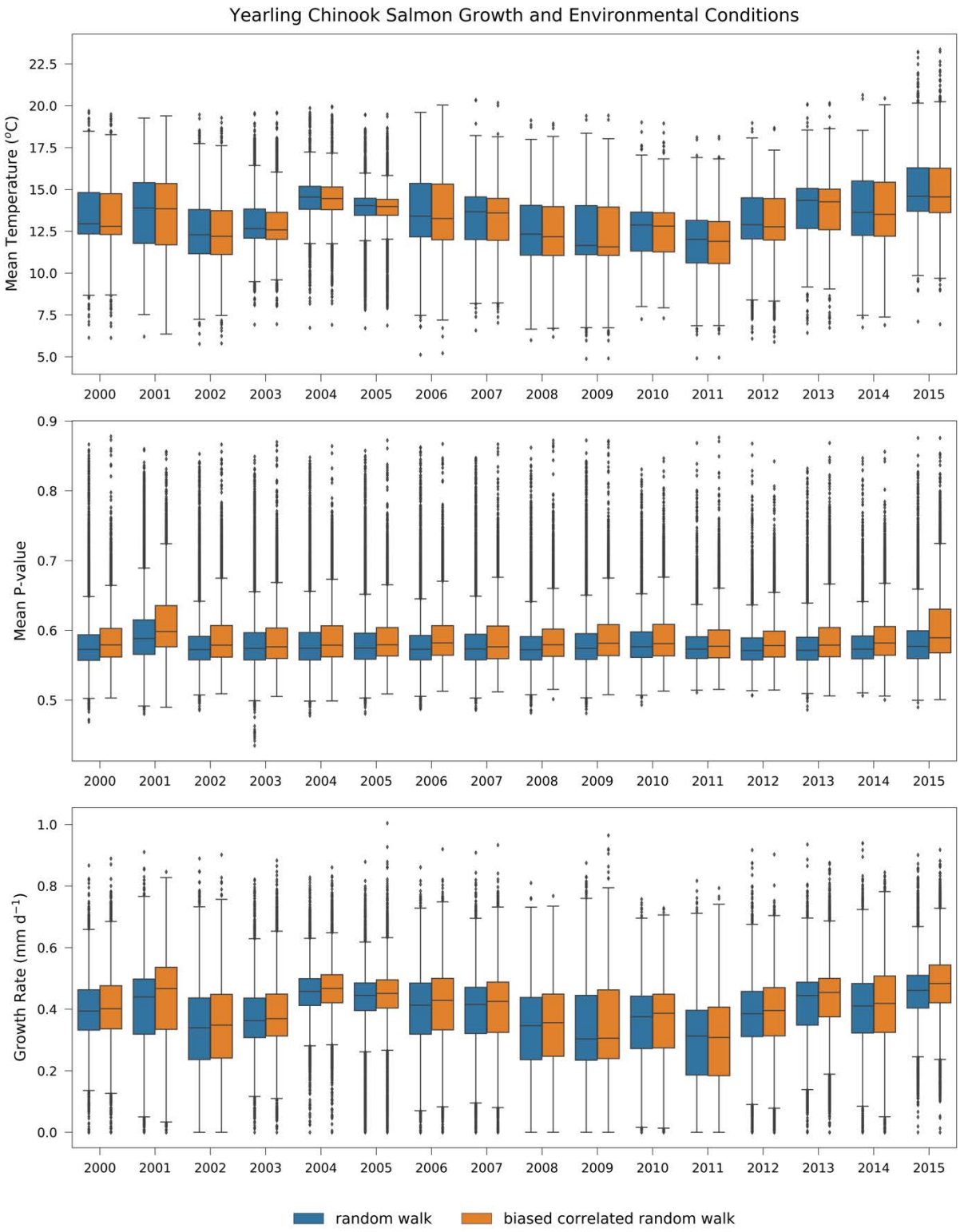

Figure 3.9. Mean temperatures (°C) (*top*) and mean P-values (*middle*) experienced by all individuals as well as growth rates for yearling Chinook salmon random walk and biased correlated random walk behaviors.

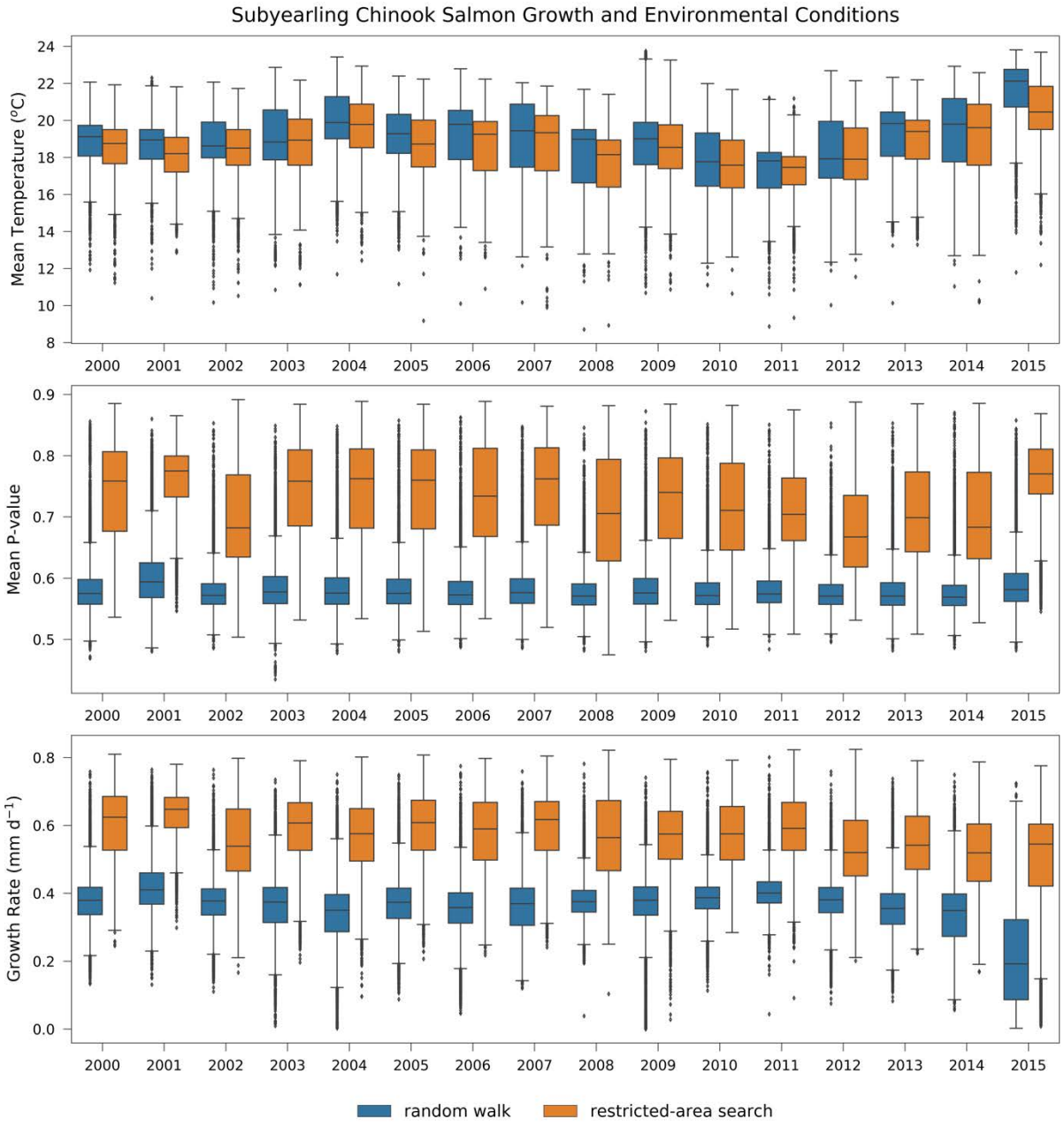

Figure 3.10. Mean temperatures (°C) (*top*) and mean P-values (*middle*) experienced by all individuals as well as growth rates for subyearling Chinook salmon random walk and restricted-area search behaviors.

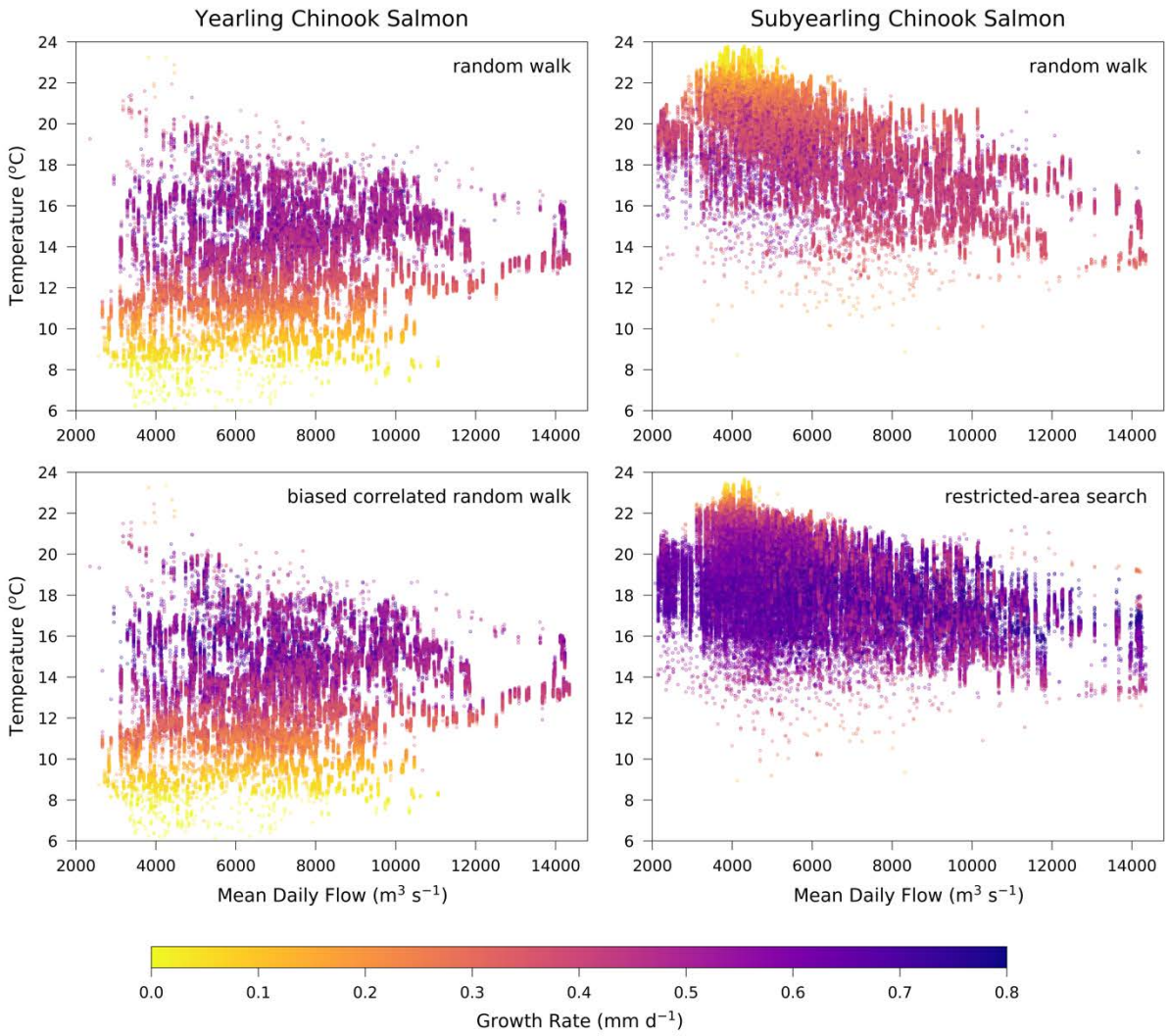

Figure 3.11. Mean daily flow (m^3 s^{-1}) upon initialization and mean temperatures (°C) experienced by simulated fish colored by their daily growth rate (mm d^{-1}) during their estuarine residence.

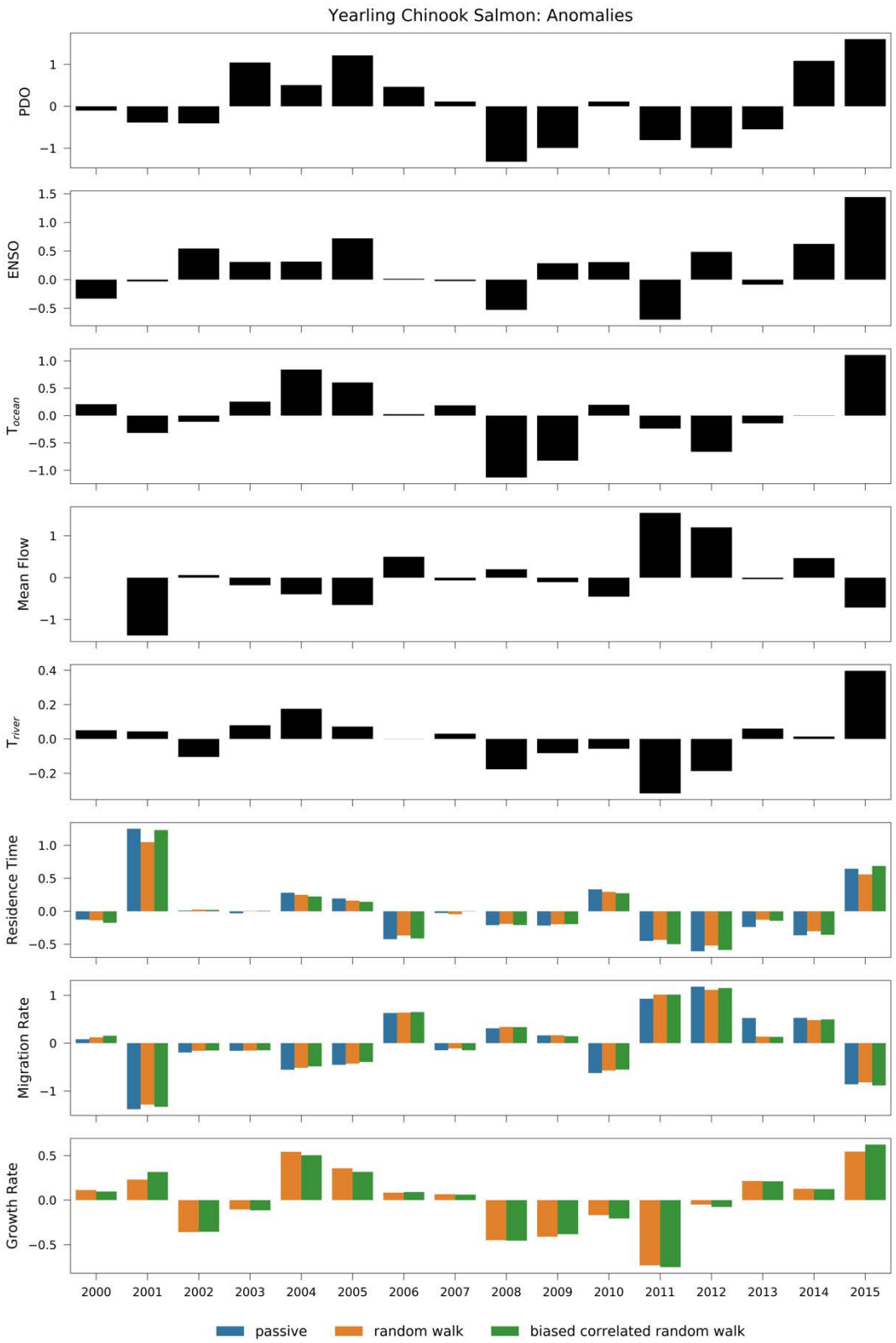

Figure 3.12. Ocean indices, river discharge, and river temperature anomalies over time averaged over the period that yearling Chinook salmon were simulated (March through July). Z-scores are also shown for residence times, migration rates, and growth rates, computed for each behavior.

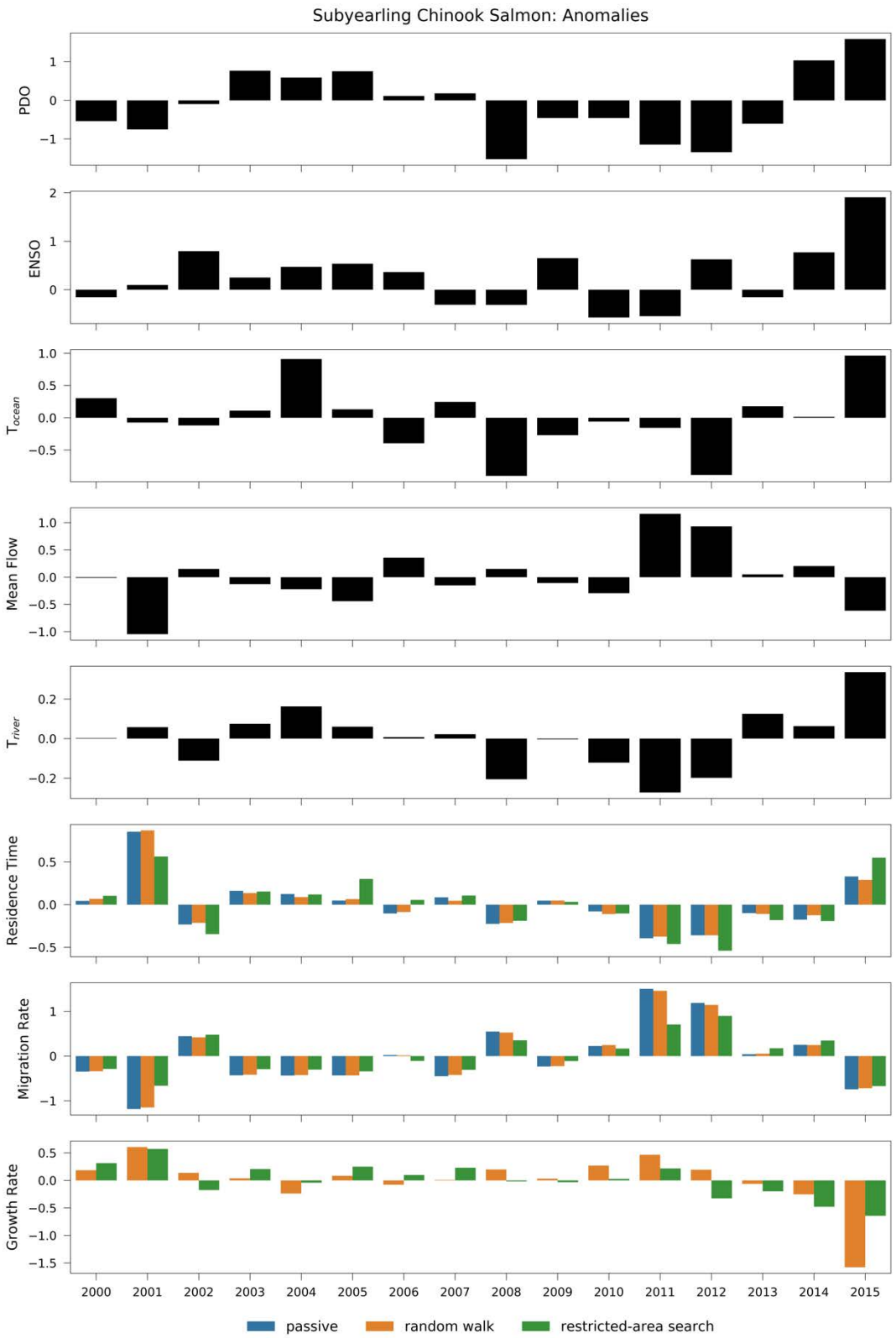

Figure 3.13. Ocean indices, river discharge, and river temperature anomalies over time averaged over the period that subyearling Chinook salmon were simulated (April through September). Z-scores are also shown for residence times, migration rates, and growth rates.

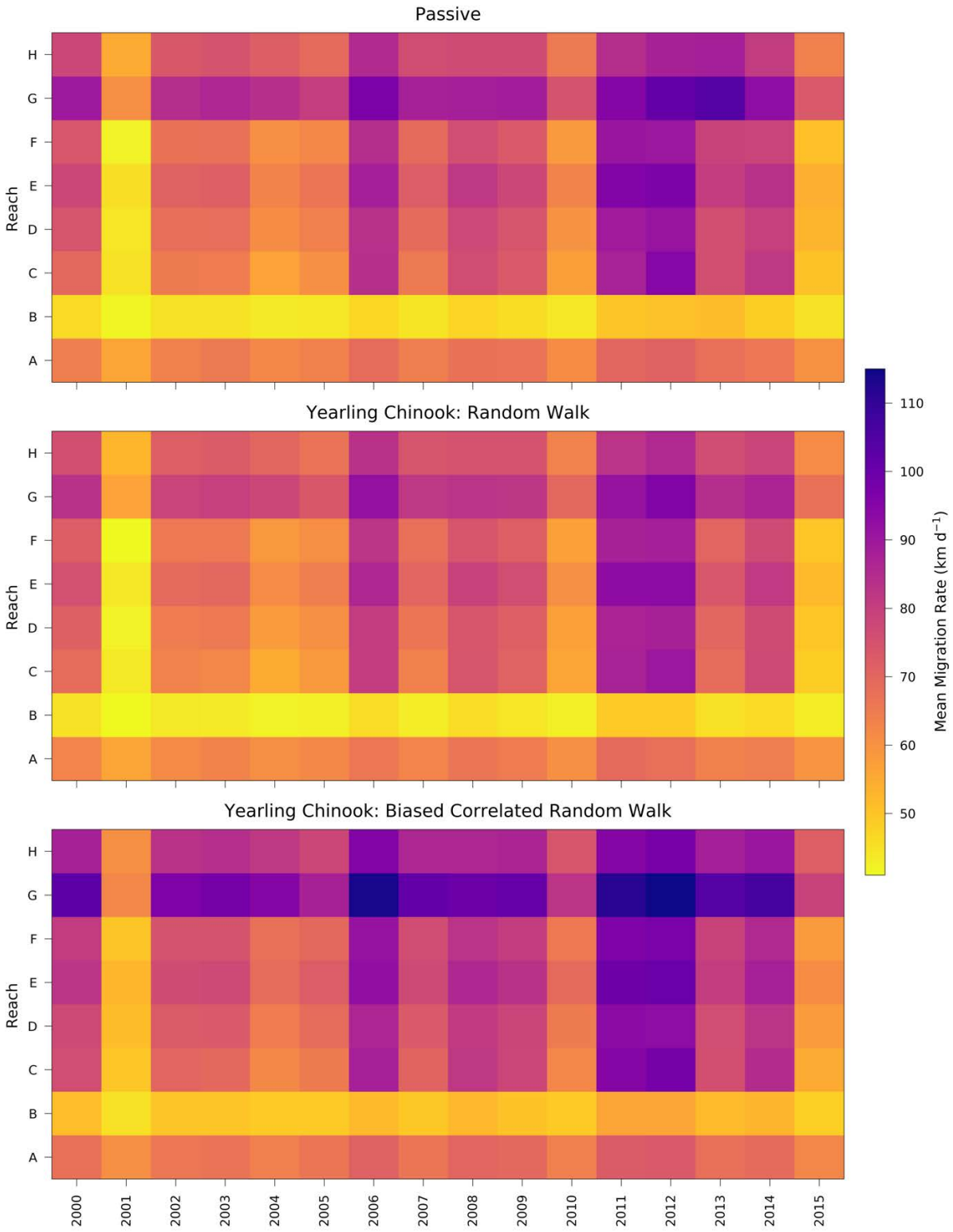

Figure 3.14. Mean migration rate (km d^{-1}) from 2000 - 2015 across hydrogeomorphic reaches for passive particles (*top*), the random walk behavior (*middle*), and the biased correlated random walk behavior (*bottom*) for yearling Chinook salmon.

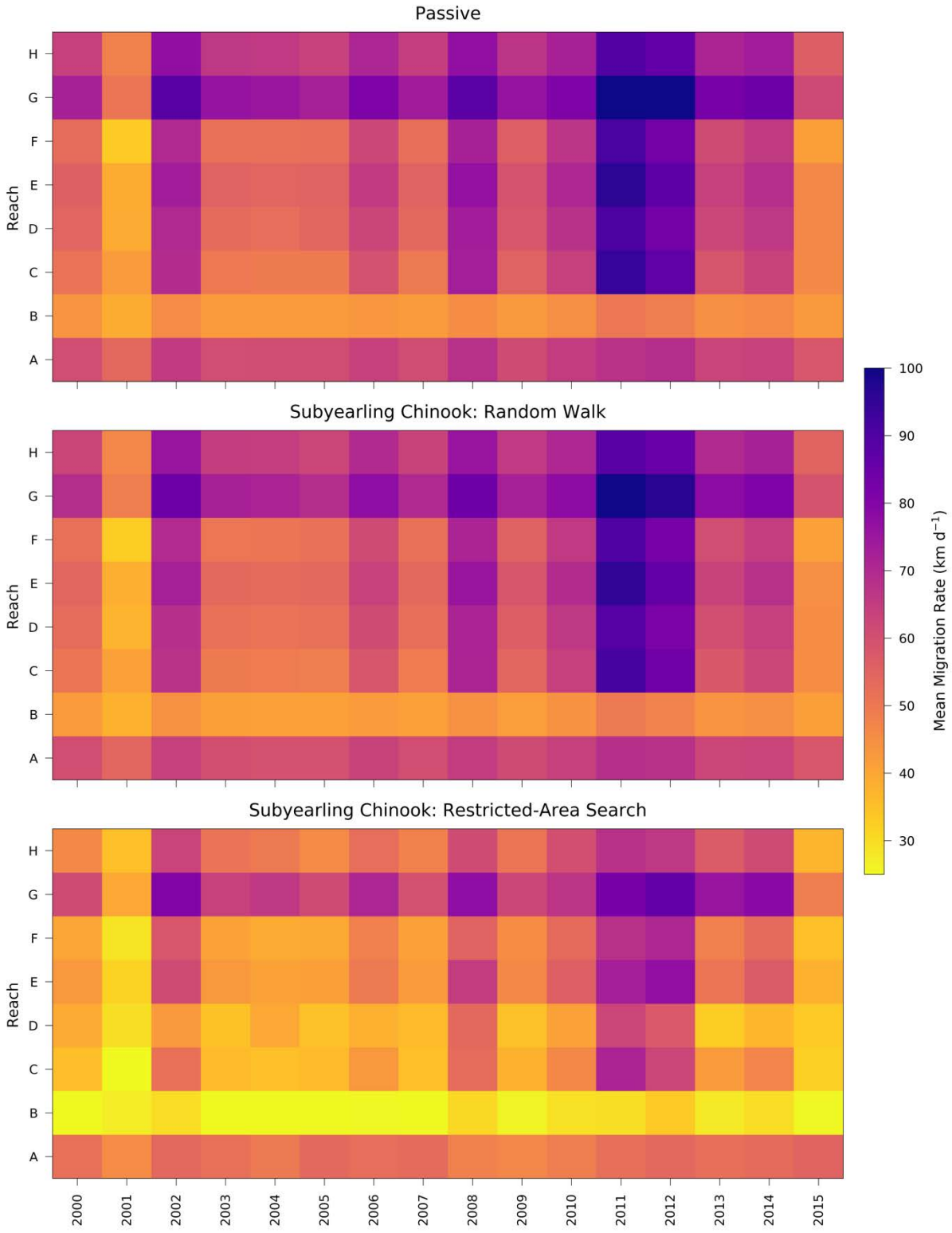

Figure 3.15. Mean migration rate (km d^{-1}) from 2000 – 2015 across hydrogeomorphic reaches for passive particles (*top*), the random walk behavior (*middle*), and the restricted-area search behavior (*bottom*) for subyearling Chinook salmon.

Figure 3.16. Mean growth rate (mm d^{-1}) from 2000 - 2015 across hydrogeomorphic reaches for random walk (*middle*) and biased correlated random walk (*bottom*) behaviors for yearling Chinook salmon.

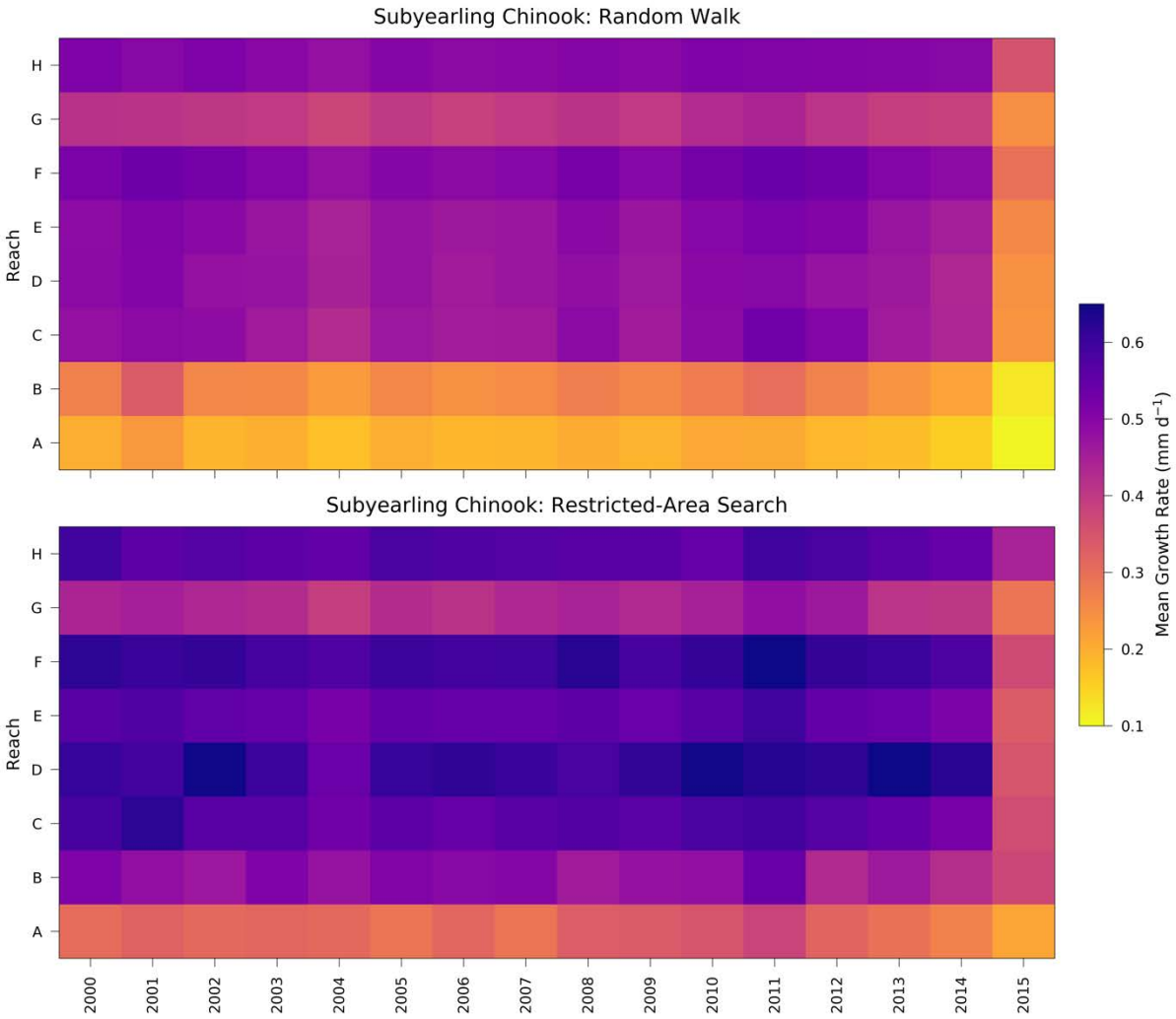

Figure 3.17. Mean growth rate (mm d^{-1}) from 2000 - 2015 across hydrogeomorphic reaches for random walk (*middle*) and restricted-area search (*bottom*) behaviors for subyearling Chinook salmon.

4 Modeling predation impacts along juvenile Chinook salmon migration pathways

Abstract

An individual-based model was used to explore how simulated predation impacts by avian predators in the lower Columbia River estuary influence patterns of survival in yearling Chinook salmon across different flow regimes. The IBM used a super-individual approach as well as a spatially- and temporally-varying predation model based on the foraging ranges of two common avian predators, Caspian terns and double-crested cormorants. In addition, the presence of marine forage fish as an alternate prey was considered in the predation model and was approximated based on the salinity intrusion length, which relates to the magnitude of river discharge. Years 2010 – 2015 were modeled to capture a range of flow regimes, and multiple swimming behaviors were modeled. Simulation results, including residence times, growth rates, and the percent of surviving individuals were assessed to identify how patterns in river discharge influence survival of outmigrating yearling Chinook salmon. In addition, migration pathways were analyzed to identify pathways associated with increased survival and growth. Results from the IBM showed that the percent survival was strongly related to individual residence times. Since residence times were driven by flow conditions, river discharge largely determined the number of simulated individuals lost due to predation. In years where flows were elevated, there were more individuals that successfully exited the estuary, whereas in low flow years, there were more individuals lost to predation. Although patterns across the lower estuary seemed to suggest that pathways with increased survival were associated with below-average growth rates, there was no clear relationship between the two.

4.1 Introduction

Since the late-1800s, there have been major declines in Pacific salmonid populations in the Columbia River basin (Bottom et al. 2005). Of the twenty recognized evolutionarily significant units (ESUs) in the system, thirteen are listed under the Endangered Species Act as threatened or endangered (https://www.fisheries.noaa.gov/species-directory/threatened-endangered). A number of factors have contributed to these population declines, including hydroelectric dams, overharvesting, and loss of wetland habitat (Bottom et al. 2005). The increasing reliance on hatcheries as a management strategy to maintain populations has likewise been problematic, leading to reduced genetic diversity. Aside from more direct anthropogenic stressors, the effects of climate change, including warming river temperatures and changes to seasonal flow patterns, pose additional threats.

For outmigrating juvenile salmonids, factors such as predation, delayed mortality associated with hydrosystem experiences (Schaller and Petrosky 2007), and rear type influence survival. Between Bonneville Dam and the Columbia River estuary, juvenile salmon populations are impacted by piscine (Zimmerman 1999), pinniped (Laake et al. 2002), and avian predators (Collis et al. 2002; Ryan et al. 2003). In the lower river upstream of the estuary, northern pikeminnow (*Ptychocheilus oregonensis*) are a common piscine predator (Ward et al. 1995). Although piscine and pinniped predation are recognized as important, more is known about avian predation impacts on juvenile salmonid abundance than other predators in the system. Predation by piscivorous colonial waterbirds is also considered one of the greatest mortality factors for juvenile salmonids in the Columbia River estuary (Evans et al. 2012).

In the late 20th century, there was a dramatic increase in waterbird populations in the lower river and estuary, with estimated values of more than 80,000 individuals (Collis et al.

2002), and the most common taxa including Caspian terns (*Hydroprogne caspia*), double-crested cormorants (*Phalacrocorax auritus*), and several gull species (*Larus* spp.). The Columbia River estuary was eventually recognized as having one of the largest colonies of double-crested cormorants and Caspian terns on the Pacific Coast and in North America. The creation of artificial dredge spoil islands due to dredging activity throughout the 1900s contributed to this region's popularity for nesting sites. In addition, the overlap between the breading seasons of avian predators with the migration timing of juvenile salmonids provided abundant food resources (Collis et al. 2002).

Research on avian predation impacts in the late 1990s indicated that the number of juvenile salmonids lost to avian predation based on PIT tags observed on Rice Island was in the millions (Collis et al. 2001). This led to efforts to discourage nesting on Rice Island and the relocation of avian predator colonies to East Sand Island near the mouth of the estuary where marine forage fish were more abundant (Roby et al. 2002). Despite the relocation, predation on salmonids has remained high in the lower estuary due to the large populations of Caspian terns and double crested cormorants, which has prompted further investigation.

There have been numerous studies that quantified avian predator impacts on juvenile salmonids, including detections of PIT-tags deposited near or on the nesting colonies on East Sand Island to assess predation rates (Evans et al. 2012; Sebring et al. 2013a; Sebring et al. 2013b). Sebring et al. (2013b) estimated predation rates of PIT-tagged Chinook, coho, and sockeye salmon that were detected at Bonneville Dam by Caspian terns and double-crested cormorants of less than 4%; however, this was a conservative estimate as it did not account for PIT-tags that were not deposited on land. Bioenergetics modeling studies have also been used to estimate the consumption rate of smolts by double-crested cormorants, an analog of predation

probability, that has proven useful to assess potential predation impacts at the species level (Lyons et al. 2014).

Both Caspian terns and double-crested cormorants have ranges outside of their nesting locations where foraging activity is increased. The foraging range of double-crested cormorants is approximately 40 km (Custer and Bunck 1992), and they primarily forage in freshwater and marine mixing zones within the estuary (Anderson et al. 2004). Caspian terns have a foraging range of approximately 60 km (Soikkeli 1973); however, observations by Anderson et al. (2004) found foraging activity to be mostly within 8 km of nesting sites. As juvenile salmon approach the lower estuary, their avian predation risk increases based on their proximity to the colonies. Reducing their exposure to predation risk therefore relies on minimizing their residence times spent in the lower estuary. Their vertical position in the water column may also influence their susceptibility to predation, especially by Caspian terns that forage mostly in shallower depths.

Increasing the survival of juvenile salmonids is recognized as a high priority objective that will benefit the recovery of salmonids listed as endangered or threatened under the ESA. While numerous studies investigating predation and survival in the lower estuary have advanced our understanding of the dynamics between avian predation and juvenile salmonid survival, there is an opportunity to better understand how survival is impacted by migration patterns in the estuary and therefore by environmental conditions, including river discharge. An individual-based model (IBM) is well suited for this as it couples physical habitat conditions with swimming behavior and bioenergetics models and allows for potential predation impacts to be considered as well.

The goals of this work were to address the following questions:

1. How do environmental conditions and swimming behaviors influence survival of yearling Chinook salmon as they migrate through the Columbia River estuary?
2. What migration pathways are associated with increased survival and growth rates, and what are the potential tradeoffs between the two?

4.2 Methods

4.2.1 Overview

These research questions were investigated through the use of an IBM that simulated estuarine migration, growth, and survival of yearling Chinook salmon in the Columbia River estuary. Years 2010 – 2015 were modeled to explore the impact of flow conditions and migration pathways on survival. Data on run timing and size at passage at Bonneville Dam informed the simulation design. The virtual environment upon which the IBM was built consisted of outputs from a hydrodynamic model that simulated the estuary from Bonneville Dam to the Pacific Ocean; however, the IBM domain only considered the estuary to the mouth. The IBM simulated multiple swimming behaviors for yearling Chinook salmon, including a random walk and biased correlated random walks. Growth was simulated using the Wisconsin bioenergetics model (Hanson 1997). Predation was simulated in the lower estuary based on the foraging ranges of Caspian terns and double-crested cormorants and assumptions regarding how the abundance of alternate prey types influences predation rates of juvenile salmonids. Although it is recognized that predation impacts occur throughout the system by multiple predator types, including piscivorous fish, colonial waterbirds, and marine mammals, this work only considered predation by birds as more is known about their impact than other predators. Details regarding the hydrodynamic model and the initial conditions for the IBM are described below, as well as the swimming behavior, bioenergetics, and predation sub-models.

4.2.2 Hydrodynamic Model

The environmental variables used in the IBM were from the hindcast simulation database db33. This database was previously generated by the finite element model SELFE (Zhang and Baptista 2008) that was benchmarked for the Columbia River estuary (Kärnä and Baptista 2016a; Kärnä et al. 2015) and skill-assessed using data collected by an observation network deployed in the estuary (Baptista et al. 2015). SELFE uses an unstructured mesh in the horizontal and a hybrid terrain-following and free-surface adapted *S* grid in the vertical dimension that shifts to an equipotential *z* grid in the ocean at depths greater than 100 m. The horizontal mesh covers the Northeast Pacific Ocean from 39 – 50 ° N and covers approximately 300 km from the shore while extending 234 river kilometers into the Columbia River from the estuary to Bonneville Dam (Figure 2.1).

Several external models were used as forcings, initial conditions, and for maintaining temperature, salinity, and water elevations along the ocean boundary. Model outputs from the NOAA/NCEP North American Mesoscale Forecast System were used for atmospheric forcing. A regional inverse model (Myers and Baptista 2001) was used to simulate the tides at the ocean boundary. Other variables imposed along the ocean boundary included temperature, salinity, and water elevations from the global Navy Coastal Ocean Model (NCOM) (Barron et al. 2006). River data from USGS included discharge, water elevations, and temperatures for the Columbia, Willamette, Lewis, and Cowlitz rivers.

4.2.3 Individual-based Model

4.2.3.1 Overview of model design, inputs, and processes

The objectives of the IBM in this work were to explore how survival changed over time due to simulated predation impacts and to assess potential tradeoffs between survival and growth for yearling Chinook salmon in the lower Columbia River estuary. Model simulations were conducted from 2010 – 2015 to capture a variety of flow regimes and environmental conditions. Multiple swimming behaviors were simulated to assess the role of behavioral decision-making on survival and growth outcomes. In addition to the random walk behavior, two biased correlated random walk behaviors were modeled that differed based on their response to potential predation impacts.

The IBM used a super-individual approach (Scheffer et al. 1995), where each super-individual represented a quantity of identical individuals (N) and mortality acted to reduce the quantity of identical individuals at each time step. There were 10,000 super-individuals simulated for each year that were assigned an initial worth of 1×10^5 individuals. While the number of super-individuals remained constant throughout the simulation, the worth of each super-individual decreased over time due to mortality. The final worth (i.e. the number of remaining identical individuals for each super-individual) at estuary exit was divided by the initial worth at the start of the simulation to get the rate of survival for each super-individual.

The model entity of interest in the IBM was the super-individual. All super-individuals were characterized by several state variables, including length, weight, worth, and 3D location. The worth of the super-individual decreased over time based on background mortality rates and predation rates that depended on the time of day and the location in the estuary. Additional state

variables in the IBM represented environmental properties of the virtual environment, including water temperatures, 3D velocities, and water depths all of which were time-varying. Other environmental variables included the hydrogeomorphic reaches, defined in Simenstad et al. (2011), that are defined by their hydrologic, tidal, and geomorphic processes, as well as wetland habitat data from the Lower Columbia Estuary Partnership (LCEP) land cover dataset (Sanborn Map Company 2011). A habitat index defined based on the proximity to wetland habitat was used to approximate the proportion of maximum consumption (P-value) used in the bioenergetics model. Lastly, the predation rate was defined in the lower estuary based on the proximity to East Sand Island and the foraging ranges of Caspian terns and double-crested cormorants (Figure 4.1). In addition to their spatial dependence, predation rates were also based on the time of day and the salinity intrusion length. See section 4.2.3.2.2.3 for further details on the predation model.

With the exception of the hydrogeomorphic reaches that had a large spatial extent, environmental variables in the estuary had a spatial resolution of 100 – 200 m in the horizontal and ranged from centimeters to meters in the vertical, depending on water depth. Water depths, temperatures, and velocities had a temporal resolution of 15 minutes, while the hydrogeomorphic reach and habitat index were static. The background mortality rate was likewise static; however, the predation rate varied at each time step depending on the location.

The IBM used a time step of 36 seconds, and individual movement based on local flow velocities and swimming behavior was calculated using this time step to correspond with the time step of the hydrodynamic model. After each fifteen-minute time step, growth was calculated using the bioenergetics model and the worth of the super-individual (i.e. the number of individuals represented by the super-individual) decreased based on the background mortality rate and the spatially-varying predation model. A binomial distribution was used to calculate the

number of individuals within the super-individual that were lost due to the predation rate and/or the background mortality rate, and this was subtracted from the worth at that time step to attain the number of survivors. After these processes concluded, outputs from the IBM were recorded, including individual lengths, weights, 3D locations, the occupied elements, and the worth of each super-individual (i.e. survivors).

4.2.3.2 Details

4.2.3.2.1 Initialization

Simulations for each year were conducted from March 16 through July 29 using a normal distribution for the run timing (μ = May 11, σ = 12 days). June 29 was the last date of initialization to ensure individuals had ample time to migrate from the system. Aside from the date and time of initialization, individuals were assigned a specific swimming behavior that was imposed for the duration of the simulation. Individuals were released near Bonneville Dam (45°38’06’’N, 121°57’41’’W) using a normal distribution centered at this point with a standard deviation of 20 m. Initial vertical positions were taken from a uniform distribution near the surface between 0 and 2m. Individual fork lengths were initialized from a normal distribution (μ = 141, σ = 15 mm) that was based on yearling Chinook salmon fork length data collected at Bonneville Dam by the Fish Passage Center Smolt Monitoring Program.

4.2.3.2.2 Sub-models

4.2.3.2.2.1 Movement model

At each 36-second time step, movement due to advection was first calculated using a Lagrangian method. Flow velocities were interpolated spatially and temporally using a Runge-Kutta fourth-order time integration method. After each new position was calculated, it was

checked to ensure that it was in a wet element and that it did not exceed that location's water depth or exit the water surface. When fish did move to a dry element or outside of the domain, the tangential velocity based on the intersected element edge was calculated, and the fish's trajectory was updated. If a fish vertically exited either at the bottom or surface, it was adjusted to just below the surface or above the bottom.

After movement due to advection was calculated, active swimming was simulated using a variety of swimming strategies. Three different random walk strategies were simulated, including an uncorrelated and unbiased random walk and two varieties of a biased correlated random walk. The uncorrelated and unbiased random walk behavior did not consider external environmental cues and served as an effective null behavior to compare more complex behaviors against. The first biased correlated random walk was similar to that described in Chapters 2 and 3, and was meant to simulate efficient migration from Bonneville Dam to the estuary mouth by biasing movement downstream and correlating the swimming direction from prior time steps to the current time step. Since the direction of swimming was related to the direction of displacement, fish with this behavior had a predictive sense of the surrounding flows and factored this into their decision making. In addition, since their swimming direction was based on the previous angle of displacement, their swimming direction included a rheotactic response where swimming behavior was correlated to the directions of flows.

A second biased correlated random walk was developed to assess the inclusion of predator avoidance as a behavioral response in the lower estuary. This behavior was activated in the lower estuary where there was a predation impact. During daylight hours when avian predators would be active, individuals would assess their immediately neighboring elements and move to the element with the smallest predation rate. This rate was defined based on the distance

to nesting colonies in the lower estuary for open-water elements and was also based on the availability of other forage fish, which was approximated by the salinity intrusion length. During nighttime, individuals would resume the original biased correlated random walk behavior where the swimming direction included a bias term to the downstream extent of the occupied hydrogeomorphic reach. The original biased correlated random walk behavior used a weight of 0.1 for the bias term, where most of the movement was weighted to optimize correlation between each step. This modified correlated random walk behavior used a weight of 0.5 for the bias term to direct individuals to habitats with reduced predation rates during daylight hours. To incorporate randomness into swimming behaviors, each super-individual had noise added to their swimming direction using a von Mises distribution where κ equaled two.

4.2.3.2.2.2 Growth sub-model

Growth was simulated using the Wisconsin Bioenergetics model (Hanson 1997) and parameters defined by Stewart and Ibarra (1991) for Chinook salmon. These parameters were defined for adult Chinook salmon; however, recent work by Plumb and Moffitt (2015) defined consumption parameters for juvenile Chinook salmon, so these were used instead for the consumption equations. Growth (*G*) was calculated based on consumption (*C*), respiration (*R*), egestion (*F*), and excretion (*U*) according to:

$$G = C - ((R + A + S) + (F + U))$$

All of these variables were calculated using mass- and temperature-dependent equations (see Chapter 2 for further details).

A constant prey energy density was used of 4000 J g^{-1}, and the P-value used in several equations was based on the value assigned to the occupied element which was based on the

proximity to wetland habitat. Elements within 100 m of wetland habitat had a P-value of 0.9, while those greater than 1000 m away had a P-value of 0.4. P-values were associated with proximity to wetland habitat as juvenile salmonids diet largely depends on macroinvertebrates from marsh habitats (Bottom et al. 2008; Bottom et al. 2005)

4.2.3.2.2.3 Predation and mortality sub-model

Mortality was simulated using a background mortality rate that was applied at each time step to all super-individuals. In addition, losses due to predation were calculated using a spatially and temporally varying rate that applied to individuals in the lower estuary. Since both Caspian terns and double-crested cormorants are diurnal foragers (Schreiber and Clapp 1987), the predation rate was only imposed during daylight hours. At night, there were no avian predation impacts. The background mortality rate used in the model was 9.6×10^{-3} day^{-1}, which corresponded to a rate of 1.0×10^{-4} $15\text{-}min^{-1}$ that was imposed at every fifteen-minute timestep. This value was selected based on sensitivity tests that showed reasonable agreement with observed survival probabilities of approximately 0.95 from Bonneville Dam to river kilometer 50 (McMichael et al. 2011).

The predation rate was based on multiple criteria. The first criterion was if the element was classified as open water, and this was based on the wetland habitat land cover data. The second criterion was based on the foraging range of Caspian terns and double-crested cormorants from their nesting sites on East Sand Island (46° 15’45” N, 123° 57’45” W) located near the estuary mouth at river kilometer 7. Distances were calculated between the element centers and East Sand Island, and this distance was then used to assign various predation rates. In the case of the predation rate by Caspian Terns, if an element was within 8 km of East Sand Island, the predation rate was defined as 1×10^{-3} $15\text{-}min^{-1}$. Elements that were beyond 8 km had a predation

rate that linearly decayed from 1 x 10^{-3} 15-min^{-1} to 0 at 60 km. Unlike the predation rates for Caspian terns, predation rates for double-crested cormorants were universally applied to all elements falling within 40 km of East Sand Island and were equal to 5 x 10^{-4} 15-min^{-1}. The final predation rate defined for each element within 60 km of East Sand Island was the sum of these two predation rates and was only applied during the day.

Forage fish species are commonly found in the Columbia River estuary (Bottom and Jones 1990), and their abundance influences predation impacts by avian predators on juvenile salmonids. Since river discharge impacts the forage fish community (Weitkamp et al. 2012), this therefore impacts their availability as alternative prey. To include the presence of forage fish in the predation model, the salinity intrusion length, which is inversely related to river discharge, was used. The salinity intrusion length was calculated from salinity outputs from the hydrodynamic model and represented how far into the estuary water with a salinity of 1 psu intruded. During low flow years, more saltwater enters the estuary, leading to greater salinity intrusion lengths, whereas in high flow years, the high volume of freshwater limits the intrusion of saltwater. Thus, in years when salinity intrusion lengths are greater and river discharge is lower, there are potentially more marine forage fish in the estuary versus high flow years when there would be fewer marine forage fish in the lower estuary.

The presence of forage fish and the potential to reduce predation rates on juvenile salmonids was therefore based on this salinity intrusion length. The spatially-dependent predation rate was computed for elements whose distance to the mouth was less than the salinity intrusion length according to:

$$M_{pred}(X,t) = \frac{0.5 \cdot M_{pred}(X)}{L_{sil}(t)} \cdot d + 0.5 \cdot M_{pred}(X)$$

where $M_{pred}(X, t)$ was the spatially and temporally varying mortality rate due to predation and where the temporal variance was based on the salinity intrusion length, $M_{pred}(X)$ was the spatially varying mortality rate due to predation, L_{sil} was the salinity intrusion length (km), and d was the distance (km) between the element center and the mouth. For elements where the distance to the mouth was greater than the salinity intrusion length, the mortality rate due to predation was based only on the spatially-dependent rate. This equation assumed that predation impacts at the estuary mouth were reduced by 50% due to the presence of other forage fish and that the reduction in predation on salmonids eventually decreased to 0 (i.e. no reduction in predation) at distances greater than the salinity intrusion length.

While it was desirable to base predation rates on observational studies, that was challenging to do since predation rates were typically described more broadly for an entire season. Rough approximations to these predation rates were made based on assumptions regarding residence times. However, it's important to note that predation in this case was meant to simulate more general predation impacts based on recognized foraging ranges and the presence of other prey in the estuary and was not intended to mimic exact predation processes in the lower estuary.

4.2.4 Analysis

To examine how predation and background mortality rates influenced survival of outmigrating juvenile Chinook salmon, the worth of all super-individuals that successfully exited the estuary was calculated. These results were determined for each of the swimming behaviors from 2010 - 2015, including the random walk and the two biased correlated random walks. To better understand what migration pathways were associated with improved survival, the

pathways were first computed for each year and behavior in order to visualize the common routes.

To assess the survival associated with these migration routes, the unique elements occupied by all successful outmigrants were assigned a value that represented the mean survival of all individuals that passed through that element. If individual elements had fewer than 10 individuals pass through them (equating to < 0.1% of simulated individuals), these rates were masked. This was done to limit the over-representation of one individual in setting the mean for an element. Overall, this analysis would allow for a visual representation where pathways associated with increased survival could be identified in addition to migration pathways associated with greater losses to predation. This analysis was also done for the growth rates that were calculated based on the total increase in fork length from Bonneville Dam to the estuary mouth, divided by the residence time. The mean growth rate for all individuals that passed through specific elements likewise represented pathways associated with either increased or decreased growth rates.

The z-score was computed for both metrics for each year and for each behavior, to better visualize what regions of the estuary were affiliated with improved or reduced survival as well as growth opportunities. Final growth rates and percent survival were likewise explored in the context of river flows to assess potential tradeoffs between growth rates, percent survival, and river flows.

4.3 Results

4.3.1 Trends in migration timing, growth, and survival

Years 2010 – 2015 included both low and high flow conditions allowing for comparisons between contrasting regimes. Figure 4.2 shows the mean daily flows, mean daily salinity intrusion lengths, and mean water temperatures from 2010 – 2015. In addition, the mean daily values for all years simulated are shown. Flow conditions in years 2010 and 2015 were below average and had higher than average daily mean salinity intrusion lengths. River temperatures in 2015 were above average, while temperatures in 2010 started out warmer, but decreased relative to the mean during the spring freshet. Years 2011 and 2012 flows were well above average, had reduced salinity intrusion lengths, and slightly cooler river temperatures. Compared to other years simulated, years 2013 and 2014 were average across the board.

Patterns in residence times and growth rates followed similar trends as seen in Chapter 3 (Table 4.1). High flow years were associated with shorter residence times for all behaviors, with the biased correlated random walk having shorter residence times than the random walk behavior. In 2012 when flows were above average, median residence times were 3.3 days for the random walk behavior, 3.0 days for the biased correlated random walk behavior, and 3.0 days for the predator avoidance behavior. In 2015, the lowest flow year simulated, median residence times were 6.0 days for the random walk behavior, 5.5 days for the biased correlated random walk behavior, and 5.5 days for the predator avoidance behavior. Across all years, minimum median growth rates were seen in 2011, with rates of 0.29 mm d^{-1} for the random walk behavior, and 0.30 mm d^{-1} for the other two behaviors. In 2015, median growth rates were much greater at 0.46 mm d^{-1} for the random walk behavior and 0.49 mm d^{-1} for the other two behaviors. The median percent survival, that represented the final worth of all super-individuals that successfully exited the estuary was lowest in 2015 and was 82.9 % for the random walk

behavior, 84.2 % for the biased correlated random walk behavior, and 84.1 % for the predator avoidance behavior. The median percent survival in 2012 was greatest, with 90.1 % for the random walk behavior, 91.2 % for the biased correlated random walk behavior, and 90.9 % for the predator avoidance behavior. While both 2011 and 2012 were high flow years that had greater percentage of survivors, 2012 had greater growth rates than 2011.

Distributions of the percent survival across the three behaviors varied across years. Within-behavior trends all followed the same general pattern of reduced survival during low flow years and greater survival in high flow years (Figure 4.3). There was also less variability expressed across simulated individuals in 2012 than in other years, especially low flow years when there was a greater interquartile range. For all years, the biased correlated random walk behavior had greater survival than the random walk behavior and the predator avoidance behavior. Despite factoring in predation rates in decision making, the predator avoidance behavior did not result in more survivors.

In general, the percent survival was negatively correlated with residence times and was positively associated with flow discharge (Figure 4.4). The longer residence times during low flow years also had reduced survival, whereas the shorter residence times during high flow years were associated with increased survival. Looking at trends across flow conditions with regards to growth rates and the percentage of survival, the percentage of survival did not seem to have any basis on growth rates (Figure 4.5). Years where growth rates exceeded 0.6 mm d^{-1} showed a decreasing trend in survival as growth rates increased. Growth rates for some years were associated with flows at initialization, where growth rates were greater during periods of high flow. In 2011 for instance, individuals released when daily mean flows at initialization exceeded 12,000 m^3s^{-1}, had greater growth rates, but this did not imply that they spent longer times in the

estuary growing, but rather that they likely experienced optimal temperature conditions during that period. Overall, there was no clear relationship between growth rates and the percentage of survival, as individuals at all growth rates had variable survival percentages. The exception was when growth rates began to exceed a certain threshold that survival began to drop off more distinctly.

The differences between the biased correlated random walk behavior and the modified biased correlated random walk behavior that included a predator avoidance behavior (referred to as the predator avoidance behavior) were barely noticeable for most years when looking at median residence times and percent survival. There was also no discernible difference between the growth rates between these behaviors. Although more generally, there was little within-year variability in growth rates across all the behaviors simulated, including the random walk behavior. Since this predator avoidance behavior did not appear to significantly differ from the biased correlated random walk behavior, it was not analyzed further with regards to spatial patterns.

4.3.2 Migration pathways, survival, and growth

To assess pathways associated with increased growth and survival, migration pathways were first assessed to identify common routes used across years. Figures 4.6 and 4.7 highlight the migration pathways for the random walk and the biased correlated random walk behaviors. Across all years and behaviors, individual pathways were most common in the north and south channels along with movement across Desdemona Sands and the upstream shoals. There were some noticeable differences between the random walk and biased correlated random walk behaviors for the years simulated. Whereas individuals simulated by the random walk behavior more frequently entered Baker Bay, individuals simulated under the biased correlated random

walk behavior were less likely to do so. Both behaviors showed increased occupation of Cathlamet Bay during low flow years; however, more individuals simulated under the biased correlated random walk behavior moved through this region. Pathways across the tidal flats were more common in the random walk behavior. These results alone are not necessarily meaningful in the interest of understanding pathways associated with growth and survival, but they provide context when looking at regions of the estuary that are associated with greater survival and/or growth outcomes.

Figures 4.8 and 4.9 show the z-scores associated with the percentage of survival computed for each element. This value was computed by identifying all individuals that passed through an element for a specific year and calculating the mean survival for all individuals specific to that element. Assuming that at least 10 individuals passed through, the z-score was then computed by subtracting the mean survival of all individuals and dividing by the standard deviation of all individuals for a given year. For the random walk behavior, individual pathways in Baker Bay were associated with decreased survival for all years. In most years, parts of the estuary with increased survival were primarily located in the lower estuary outside of the lateral bays. The mid-estuary region near the tidal flats had decreased survival in 2015, and this pattern seemed evident in other years as well.

Trends in survival across the estuary were much more evident for the biased correlated random walk behavior. Figure 4.9 highlights the regions associated with increased survival, and there is a clear pattern, with the exception of 2010 that individuals migrating through the main body of the lower estuary, mostly in the north and south channels have increased survival. Individuals simulated under this behavior that occupied the lateral bays, especially in 2011 - 2015 were associated with decreased survival. During 2011 and 2012 when flows were

especially high, survival was distinctly greater outside of the lateral bays. In 2010 z-scores were reduced throughout the estuary suggesting less extreme deviation in survival across pathways. Whereas the lateral bays were associated with reduced survival during most years, this was less of the case in years 2010. In 2010, the lower estuary had contrasting patterns to the other years, with decreased survival in the region of the tidal flats near the south channel. While the pathways in the main channels were typically associated with increased survival, this was not the case for that year.

Figures 4.10 and 4.11 present data in a similar fashion, but for z-scores associated with growth rates. General trends for the random walk behavior showed decreased growth rates concentrated in the mid-estuary in most years. While not true for all years, growth rates appeared to be higher in several of the lateral bays. For example, in 2010, growth rates were elevated in Baker Bay, and Grays Bay. In years 2012 and 2014, growth rates were higher in Cathlamet Bay. In some years, including 2013 and 2014, there also appeared to be a distinct pattern between the north channel and the south channels.

Z-scores of growth rates for the biased correlated random walk behavior depicted in Figure 4.11 showed similar patterns as those in Figure 4.9 that depicted survival; however, they tended to show the opposite trend. In years 2011, 2012, and 2014, pathways in the main channel were associated with increased survival. Considering these same years, growth rates were reduced across the tidal flats and in the north channel. However, growth rates in the south channel were above average. Looking at the migration pathways in Figure 4.7, these regions were associated with the most common pathways individuals took during their migrations. Years 2011, 2013, and 2015 showed different patterns regarding growth, with increased growth rates in the lower estuary except along the south channel. Whereas growth rates in years 2011, 2012, and

2014 were greater in Cathlamet Bay, growth rates in 2010, 2013, and 2015 were below average for that region.

4.4 Discussion

Results from simulations conducted from 2010 – 2015 showed that survival was closely related to residence times. Individuals that spent more time in the lower estuary were exposed to greater predation risks simply by being in the estuary for longer periods of time, and this was true for all years regardless of flow conditions. Since residence times were strongly associated with river discharge, survival was likewise related to river discharge, where the percentage of individuals surviving to marine exit was greater in years where flows were higher. Migrating during the freshet would thus be advantageous because flows are elevated during these periods and outmigrating juvenile salmonids benefit from these flow conditions as they spend less time in the estuary and are less likely to be preyed upon.

Comparing low and high flow years against one another, survival varied by as much as 6%. There were likewise differences in growth rates between these flow regimes. While high flow conditions were advantageous for the sake of survival, this was not necessarily as true when considering growth. In 2015, which was a low flow year, median survival across behaviors was roughly 83 – 84%, which was the lowest survival of all years simulated. However, median growth rates during this year were also the greatest ranging from 0.46 – 0.49 mm d^{-1} across behaviors.

Looking at the spatial patterns in survival and growth, a contrasting relationship was evident, especially for the biased correlated random walk behavior. In years when flows were high, migration pathways with high survival were mostly in the main part of the lower estuary

outside of the lateral bays; however, growth rates associated with these pathways were substantially reduced. While individuals migrating through the system may benefit from having reduced predation risks due to their faster migration in the lower estuary, they miss out on potential growth opportunities in the lower estuary as well.

Although the pattern of increased survival being associated with decreased growth and vice versa emerged from some of the model simulations, especially when looking at the spatial distributions in Figures 4.8 – 4.11, this pattern was not always so dichotomous. For example, individuals simulated in 2012 had the greatest median percentage of survival (90 – 91%), but growth rates of 0.38 – 0.39 mm d^{-1} were also elevated when compared to the other high flow year 2011 when survival was high at 90%, but median growth rates were low at 0.3 mm d^{-1}. In addition, looking at the dependence of survival on growth rates shows little evidence of any strong correlation. While the spatial patterns may hint at a strong relationship between survival and growth rates, where high survival equates to low growth rates, this does not appear to be the case when assessing the dependence of survival on growth rates. If there was indeed a strong association between the two, there would be greater indication that the two are negatively correlated, but that was not seen.

The predation model attempted to account for alternate prey in the lower estuary based on the salinity intrusion length. The way it was imposed, predation impacts on yearling Chinook salmon would be greater in the lower estuary during high flow years when fewer forage fish would enter the estuary. It could be assumed that predation could therefore be greater during high flow years; however, this did not appear to be the case. Despite trying to include the presence of other prey, fewer individuals were lost to predation in high flow years than low flow years, and residence times appeared to be the most important factor in driving predation risk.

Although predation impacts may have been reduced in a low flow year compared to a high flow year based on the presence of other forage fish, simulated yearling Chinook salmon spent more time in the lower estuary, and therefore experienced greater losses.

Overall the results show that survival was associated with residence times and the length of time that individuals spent in the estuary. While there was a spatial pattern that highlighted differences across the lower estuary in terms of survival and growth and how these patterns seemed to contrast, there was no clear relationship that showed survival being negatively correlated with growth rates. However, the greatest growth rates observed were associated with decreased survival.

4.4.1 Limitations

While the IBM proved useful for simulating potential predation impacts on outmigrating yearling Chinook salmon, it's important to account for the model limitations and how they impact our ability to make meaningful conclusions. There were many simplifying assumptions made for the predation rates and mortality rates. Rates were selected based on attempting to approximate semi-realistic values after running sensitivity tests that attempted to match observed losses through various parts of the system; however, they were only loosely based on observational data. Background mortality rates were meant to reduce the number of survivors throughout the estuary at each time step, but this also meant that at each time step, a super-individual decreased in the number of survivors it represented. This process was meant to account for multiple processes, including disease, loss to other predators, starvation, etc.; however, it's likely that this kind of rate would be more spatially and temporally variable.

The predation rate attempted to account for spatial and temporal patterns by accounting for the foraging range of avian predators and the potential presence of forage fish within open water habitat; however, there were many considerations that were not included. For example, Caspian terns primarily hunt closer to the surface such that salmonids that are closer to the surface are more impacted (Collis et al. 2002); however, this IBM did not simulate vertical swimming, and the predation rate was only in the horizontal dimension and did not vary vertically. In addition, birds are a visual predator, and the turbidity of the water would influence habitats where they forage, but the potential effects of turbidity on predation rates were not accounted for. The predation model also didn't consider more detailed information about the avian predators, including the colony size, the nesting chronology, or the percent of salmonids in their diet. Overall, there were many factors that could potentially influence predation rates that were not considered in this IBM, so the results should be considered as more of an approximation of the effects of predation under different flow conditions.

The lack of density-dependent interactions was an additional limitation, that had implications for both the predation model and the bioenergetics model. By not considering these interactions, the model assumed that there was no competition for food resources and that there was not a drawdown in prey resources over time. Similarly, predators were not simulated as an active agent so were not responding behaviorally to potential hotspots where juvenile Chinook salmon were located. This IBM also only considered yearling Chinook salmon; however, steelhead are recognized as having higher predation rates by Caspian terns.

While it is desirable to simulate ecological processes as effectively as possible, there becomes a point where adding further complexity to a model has diminishing returns, especially when it is challenging to assess the uncertainty and skill of the model. This was the case with this

predation model. A strong attempt was made to adequately simulate potential predation impacts by avian predators in the lower Columbia River estuary by considering the general habits of two main predators and the potential availability of alternate prey based on the salinity intrusion length. While there were limits to its implementation, it worked well to approximate potential predation impacts under different flow regimes.

4.5 Conclusions

The inclusion of a predation model in an IBM that simulated yearling Chinook salmon migration in the Columbia River estuary allowed for an exploration of how various flow regimes and predation influence survival. Although the predation model was based on a number of assumptions and fairly basic, it attempted to capture the dynamics of two common avian predators and their general foraging behavior. A number of years were simulated to assess how predation impacts and varying flow conditions influence the potential growth and survival outcomes of yearling Chinook salmon. The percent survival was strongly associated with residence times of individuals. Since residence times were mostly driven by flow discharge for the behaviors simulated, survival was likewise related to river flows. Looking at migration pathways associated with increased survival and growth rates showed that pathways concentrated in the main channels had increased survival but decreased growth, whereas migration pathways associated with some of the lateral bays, including Cathlamet Bay were often associated with reduced survival but increased growth rates. Although these spatial patterns suggested that survival and growth rates might be inversely related, a clear relationship between growth and survival was not established.

Tables

Table 4.1. Median residence times (d), median growth rates (mm d^{-1}), and median percent survival for years 2010 – 2015 using the random walk (RW), biased correlated random walk (BCRW), and biased correlated random walk with predator avoidance (PA).

Year	Residence Time (d)			Growth Rate (mm d^{-1})			Survival (%)		
	RW	BCRW	PA	RW	BCRW	PA	RW	BCRW	PA
2010	5.46	4.85	4.96	0.36	0.37	0.37	84.4	85.7	85.2
2011	3.65	3.29	3.33	0.29	0.30	0.30	89.5	90.3	90.1
2012	3.31	2.97	3.01	0.38	0.39	0.39	90.1	91.2	90.9
2013	4.28	3.82	3.89	0.42	0.44	0.44	87.1	88.1	87.9
2014	3.84	3.44	3.49	0.40	0.42	0.42	88.4	89.6	89.3
2015	6.04	5.47	5.49	0.46	0.49	0.49	82.9	84.2	84.1

Figures

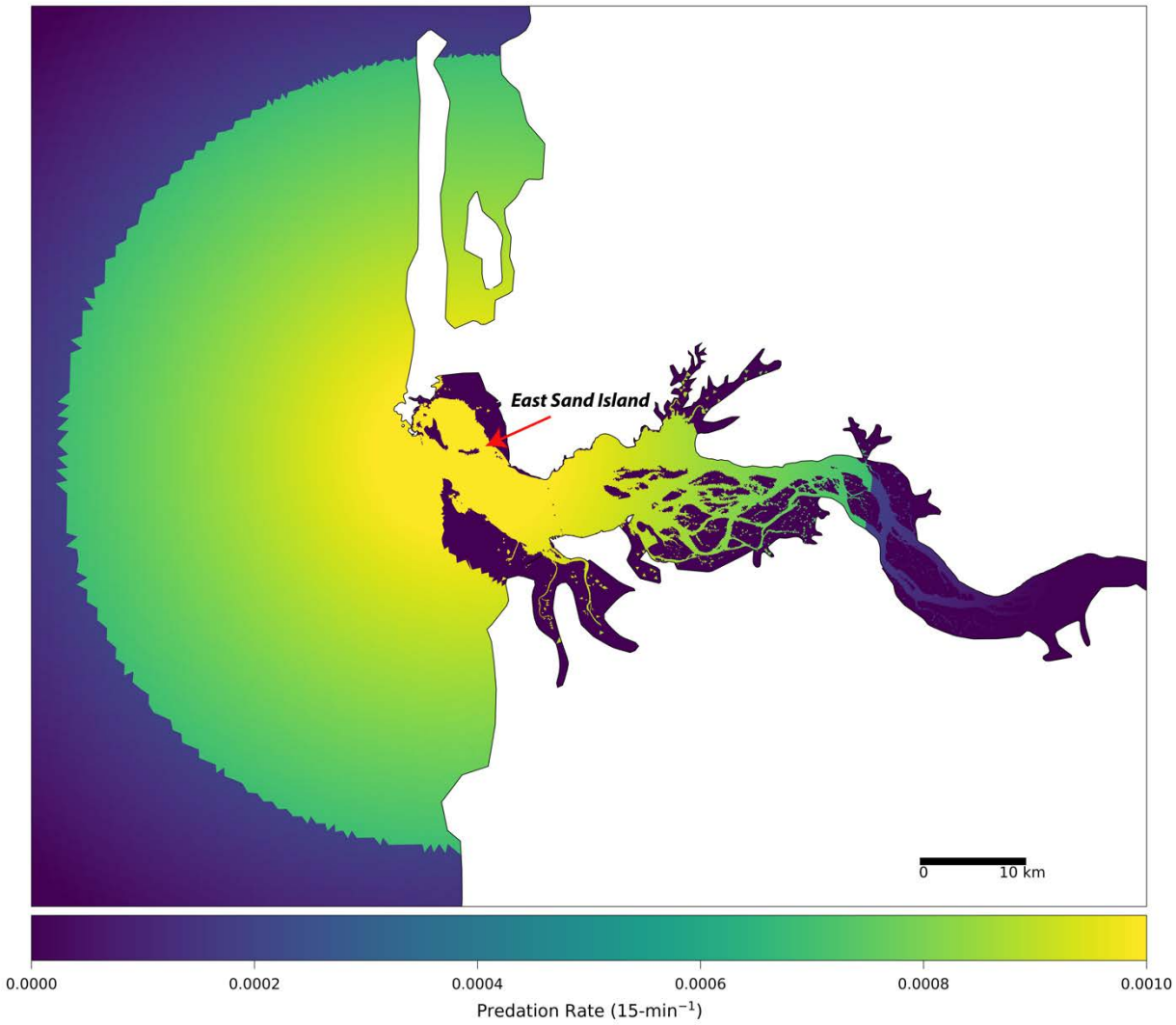

Figure 4.1. Map of the spatially variable predation rate based on the foraging range of double-crested cormorants and Caspian terns nesting at East Sand Island in the lower Columbia River estuary.

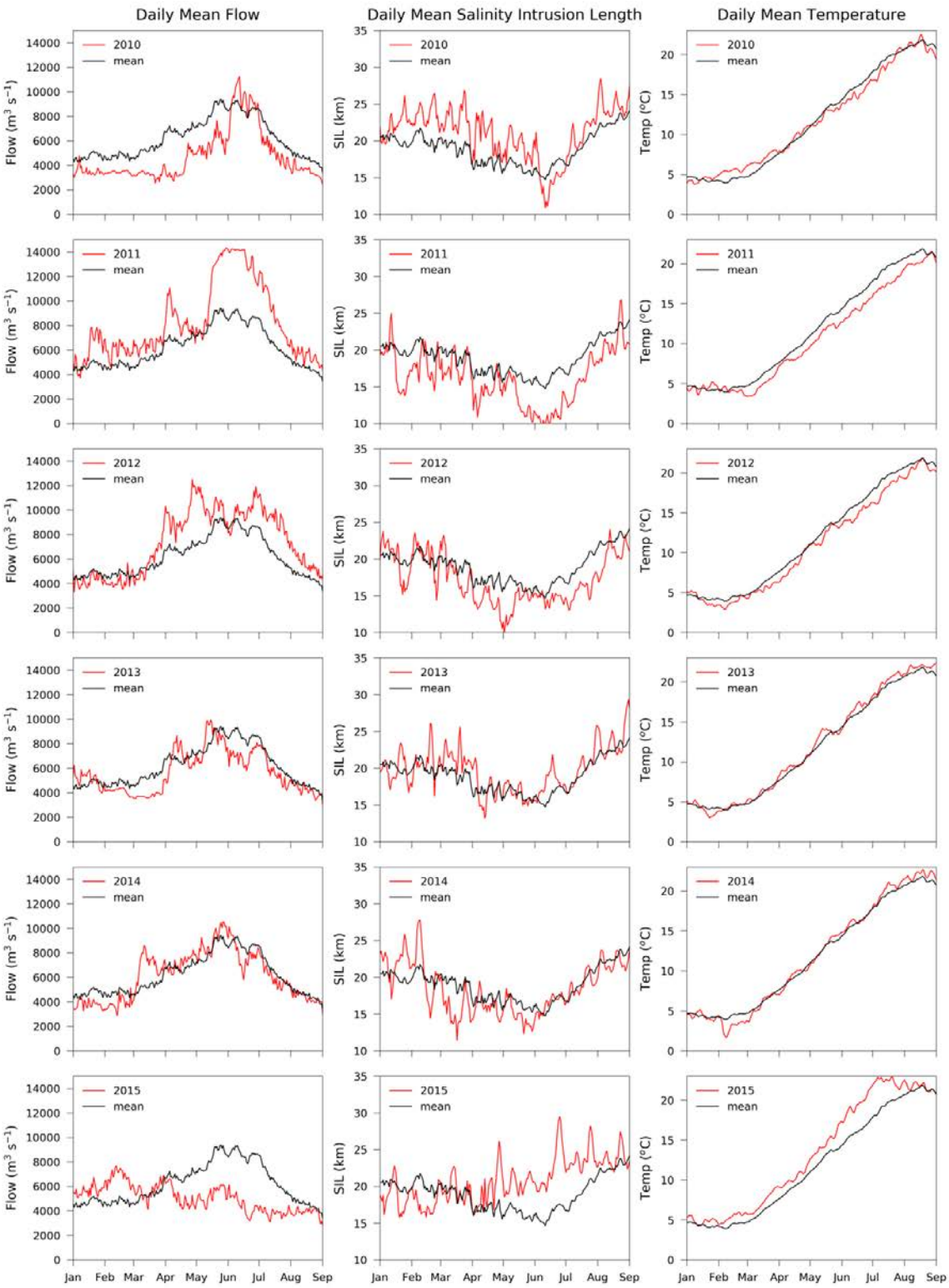

Figure 4.2. Environmental conditions from 2010 - 2015 including mean daily river discharge at Bonneville Dam (*left*), salinity intrusion length (km) in the lower estuary (*middle*), and river temperatures at Bonneville Dam (°C) (*right*) in red. Mean values for all years indicated by black line.

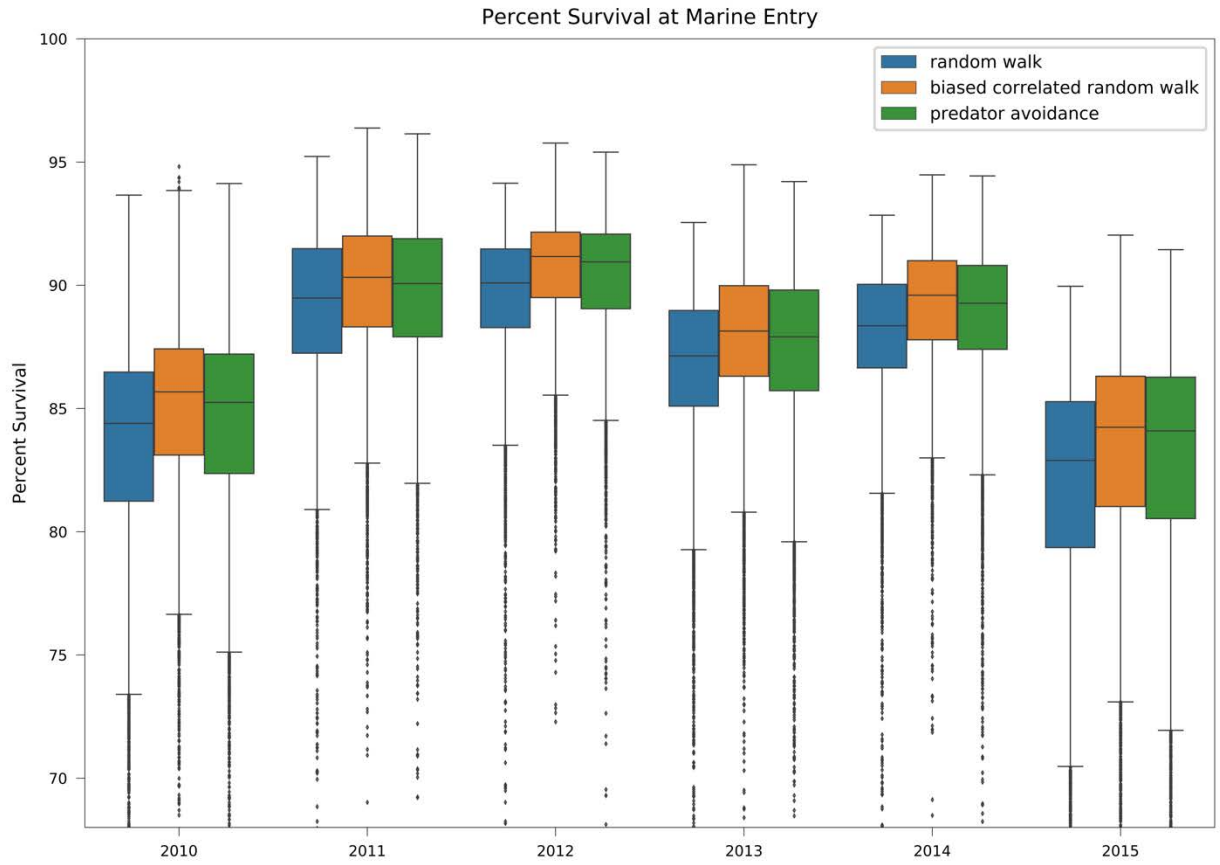

Figure 4.3. Percent survival based on the worth of all super-individuals at the time of marine entry from 2010 – 2015 for the random walk, biased correlated random walk, and modified biased corelated walk behavior with a predator avoidance component.

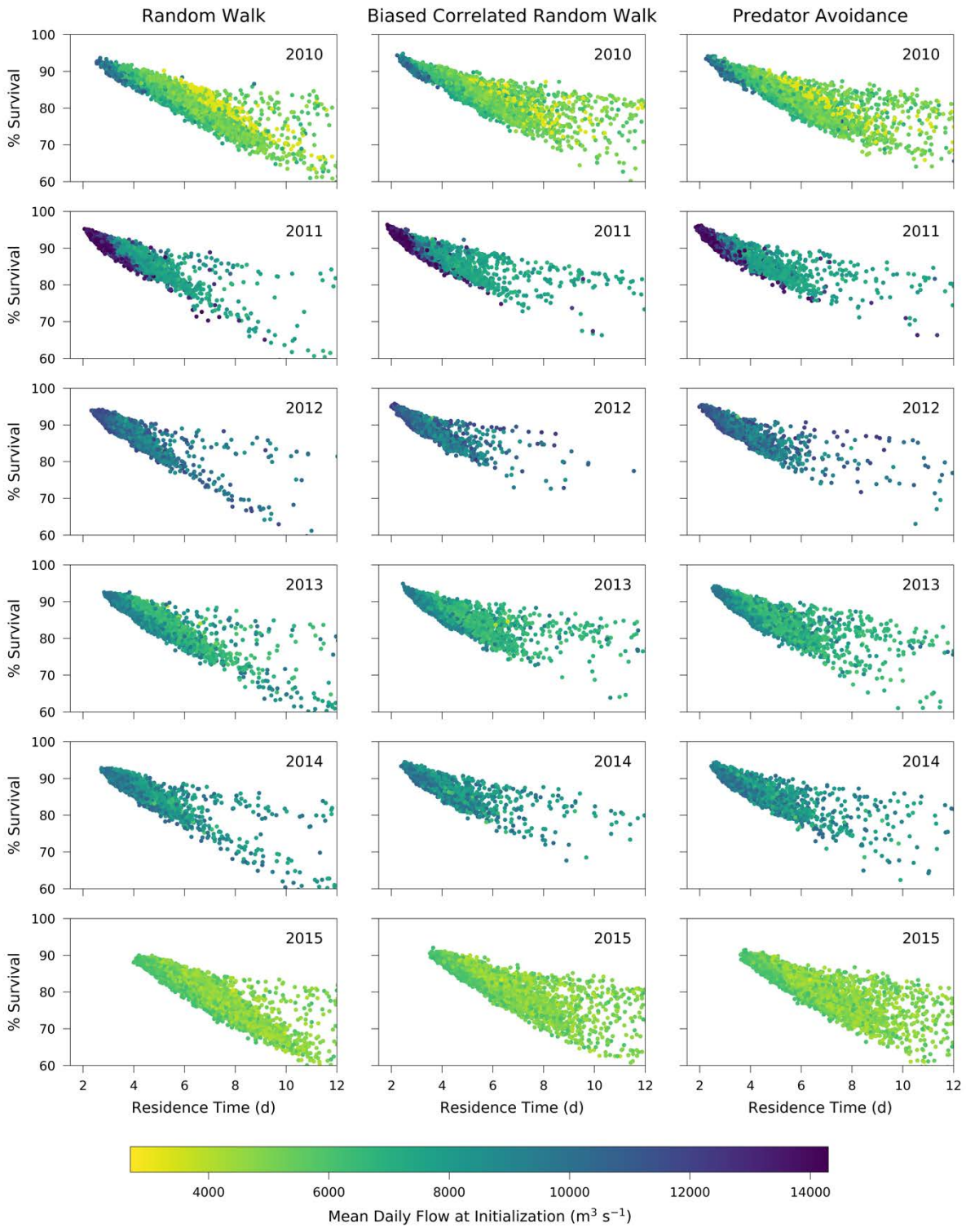

Figure 4.4. Residence times (d) and percent survival based on the worth of all super-individuals at the time of marine entry from 2010 – 2015 for the random walk (*left*), biased correlated random walk (*middle*), and modified biased corelated walk behavior with a predator avoidance component (*right)*. Values are colored by the mean daily flow at initialization (m^3 s^{-1}).

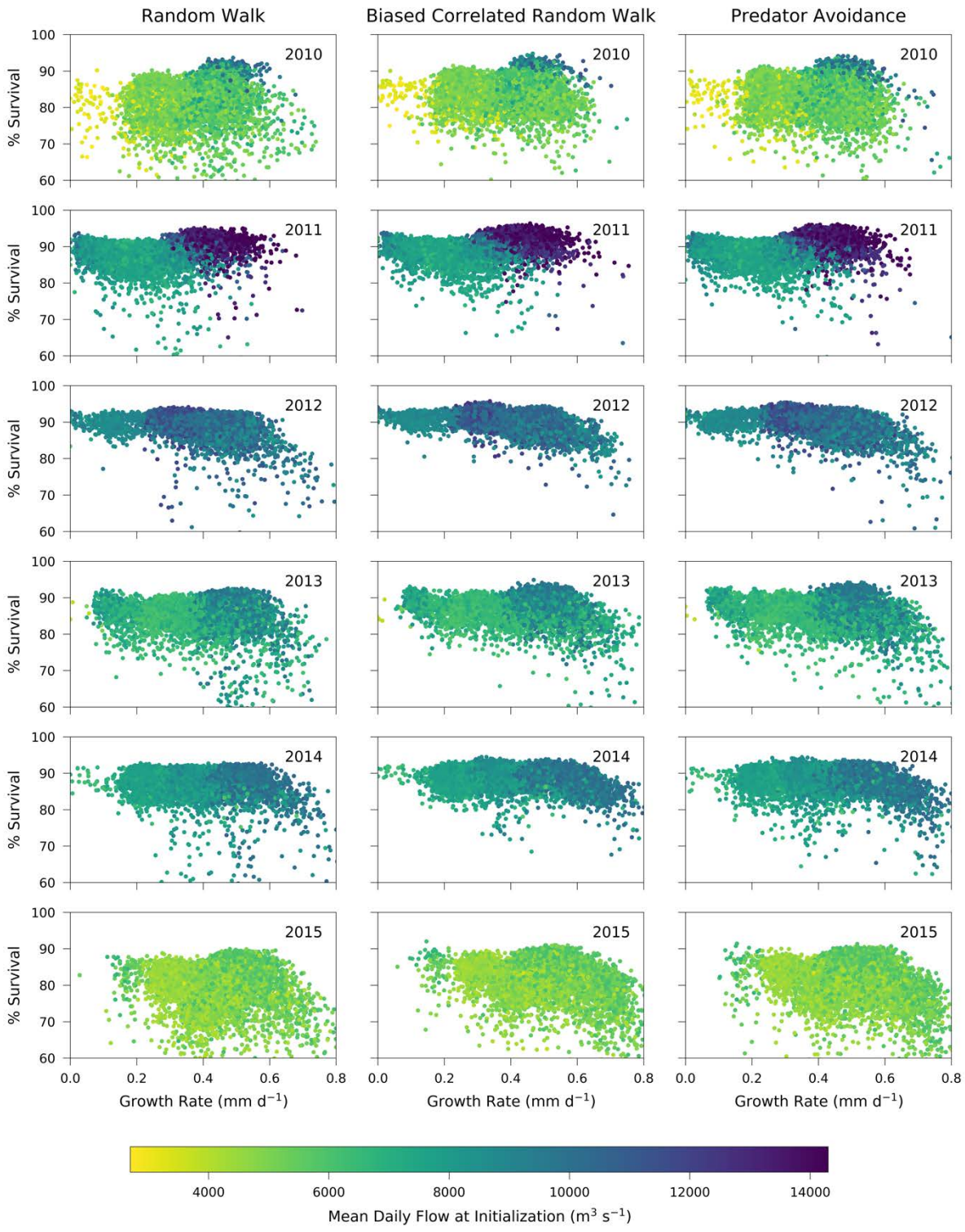

Figure 4.5. Growth rates (mm d^{-1}) and percent survival based on the worth of all super-individuals at the time of marine entry from 2010 – 2015 for the random walk (*left*), biased correlated random walk (*middle*), and modified biased corelated walk behavior with a predator avoidance component (*right)*. Values are colored by the mean daily flow at initialization (m^3 s^{-1}).

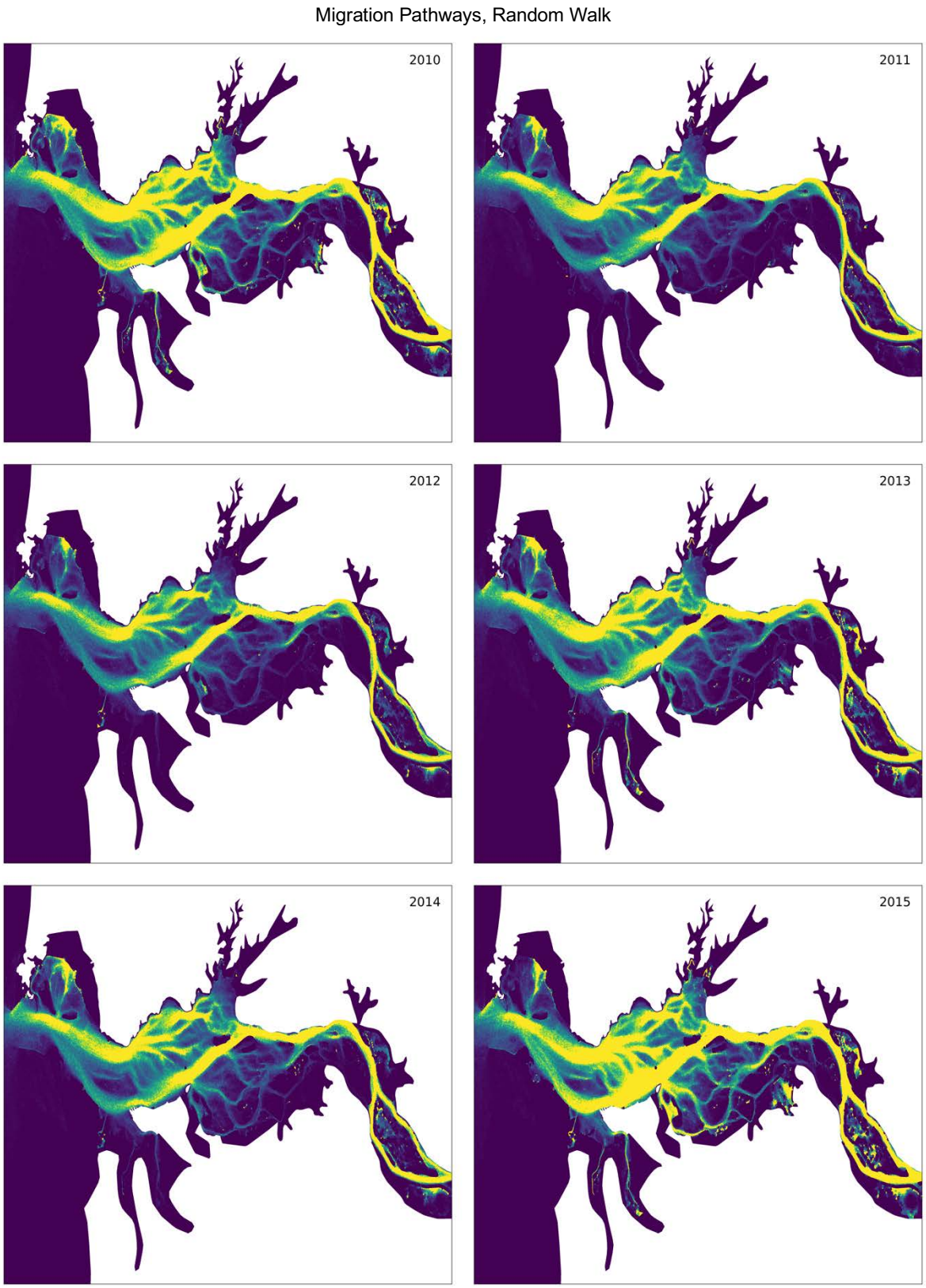

Figure 4.6. Migration pathways from 2010 – 2015 for the random walk behavior. Common pathways are indicated in yellow.

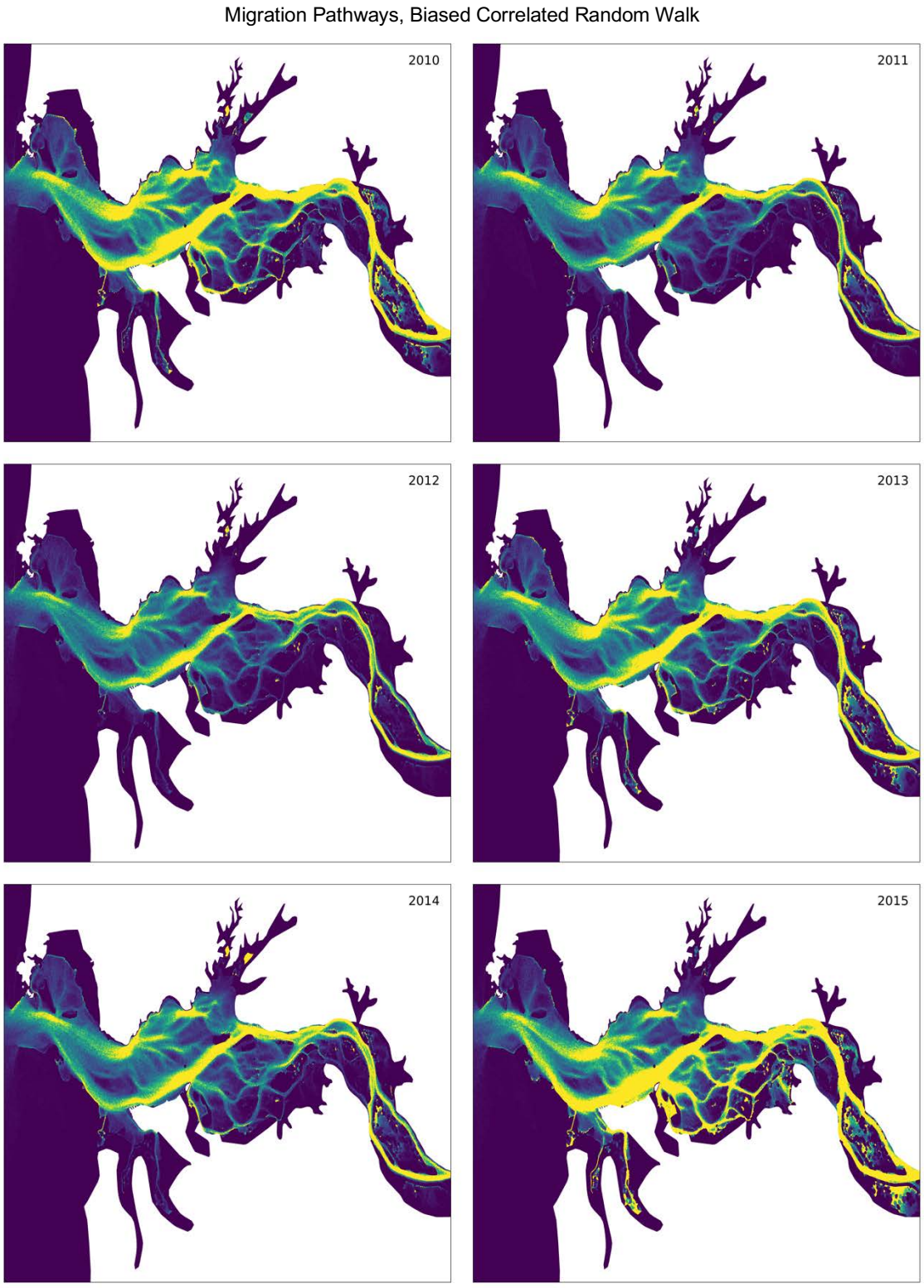

Figure 4.7. Migration pathways from 2010 – 2015 for the biased correlated random walk behavior. Common pathways are indicated in yellow.

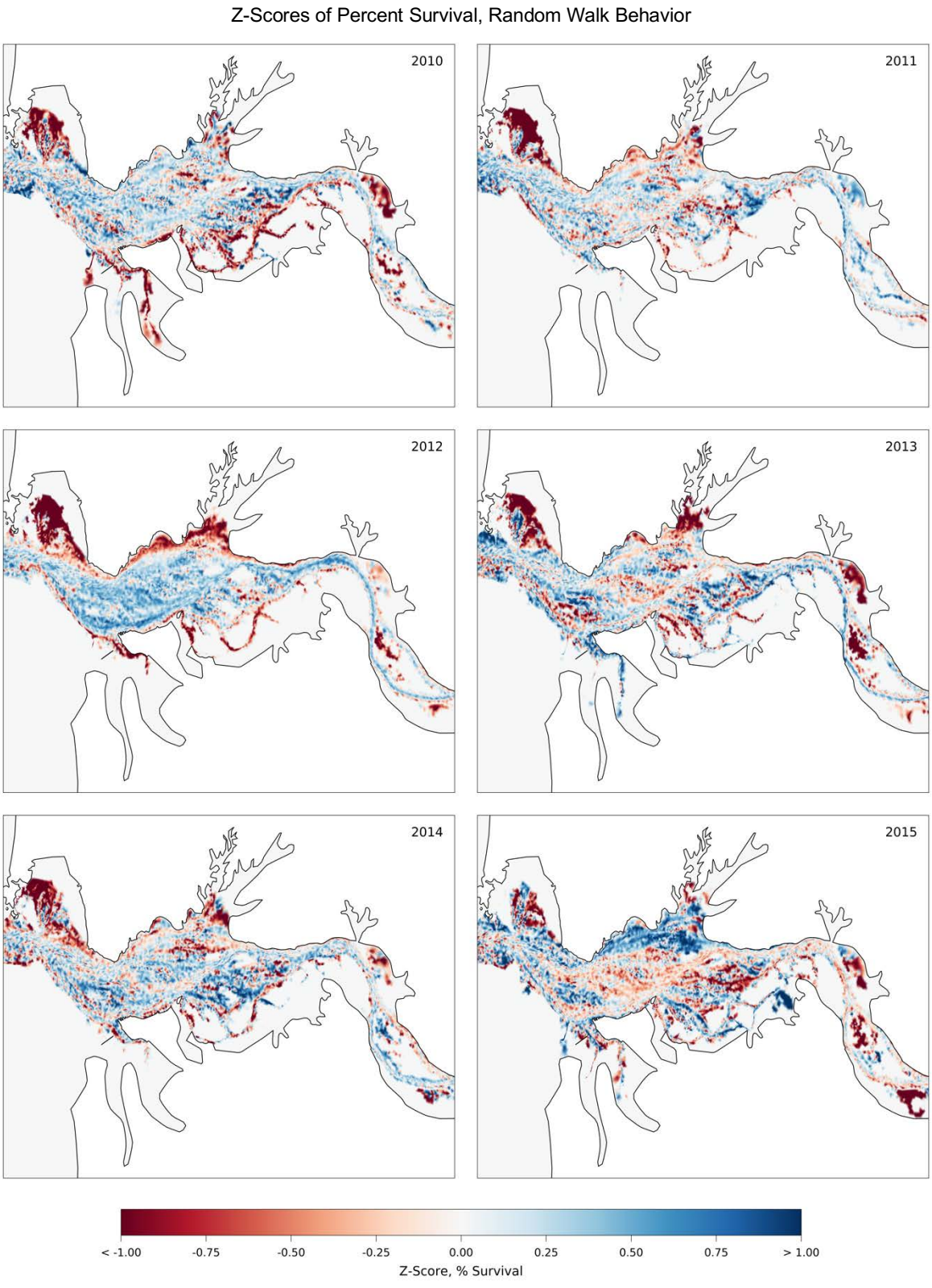

Figure 4.8. Z-scores for the element-based percent survival for yearling Chinook salmon random walk behaviors from 2010 – 2015.

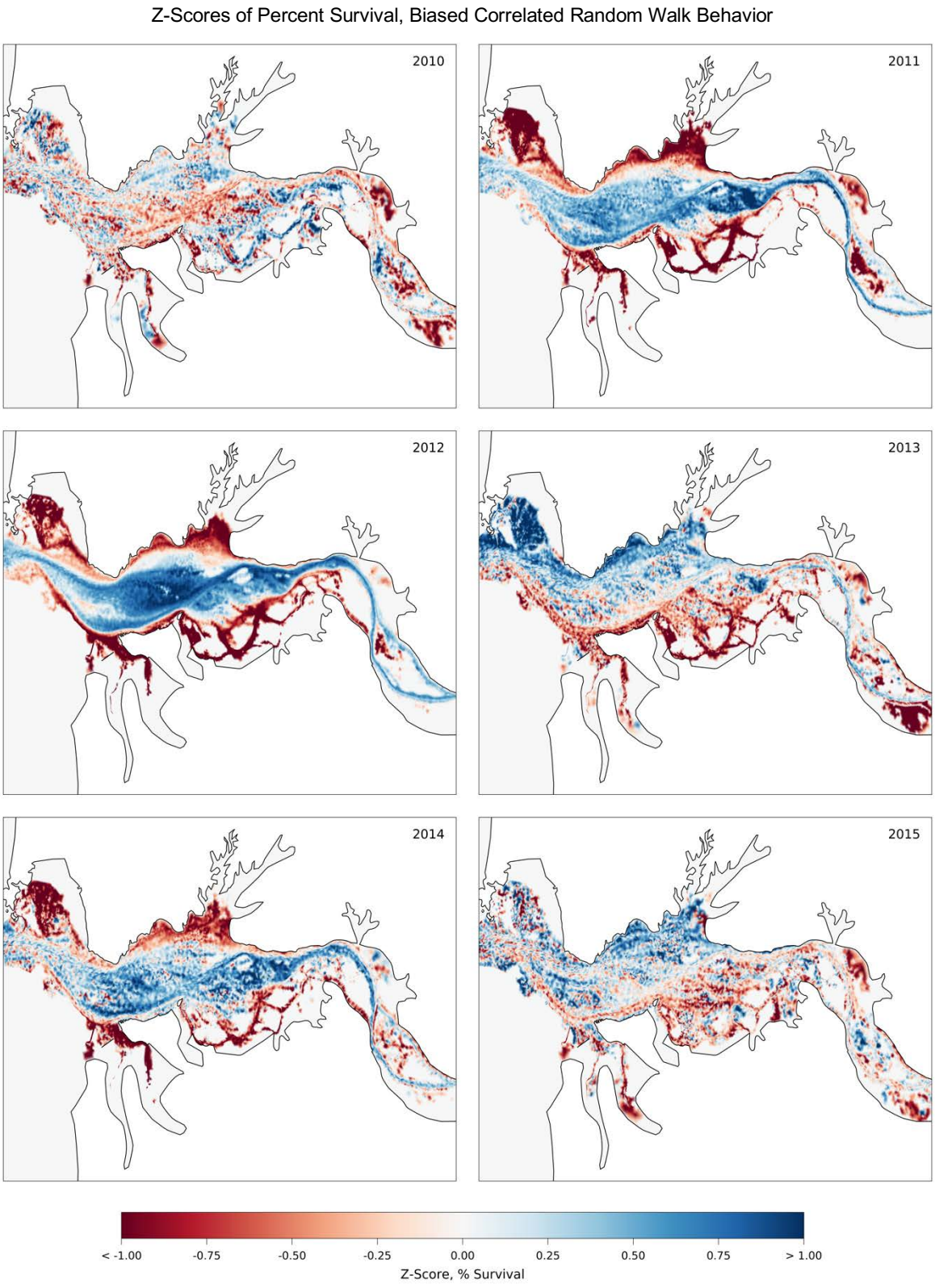

Figure 4.9. Z-scores for the element-based percent survival for yearling Chinook salmon biased correlated random walk behaviors from 2010 – 2015.

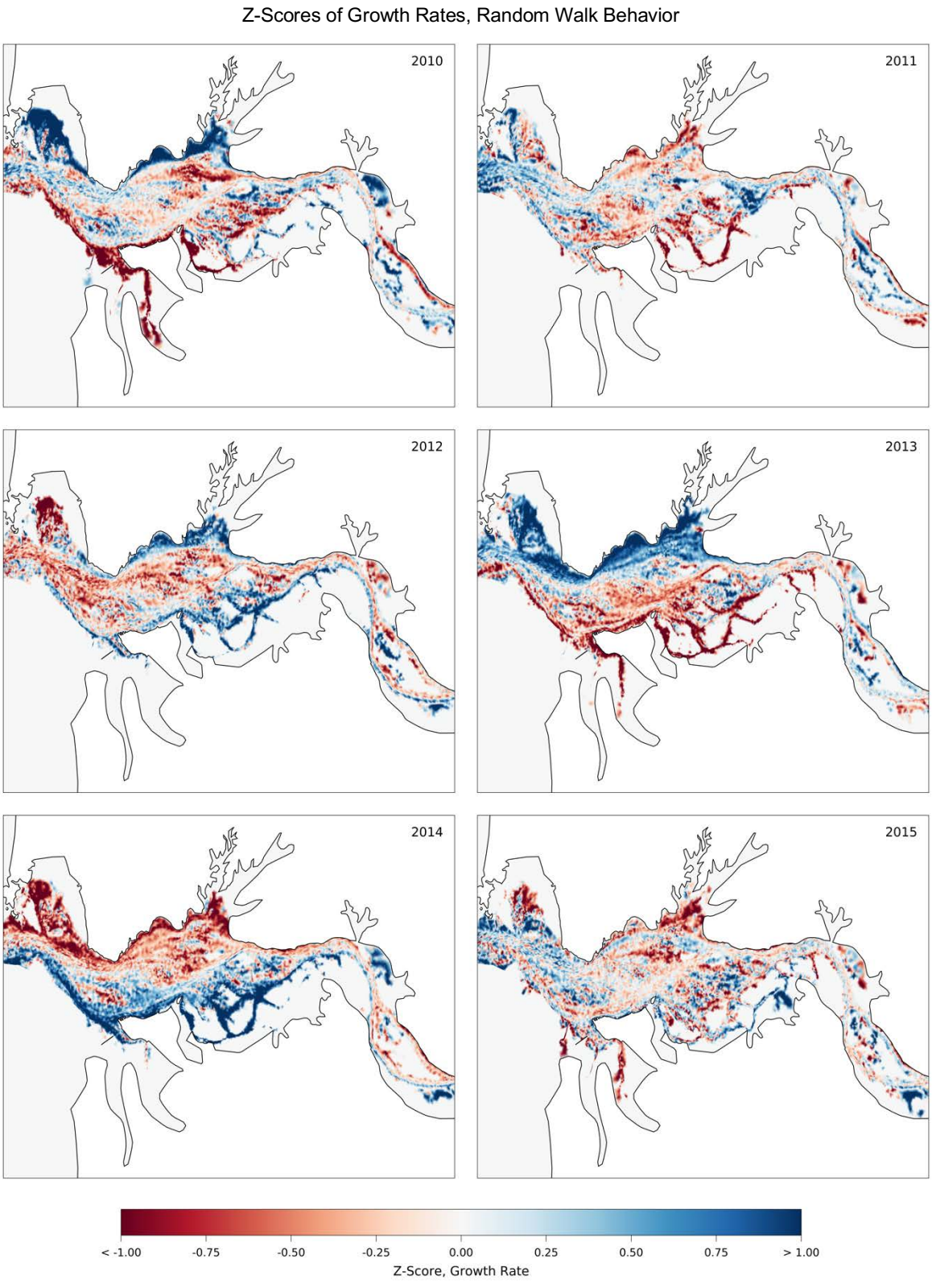

Figure 4.10. Z-scores for the element-based growth rates (mm d^{-1}) for yearling Chinook salmon random walk behaviors from 2010 – 2015.

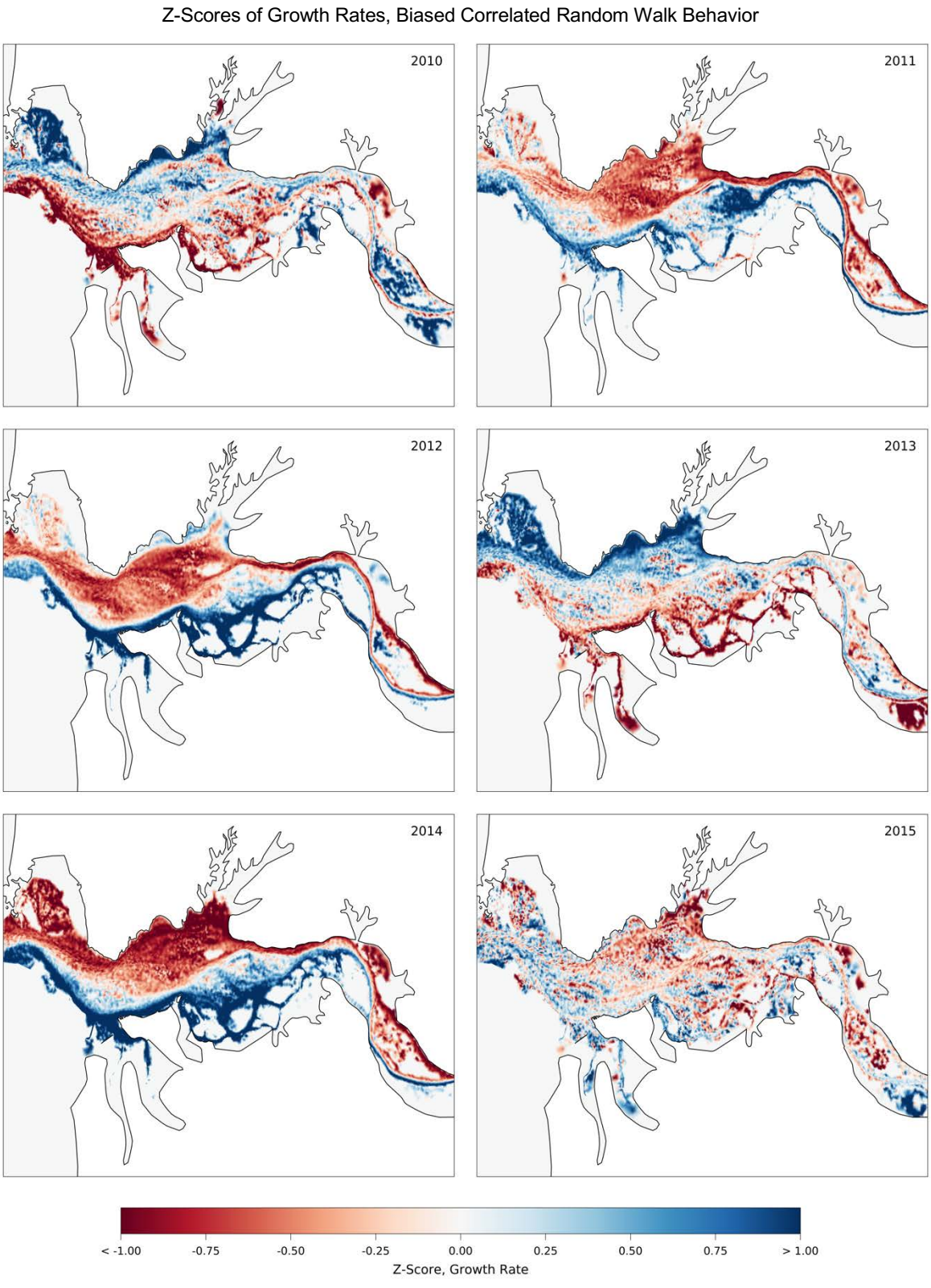

Figure 4.11. Z-scores for the element-based growth rates (mm d^{-1}) for yearling Chinook salmon biased correlated random walk behaviors from 2010 – 2015.

5 Summary and Conclusions

The main objective of this work was to develop an IBM of juvenile Chinook salmon in the Columbia River estuary to characterize migration patterns, residence times, growth rates, and survival. This was successfully accomplished through the development of an IBM that leveraged outputs from a three-dimensional hydrodynamic model, to create a virtual environment with high-resolution flow velocities and water temperatures. Active swimming was effectively modeled for two life-history types based on assumptions regarding their habitat usage. Water temperatures from the hydrodynamic model as well as land cover data representing wetland habitat enabled the successful development of a bioenergetics model so that growth could be simulated over time.

In the last several decades, there has been dedicated research to better understand how juvenile Chinook salmon use habitats in the Columbia River estuary during their migration. This work contributes to that body of knowledge by highlighting common migration pathways for juvenile Chinook salmon, and how various characteristics associated with migration, including residence times, migration rates, and growth rates vary across flow regimes. Previous work that quantified physical habitat in the estuary specifically called out the need for this type of model (Rostaminia 2017) to better understand how juvenile Chinook salmon utilize and benefit from estuarine habitat.

Looking back at the objectives laid out in Chapter 1, this dissertation described the development of a spatially-explicit and time-varying IBM of juvenile Chinook salmon, where movement, growth, and survival were tracked over time. In Chapter 2, model-data comparisons with observed travel times from the Jones Beach pair-trawl experiment as well as from the 2010 JSATS study helped to assess the IBM's performance. Through these comparisons, it was

possible to establish the legitimacy of the IBM as a tool to simulate juvenile Chinook salmon migration. This helped to support further findings regarding impacts of environmental drivers (e.g., river flow discharge, tides, large-scale indices, and water temperatures) on estuarine residence and growth.

Both chapters 2 and 4 characterized common migration pathways in the estuary and highlighted the clear association between migration pathways and the main channels of the estuary. For yearling Chinook salmon, behaviors that optimized migration resulted in slightly reduced residence times and increased survival. While it's not possible to prove specific swimming behaviors employed by living fish, this model suggests that in some cases, swimming behavior may be less important. For yearling Chinook salmon that migrate during the spring freshet, it's possible that they take advantage of existing flows and do not expend much energy actively swimming to reach the estuary mouth.

While most of the behaviors did not stand out significantly from others, this was not the case for the subyearling Chinook salmon restricted-area search behavior. This behavior showed the strongest behavioral effect as evidenced by the increased occupation of lateral bays as well as the longer residence times and elevated growth rates. While it could be argued that swimming behavior may be less significant than movement resulting from advection, swimming behaviors that optimized growth highlighted the importance of directed swimming to identify potentially more productive habitats.

Additional contributions from this work clarified the effects of interannual and spatial variability on migration patterns and growth rates. The impacts of flow variability were especially evident in upstream reaches and resulted in greater migration rates through those

regions. Migration patterns in the lower estuary near the mouth did not deviate as much over time, suggesting that interannual variability in this region was less influential. Growth rates were likewise impacted by interannual variability in river temperatures. Spatial patterns in growth across the estuarine continuum revealed that unless individuals actively sought regions of increased growth, growth in the lower estuary was reduced compared to upstream reaches. However, it's important to note that this finding could largely be the result of how the bioenergetics model was parameterized that led to reduced growth outside of regions with wetland habitat.

This dissertation also showed how residence times and migration behavior in the estuary impact survival. Individuals that spent less time in the estuary were more likely to survive, and longer residence, especially during low flow periods, resulted in greater mortality. The IBM likewise demonstrated a contrasting pattern between pathways associated with increased survival and greater growth. Pathways confined to the main channels were associated with increased survival but reduced growth, especially in high flow years. In contrast, pathways with greater occupation in the lateral bays displayed increased growth, but were associated with reduced survival.

5.1 Future work

This dissertation made important contributions to our understanding of the role of system variability in impacting juvenile Chinook salmon migration rates, residence times, growth rates, and survival. While this work was an improvement from previous work that focused solely on quantifying physical habitat in the estuary based on specific temperature, velocity, water depth, and salinity criteria, there are still many improvements that could be made.

One area of improvement is how the bioenergetics model is simulated. The Wisconsin bioenergetics model performed well in this IBM; however, some limitations in this application included the representation of P-values as well as prey energy densities. In future iterations of the model, it would be advantageous to more effectively characterize how prey types differ across the estuary from freshwater environments to estuarine environments. While the approximation of P-values simplified the bioenergetics model, it would be more meaningful to have this value be more reflective of habitat quality and to also consider the drawdown of prey resources over time.

An additional direction that would be helpful includes conducting a sensitivity analysis to more closely examine how swimming speed and specific parameters used in the bioenergetics model (e.g., P-values and prey energy density) and swimming behaviors impact IBM results. For example, performing an Individual Parameter Perturbation or a Latin Hypercube sensitivity analysis could help to identify what parts of the model are most significantly impacting results. However, even without conducting a sophisticated sensitivity analysis, there are certain parameters that stand out as having a noticeable effect on results. The swim speed multiplier used for most swimming behaviors was set at one body length per second; however, swimming speeds are much more dynamic than that. This value likely underestimates swimming speeds, especially for individuals that prioritize movement to specific habitats. This could act to underrepresent the role of swimming behaviors which has important implications on the IBM results. Similarly, the constant prey energy density and P-values used largely influenced results from the bioenergetics model. These values could be better parameterized through a sensitivity analysis that considers material flux from wetland habitats based on flow environments and the areal extent of wetland habitat.

The model could also be improved by including competition or density-dependent processes. This could have major implications on residence times, especially for behaviors optimizing growth. If numerous individuals occupy the same habitat, the drawdown of prey resources would increase competition for food, and this could limit the amount of time fish occupy that area. There could also be an emergence of size-dependent effects if larger juvenile salmon have a competitive advantage. Similarly, density-dependent interactions could influence predation impacts, such that predation risk would be reduced if there were many individuals present in an area. Incorporating competition and density-dependence in IBM processes would likely require that more fish be simulated to more accurately represent the number of outmigrating yearling and subyearling Chinook salmon. Additionally, it would be important to consider the presence of other juvenile salmonids and estuarine fish with regards to competition for food resources and predation risk.

With regards to the IBM, an additional area to explore would be to improve swimming behaviors. The behaviors used were mostly based on simple rules regarding habitat usage that either prioritized migration or growth. While these rules were effective for drawing general conclusions about yearling and subyearling Chinook salmon residence times and migration rates, these rules did not adequately represent certain processes. For example, swimming behavior is often adaptive to short-term goals such as feeding or predator avoidance based on an individual's current state or based on the individual's prior history. Prioritizing these needs based on an individual's memory of recent events as well as their current condition could be more representative. In addition, behaviors associated with marine entry were not well simulated in the model. All behaviors maintained consistent rules from Bonneville Dam to the estuary mouth; however, it's likely that as individuals get closer to the estuary mouth, they prioritize exit.

Having a behavior that reflects the immediate biological needs of an individual as well as their desire to exit the system could more accurately address the role of behavioral decision-making during outmigration.

A meaningful future application of this work would be to evaluate potential flow management scenarios to better understand how hydropower operations impact how juvenile Chinook salmon interact with estuarine habitat. The IBM could likewise explore various climate change scenarios to better understand how warming temperatures and shifting hydrographs would impact residence times and growth of juvenile Chinook salmon. This work could also prove informative when considering future restoration work; however, this would likely necessitate the use of a much more highly resolved mesh. In addition, this IBM could be adapted for other species of importance in the Columbia River estuary, including other salmonid species and Pacific lamprey. The model could likewise be used to explore the return of adult salmon to the Columbia River estuary and how environmental conditions and hydropower operations impact their migration from the marine environment to their natal spawning habitats.

References

Anderson, C.D., D.D. Roby, and K. Collis. 2004. Foraging patterns of male and female double-crested cormorants nesting in the Columbia River estuary. *Canadian Journal of Zoology* 82: 541-554.

Bailey, J.D., J. Wallis, and E.A. Codling. 2018. Navigational efficiency in a biased and correlated random walk model of individual animal movement. *Ecology* 99: 217-223.

Baptista, A.M., C. Seaton, M.P. Wilkin, S.F. Riseman, J.A. Needoba, D. Maier, P.J. Turner, T. Kärnä, J.E. Lopez, L. Herfort, V.M. Megler, C. McNeil, B.C. Crump, T.D. Peterson, Y.H. Spitz, and H.M. Simon. 2015. Infrastructure for collaborative science and societal applications in the Columbia River estuary. *Frontiers of Earth Science* 9: 659-682.

Barnes, C.A., A.C. Duxbury, and B.-A. Morse. 1972. *Circulation and selected properties of the Columbia River effluent at sea.* Seattle, WA: University of Washington Press.

Barron, C.N., A.B. Kara, P.J. Martin, R.C. Rhodes, and L.F. Smedstad. 2006. Formulation, implementation and examination of vertical coordinate choices in the Global Navy Coastal Ocean Model (NCOM). *Ocean Modelling* 11: 347-375.

Beauchamp, D.A., D.J. Stewart, and G.L. Thomas. 1989. Corroboration of a bioenergetics model for Sockeye salmon. *Transactions of the American Fisheries Society* 118: 597-607.

Benhamou, S., and P. Bovet. 1992. Distinguishing between elementary orientation mechanisms by means of path analysis. *Animal Behaviour* 43: 371-377.

Booker, D.J., N.C. Wells, and I.P. Smith. 2008. Modelling the trajectories of migrating Atlantic salmon (Salmo salar). *Canadian Journal of Fisheries and Aquatic Sciences* 65: 352-361.

Bottom, D.L., G. Anderson, A. Baptista, J. Burke, M. Burla, M. Bhuthimethee, L. Campbell, E. Casillas, S. Hinton, K. Jacobsen, D. Jay, R. McNatt, P. Moran, G.C. Roegner, C.A. Simenstad, V. Stamatiou, D. Teel, and J.E. Zamon. 2008. Salmon Life Histories, Habitat, and Food Webs in the Columbia River Estuary: An Overview of Research Results, 2002-2006, 52: National Oceanic and Atmospheric Administration, National Marine Fisheries Service, Northwest Fisheries Science Center, Fish Ecology and Conservation Biology Divisions, Seattle.

Bottom, D.L., A. Baptista, J. Burke, L. Campbell, E. Casillas, S. Hinton, D.A. Jay, M.A. Lott, G. Mccabe, R. Mcnatt, M. Ramirez, G.C. Roegner, C.A. Simenstad, S. Spilseth, L. Stamatiou, D. Teel, and J.E. Zamon. 2011. Estuarine habitat and juvenile salmon: current and historical linkages in the lower Columbia River and estuary: Final Report 2002-2008. *National Marine Fisheries Service Report to the U.S. Army Corps of Engineers Contract W66QKZ20374382*: 200 pp.

Bottom, D.L., and K.K. Jones. 1990. Species composition, distribution, and invertebrate prey of fish assemblages in the Columbia River estuary. *Progress in Oceanography* 25: 243-270.

Bottom, D.L., C.A. Simenstad, J. Burke, A.M. Baptista, D.A. Jay, K.K. Jones, E. Casillas, and M.H. Schiewe. 2005. Salmon at river's end: the role of the estuary in the decline and recovery of Columbia River salmon. NOAA Technical Memorandum NMFS-NWFSC-68.

Brosnan, I. 2014. Death of a Salmon: An Investigation of the Processes Affecting Survival and Migration of Juvenile Yearling Chinook Salmon (Oncorhynchus Tshawytscha) in the Lower Columbia River and Ocean Plume. PhD, Cornell University Ithaca, New York.

Burke, B.J., J.J. Anderson, and A.M. Baptista. 2014. Evidence for multiple navigational sensory capabilities of Chinook salmon. *Aquatic Biology* 20: 77-90.

Burke, B.J., J.J. Anderson, J.A. Miller, L. Tomaro, D.J. Teel, N.S. Banas, and A.M. Baptista. 2016. Estimating behavior in a black box: how coastal oceanographic dynamics influence

yearling Chinook salmon marine growth and migration behaviors. *Environmental Biology of Fishes* 99: 671-686.
Burke, J.L. 2004. Life histories of juvenile Chinook salmon in the Columbia River estuary: 1916 to the present.
Burla, M. 2009. The Columbia River Estuary and Plume: Natural Variability, Anthropogenic Change and Physical Habitat for Salmon. Doctoral Thesis, Oregon Health & Science University Portland, Oregon.
Byron, C.J., and B.J. Burke. 2014. Salmon ocean migration models suggest a variety of population-specific strategies. *Reviews in Fish Biology and Fisheries* 24: 737-756.
Campbell, L.A. 2010. Life histories of juvenile Chinook salmon (Oncorhynchus tshawytscha) in the Columbia River estuary as inferred from scale and otolith microchemistry. Master's Thesis, Oregon State University Corvallis, Oregon.
Carter, J.A., G.A. McMichael, I.D. Welch, R.A. Harnish, and B.J. Bellgraph. 2009. Seasonal Juvenile Salmonid Presence and Migratory Behavior in the Lower Columbia River. PNNL-18246. Richland, Washington: Pacific Northwest National Laboratory.
Chawla, A., D.A. Jay, A.M. Baptista, M. Wilkin, and C. Seaton. 2008. Seasonal variability and estuary–shelf interactions in circulation dynamics of a river-dominated estuary. *Estuaries and Coasts* 31: 269-288.
Clarke, W.C., R.E. Withler, and J.E. Shelbourn. 1992. Genetic Control of Juvenile Life History Pattern in Chinook Salmon (Oncorhynchus tshawytscha). *Canadian Journal of Fisheries and Aquatic Sciences* 49: 2300-2306.
Codling, E.A., N.A. Hill, J.W. Pitchford, and S.D. Simpson. 2004. Random walk models for the movement and recruitment of reef fish larvae. *Marine Ecology Progress Series* 279: 215-224.
Codling, E.A., M.J. Plank, and S. Benhamou. 2008. Random walk models in biology. *Journal of the Royal society interface* 5: 813-834.
Collis, K., D.D. Roby, D.P. Craig, S. Adamany, J.Y. Adkins, and D.E. Lyons. 2002. Colony Size and Diet Composition of Piscivorous Waterbirds on the Lower Columbia River: Implications for Losses of Juvenile Salmonids to Avian Predation. *Transactions of the American Fisheries Society* 131: 537-550.
Collis, K., D.D. Roby, D.P. Craig, B.A. Ryan, and R.D. Ledgerwood. 2001. Colonial waterbird predation on juvenile salmonids tagged with passive integrated transponders in the Columbia River estuary: vulnerability of different salmonid species, stocks, and rearing types. *Transactions of the American Fisheries Society* 130: 385-396.
Cooke, S., G. Crossin, and S. Hinch. 2011. Fish migrations | Pacific Salmon Migration: Completing the Cycle. *Encyclopedia of Fish Physiology* 3: 1945-1952.
Custer, T.W., and C. Bunck. 1992. Feeding flights of breeding double-crested cormorants at two Wisconsin colonies. *Journal of Field Ornithology*: 203-211.
Dawley, E.M., R.D. Ledgerwood, T.H. Blahm, C.W. Sims, J.T. Durkin, R.A. Kirn, A.E. Rankis, G.E. Monan, and F.J. Ossiander. 1986. *Migrational characteristics, biological observations, and relative survival of juvenile salmonids entering the Columbia River estuary, 1966-1983*: US Department of Energy, Bonneville Power Administration, Division of Fish & Wildlife.
Duffy, E.J., and D.A. Beauchamp. 2011. Rapid growth in the early marine period improves the marine survival of Chinook salmon (Oncorhynchus tshawytscha) in Puget Sound, Washington. *Canadian Journal of Fisheries and Aquatic Sciences* 68: 232-240.

Elliott, J.M. 1976. Energy losses in the waste products of brown trout (Salmo trutta L.). *The Journal of Animal Ecology*: 561-580.

Emmett, R.L., G.K. Krutzikowsky, and P. Bentley. 2006. Abundance and distribution of pelagic piscivorous fishes in the Columbia River plume during spring/early summer 1998–2003: Relationship to oceanographic conditions, forage fishes, and juvenile salmonids. *Progress in Oceanography* 68: 1-26.

Evans, A.F., N.J. Hostetter, D.D. Roby, K. Collis, D.E. Lyons, B.P. Sandford, R.D. Ledgerwood, and S. Sebring. 2012. Systemwide Evaluation of Avian Predation on Juvenile Salmonids from the Columbia River Based on Recoveries of Passive Integrated Transponder Tags. *Transactions of the American Fisheries Society* 141: 975-989.

Fiechter, J., D.D. Huff, B.T. Martin, D.W. Jackson, C.A. Edwards, K.A. Rose, E.N. Curchitser, K.S. Hedstrom, S.T. Lindley, and B.K. Wells. 2015a. Environmental conditions impacting juvenile Chinook salmon growth off central California: An ecosystem model analysis. *Geophysical Research Letters* 42: 2910-2917.

Fiechter, J., K.A. Rose, E.N. Curchitser, and K.S. Hedstrom. 2015b. The role of environmental controls in determining sardine and anchovy population cycles in the California Current: Analysis of an end-to-end model. *Progress in Oceanography* 138: 381-398.

Fraenkel, G.S., and D.L. Gunn. 1940. The Orientation of Animals: Kineses, Taxes and Compass Reactions, 352: Oxford.

Giske, J., G. Huse, and O. Fiksen. 1998. Modelling spatial dynamics of fish. *Reviews in Fish Biology and Fisheries* 8: 57-91.

Goodwin, R.A., J.M. Nestler, J.J. Anderson, L.J. Weber, and D.P. Loucks. 2006. Forecasting 3-D fish movement behavior using a Eulerian–Lagrangian–agent method (ELAM). *Ecological Modelling* 192: 197-223.

Grimm, V., U. Berger, F. Bastiansen, S. Eliassen, V. Ginot, J. Giske, J. Goss-Custard, T. Grand, S.K. Heinz, G. Huse, A. Huth, J.U. Jepsen, C. Jørgensen, W.M. Mooij, B. Müller, G. Pe'er, C. Piou, S.F. Railsback, A.M. Robbins, M.M. Robbins, E. Rossmanith, N. Rüger, E. Strand, S. Souissi, R.A. Stillman, R. Vabø, U. Visser, and D.L. DeAngelis. 2006. A standard protocol for describing individual-based and agent-based models. *Ecological Modelling* 198: 115-126.

Groot, C., and L. Margolis. 1991. *Pacific salmon life histories*. Vancouver: Univ. British Columbia Press.

Haeseker, S.L., J.A. McCann, J. Tuomikoski, and B. Chockley. 2012. Assessing freshwater and marine environmental influences on life-stage-specific survival rates of Snake River spring–summer Chinook salmon and steelhead. *Transactions of the American Fisheries Society* 141: 121-138.

Hamilton, K., and L.A. Mysak. 1986. Possible Effects of the Sitka Eddy on Sockeye (Oncorhynchus nerka) and Pink Salmon (Oncorhynchus gorbuscha) Migration off Southeast Alaska. *Canadian Journal of Fisheries and Aquatic Sciences* 43: 498-504.

Hanson, P.C. 1997. Fish bioenergetics 3.0 for Windows. Madison, Wisconsin: University of Wisconsin Sea Grant Institute.

Harnish, R.A., G.E. Johnson, G.A. McMichael, M.S. Hughes, and B.D. Ebberts. 2012. Effect of migration pathway on travel time and survival of acoustic-tagged juvenile salmonids in the Columbia River estuary. *Transactions of the American Fisheries Society* 141: 507-519.

Healey, M.C. 1982. Juvenile Pacific salmon in estuaries: the life support system. In *Estuarine Comparisons*, ed. V.S. Kennedy, 315-341. New York: Academic Press.

Healey, M.C., K.A. Thomson, P.H. Leblond, L. Huato, S.G. Hinch, and C.J. Walters. 2000. Computer simulations of the effects of the Sitka eddy on the migration of sockeye salmon returning to British Columbia. *Fisheries Oceanography* 9: 271-281.

Hinckley, S., A.J. Hermann, and B.A. Megrey. 1996. Development of a spatially explicit, individual-based model of marine fish early life history. *Marine Ecology Progress Series* 139: 47-68.

Humston, R., J.S. Ault, M. Lutcavage, and D.B. Olson. 2000. Schooling and migration of large pelagic fishes relative to environmental cues. *Fisheries Oceanography* 9: 136-146.

Humston, R., D.B. Olson, and J.S. Ault. 2004. Behavioral assumptions in models of fish movement and their influence on population dynamics. *Transactions of the American Fisheries Society* 133: 1304-1328.

Johnson, G.E., G.R. Ploskey, N.K. Sather, D.J. Teel, and A. Fisk. 2015. Residence times of juvenile salmon and steelhead in off-channel tidal freshwater habitats, Columbia River, USA. *Canadian Journal of Fisheries and Aquatic Sciences* 72: 684-696.

Kärnä, T., and A.M. Baptista. 2016a. Evaluation of a long-term hindcast simulation for the Columbia River estuary. *Ocean Modelling* 99: 1-14.

Kärnä, T., and A.M. Baptista. 2016b. Water age in the Columbia River estuary. *Estuarine, Coastal and Shelf Science* 183: 249-259.

Kärnä, T., A.M. Baptista, J.E. Lopez, P.J. Turner, C. McNeil, and T.B. Sanford. 2015. Numerical modeling of circulation in high-energy estuaries: a Columbia River Estuary benchmark. *Ocean Modelling* 88: 54-71.

Koehler, M.E., K.L. Fresh, D.A. Beauchamp, J.R. Cordell, C.A. Simenstad, and D.E. Seiler. 2006. Diet and bioenergetics of lake-rearing juvenile Chinook salmon in Lake Washington. *Transactions of the American Fisheries Society* 135: 1580-1591.

Kukulka, T., and D.A. Jay. 2003a. Impacts of Columbia River discharge on salmonid habitat: 1. A nonstationary fluvial tide model. *Journal of Geophysical Research: Oceans* 108.

Kukulka, T., and D.A. Jay. 2003b. Impacts of Columbia River discharge on salmonid habitat: 2. Changes in shallow-water habitat. *Journal of Geophysical Research: Oceans* 108.

Laake, J.L., P. Browne, R.L. DeLong, and H.R. Huber. 2002. Pinniped diet composition: a comparison of estimation models. *Fishery Bulletin* 100: 434-447.

Ledgerwood, R.D., B.A. Ryan, E.M. Dawley, E.P. Nunnallee, and J.W. Ferguson. 2004. A surface trawl to detect migrating juvenile salmonids tagged with passive integrated transponder tags. *North American Journal of Fisheries Management* 24: 440-451.

Lyons, D., A. Evans, N. Hostetter, A. Piggott, L. Weitkamp, T. Good, D. Roby, K. Collis, P. Loschl, and B. Cramer. 2014. Factors influencing predation on juvenile salmonids by double-crested cormorants in the Columbia River estuary: a retrospective analysis. *Report to the US Army Corps of Engineers, Portland District, Portland, Oregon.*

Mantua, N.J., S.R. Hare, and Y. Zhang. 1997. A Pacific interdecadal climate oscillation with impacts on salmon production. *Bulletin of the American Meteorological Society*: 1069-1079.

McCabe, G.T., R.L. Emmett, W.D. Muir, and T.H. Blahm. 1986. Utilization of the Columbia River estuary by subyearling chinook Salmon. *Northwest Science* 60: 113-124.

McComas, R.L., G.A. McMichael, J.A. Vucelick, L. Gilbreath, J.P. Everett, S.G. Smith, T. Carlson, G. Matthews, and J.W. Ferguson. 2008. A study to estimate salmonid survival through the Columbia River estuary using acoustic tags, 2006. *Fish Ecology Division,*

Northwest Fisheries Science Center, National Marine Fisheries Service: Seattle, WA, USA.

McMichael, G.A., M.B. Eppard, T.J. Carlson, J.A. Carter, B.D. Ebberts, R.S. Brown, M. Weiland, G.R. Ploskey, R.A. Harnish, and Z.D. Deng. 2010. The juvenile salmon acoustic telemetry system: a new tool. *Fisheries* 35: 9-22.

McMichael, G.A., R.A. Harnish, J.R. Skalski, K.A. Deters, K.D. Ham, R.L. Townsend, P.S. Titzler, M.S. Hughes, J.A. Kim, and D.M. Trott. 2011. Migratory behavior and survival of juvenile salmonids in the lower Columbia River, estuary, and plume in 2010: PNNL-20443, Pacific Northwest National Lab. Richland, WA.

McNatt, R., and S. Hinton. 2017. Evidence for direct use of tidal wetlands by interior stocks of juvenile salmon. In Anadromous Fish Evaluation Program, Annual Meeting. Richland, Washington.

McNatt, R.A., D.L. Bottom, and S.A. Hinton. 2016. Residency and movement of juvenile Chinook salmon at multiple spatial scales in a tidal marsh of the Columbia River estuary. *Transactions of the American Fisheries Society* 145: 774-785.

Miller, T.J. 2007. Contribution of individual-based coupled physical-biological models to understanding recruitment in marine fish populations. *Marine Ecology Progress Series* 347: 127-138.

Mork, K.A., J. Gilbey, L.P. Hansen, A.J. Jensen, J.A. Jacobsen, M. Holm, J.C. Holst, N. Ó Maoiléidigh, F. Vikebø, P. McGinnity, W. Melle, K. Thomas, E. Verspoor, and V. Wennevik. 2012. Modelling the migration of post-smolt Atlantic salmon (Salmo salar) in the Northeast Atlantic. *ICES Journal of Marine Science* 69: 1616-1624.

Myers, E.P., and A.M. Baptista. 2001. Inversion for tides in the Eastern North Pacific Ocean. *Advances in Water Resources* 24: 505-519.

Myers, J.M., R.G. Kope, G.J. Bryant, D. Teel, L.J. Lierheimer, T.C. Wainwright, W.S. Grant, F.W. Waknitz, K. Neely, and S.T. Lindley. 1998. Status review of chinook salmon from Washington, Idaho, Oregon, and California. *NOAA Technical Memorandum NMFS-NWFSC* 35: 443.

Okunishi, T., S.-I. Ito, D. Ambe, A. Takasuka, T. Kameda, K. Tadokoro, T. Setou, K. Komatsu, A. Kawabata, H. Kubota, T. Ichikawa, H. Sugisaki, T. Hashioka, Y. Yamanaka, N. Yoshie, and T. Watanabe. 2012. A modeling approach to evaluate growth and movement for recruitment success of Japanese sardine (Sardinops melanostictus) in the western Pacific. *Fisheries Oceanography* 21: 44-57.

Petrosky, C., and H. Schaller. 2010. Influence of river conditions during seaward migration and ocean conditions on survival rates of Snake River Chinook salmon and steelhead. *Ecology of Freshwater Fish* 19: 520-536.

Plumb, J.M., and C.M. Moffitt. 2015. Re-estimating temperature-dependent consumption parameters in bioenergetics models for juvenile Chinook salmon. *Transactions of the American Fisheries Society* 144: 323-330.

Politikos, D.V., M. Huret, and P. Petitgas. 2015. A coupled movement and bioenergetics model to explore the spawning migration of anchovy in the Bay of Biscay. *Ecological Modelling* 313: 212-222.

Prentice, E.F., T.A. Flagg, C.S. McCutcheon, and D.F. Brastow. 1990. PIT-tag monitoring systems for hydroelectric dams and fish hatcheries. *American Fisheries Society Symposium* 7: 323-334.

Quinn, T.P. 2005. *The behavior and ecology of Pacific salmon and trout*. Seattle, WA: University of Washington Press.

Railsback, S.F., R.H. Lamberson, B.C. Harvey, and W.E. Duffy. 1999. Movement rules for individual-based models of stream fish. *Ecological Modelling* 123: 73-89.

Raymond, H.L. 1988. Effects of Hydroelectric Development and Fisheries Enhancement on Spring and Summer Chinook Salmon and Steelhead in the Columbia River Basin. *North American Journal of Fisheries Management* 8: 1-24.

Rich, W.H. 1920. Early history and seaward migration of Chinook salmon in the Columbia and Sacramento rivers. *Fishery Bulletin* 37: 1-74.

Roby, D.D., K. Collis, D.E. Lyons, D.P. Craig, J.Y. Adkins, A.M. Myers, and R.M. Suryan. 2002. Effects of colony relocation on diet and productivity of Caspian terns. *The Journal of Wildlife Management*: 662-673.

Roegner, G.C., R. McNatt, D.J. Teel, and D.L. Bottom. 2012. Distribution, size, and origin of juvenile Chinook salmon in shallow-water habitats of the lower Columbia River and estuary, 2002–2007. *Marine and Coastal Fisheries* 4: 450-472.

Rogers, E., G. DiMego, T. Black, M. Ek, B. Ferrier, G. Gayno, Z. Janjic, Y. Lin, M. Pyle, and V. Wong. 2009. The NCEP North American mesoscale modeling system: Recent changes and future plans. In Preprints, 23rd Conference on Weather Analysis and Forecasting/19th Conference on Numerical Weather Prediction.

Rose, K.A., J. Fiechter, E.N. Curchitser, K. Hedstrom, M. Bernal, S. Creekmore, A. Haynie, S.i. Ito, S. Lluch-Cota, B.A. Megrey, C.A. Edwards, D. Checkley, T. Koslow, S. McClatchie, F. Werner, A. MacCall, and V. Agostini. 2015. Demonstration of a fully-coupled end-to-end model for small pelagic fish using sardine and anchovy in the California Current. *Progress in Oceanography* 138: 348-380.

Rostaminia, M. 2017. Change in variability in the Columbia River estuary: a habitat perspective. Doctoral Thesis, Oregon Health & Science University Portland, Oregon.

Royce, W.F., L.S. Smith, and A.C. Hartt. 1968. Models of oceanic migrations of Pacific salmon and comments on guidance mechanisms. *Fishery Bulletin* 66: 441-462.

Ryan, B.A., S.G. Smith, J.A.M. Butzerin, and J.W. Ferguson. 2003. Relative vulnerability to avian predation of juvenile salmonids tagged with passive integrated transponders in the Columbia River estuary, 1998–2000. *Transactions of the American Fisheries Society* 132: 275-288.

Sanborn Map Company. 2011. High Resolution Land Cover, Lower Columbia River Estuary. OR & WA, United States, 2007-2010. Portland, OR: Sanborn Map Company.

Schaller, H.A., and C.E. Petrosky. 2007. Assessing hydrosystem influence on delayed mortality of Snake River stream-type Chinook salmon. *North American Journal of Fisheries Management* 27: 810-824.

Schaller, H.A., C.E. Petrosky, and E.S. Tinus. 2014. Evaluating river management during seaward migration to recover Columbia River stream-type Chinook salmon considering the variation in marine conditions. *Canadian Journal of Fisheries and Aquatic Sciences* 71: 259-271.

Scheuerell, M.D., R.W. Zabel, and B.P. Sandford. 2009. Relating juvenile migration timing and survival to adulthood in two species of threatened Pacific salmon (Oncorhynchus spp.). *Journal of Applied Ecology* 46: 983-990.

Schreiber, R.W., and R.B. Clapp. 1987. Pelecaniform feeding ecology.

Sebring, S.H., M.C. Carper, R.D. Ledgerwood, B.P. Sandford, G.M. Matthews, and A.F. Evans. 2013a. Relative vulnerability of PIT-tagged subyearling fall Chinook Salmon to predation by Caspian terns and double-crested cormorants in the Columbia River estuary. *Transactions of the American Fisheries Society* 142: 1321-1334.

Sebring, S.H., G. Murphey, B.P. Sandford, A. Evans, and R.D. Ledgerwood. 2013b. Detection of passive integrated transponder (PIT) tags on piscivorous avian colonies in the Columbia River Basin, 2011: Fish Ecology Division, Northwest Fisheries Science Center, National Marine Fisheries Service.

Simenstad, C.A., J.L. Burke, J.E. O'Connor, C. Cannon, D.W. Heatwole, M.F. Ramirez, I.R. Waite, T.D. Counihan, and K.L. Jones. 2011. Columbia River estuary ecosystem classification—concept and application: US Geological Survey.

Simenstad, C.A., and J.R. Cordell. 2000. Ecological assessment criteria for restoring anadromous salmonid habitat in Pacific Northwest estuaries. *Ecological Engineering* 15: 283-302.

Simenstad, C.A., K.L. Fresh, and E.O. Salo. 1982. The role of Puget Sound and Washington coastal estuaries in the life history of Pacific salmon: an unappreciated function. *Estuarine Comparisons. Academic Press, New York* 14: 343-364.

Soikkeli, M. 1973. Long distance fishing flights of the breeding Caspian tern Hydroprogne caspia. *Ornis Fennica* 50: 47-48.

Song, Y., and D. Haidvogel. 1994. A semi-implicit ocean circulation model using a generalized topography-following coordinate system. *Journal of Computational Physics* 115: 228-244.

Stewart, D.J., and M. Ibarra. 1991. Predation and production by salmonine fishes in Lake Michigan, 1978–88. *Canadian Journal of Fisheries and Aquatic Sciences* 48: 909-922.

Stewart, D.J., D. Weininger, D.V. Rottiers, and T.A. Edsall. 1983. An energetics model for lake trout, Salvelinus namaycush: application to the Lake Michigan population. *Canadian Journal of Fisheries and Aquatic Sciences* 40: 681-698.

Thom, R.M., S.A. Breithaupt, H.L. Diefenderfer, A.B. Borde, G.C. Roegner, G.E. Johnson, and D.L. Woodruff. 2018. Storm-driven particulate organic matter flux connects a tidal tributary floodplain wetland, mainstem river, and estuary. *Ecological Applications* 28: 1420-1434.

Thornton, K.W., and A.S. Lessem. 1978. A temperature algorithm for modifying biological rates. *Transactions of the American Fisheries Society* 107: 284-287.

Thorpe, J.E. 1994. Salmonid fishes and the estuarine environment. *Estuaries* 17: 76-93.

Tyler, J.A., and K.A. Rose. 1994. Individual variability and spatial heterogeneity in fish population models. *Reviews in Fish Biology and Fisheries* 4: 91-123.

Waples, R.S., D.J. Teel, J.M. Myers, and A.R. Marshall. 2004. Life-history divergence in Chinook salmon: historic contingency and parallel evolution. *Evolution* 58: 386-403, 318.

Ward, D.L., J.H. Petersen, and J.J. Loch. 1995. Index of predation on juvenile salmonids by northern squawfish in the lower and middle Columbia River and in the lower Snake River. *Transactions of the American Fisheries Society* 124: 321-334.

Ware, D. 1978. Bioenergetics of pelagic fish: theoretical change in swimming speed and ration with body size. *Journal of the Fisheries Board of Canada* 35: 220-228.

Watkins, K.S., and K.A. Rose. 2013. Evaluating the performance of individual-based animal movement models in novel environments. *Ecological Modelling* 250: 214-234.

Watkins, K.S., and K.A. Rose. 2017. Simulating individual-based movement in dynamic environments. *Ecological Modelling* 356: 59-72.

Weitkamp, L.A., P.J. Bentley, and M.N.C. Litz. 2012. Seasonal and interannual variation in juvenile salmonids and associated fish assemblage in open waters of the lower Columbia river estuary. *Fishery Bulletin* 110: 426-450.

Weitkamp, L.A., G. Goulette, J. Hawkes, M. O'Malley, and C. Lipsky. 2014. Juvenile salmon in estuaries: comparisons between North American Atlantic and Pacific salmon populations. *Reviews in Fish Biology and Fisheries* 24: 713-736.

Williams, J.G., S.G. Smith, R. Zabel, W. Muir, M. Scheuerell, B. Sandford, D.M. Marsh, R. McNatt, and S. Achord. 2005. Effects of the federal Columbia River power system on salmon populations. *NOAA Technical Memorandum, NMFS-NWFSC* 63.

Willis, J. 2011. Modelling swimming aquatic animals in hydrodynamic models. *Ecological Modelling* 222: 3869-3887.

Zabel, R.W., and J.G. Williams. 2002. Selective mortality in Chinook salmon: what is the role of human disturbance? *Ecological Applications* 12: 173-183.

Zhang, Y., and A.M. Baptista. 2008. SELFE: A semi-implicit Eulerian–Lagrangian finite-element model for cross-scale ocean circulation. *Ocean Modelling* 21: 71-96.

Zimmerman, M.P. 1999. Food Habits of Smallmouth Bass, Walleyes, and Northern Pikeminnow in the Lower Columbia River Basin during Outmigration of Juvenile Anadromous Salmonids. *Transactions of the American Fisheries Society* 128: 1036-1054.